CHARACTERIZATION OF THE ALLOSTERIC PROPERTIES OF *THERMUS THERMOPHILUS* PHOSPHOFRUCTOKINASE AND THE SOURCES OF STRONG INHIBITOR BINDING AFFINITY AND WEAK INHIBITORY RESPONSE

A Dissertation

by

MARIA SHUBINA-MCGRESHAM

Submitted to the Office of Graduate Studies of
Texas A&M University
in partial fulfillment of the requirements for the degree of

DOCTOR OF PHILOSOPHY

August 2012

Major Subject: Biochemistry

CHARACTERIZATION OF THE ALLOSTERIC PROPERTIES OF *THERMUS THERMOPHILUS* PHOSPHOFRUCTOKINASE AND THE SOURCES OF STRONG INHIBITOR BINDING AFFINITY AND WEAK INHIBITORY RESPONSE

A Dissertation

by

MARIA SHUBINA-MCGRESHAM

Submitted to the Office of Graduate Studies of
Texas A&M University
in partial fulfillment of the requirements for the degree of

DOCTOR OF PHILOSOPHY

Approved by:

Chair of Committee,	Gregory Reinhart
Committee Members,	Jorge Cruz-Reyes
	Tatyana Igumenova
	Siegfried Musser
Head of Department,	Gregory Reinhart

August 2012

Major Subject: Biochemistry

ABSTRACT

Characterization of the Allosteric Properties of *Thermus thermophilus* Phosphofructokinase and the Sources of Strong Inhibitor Binding Affinity and Weak Inhibitory Response. (August 2012)

Maria Shubina-McGresham, B.S. The University of Texas at Tyler

Chair of Advisory Committee: Dr. Gregory Reinhart

Characterization of allosteric properties of phosphofructokinase from the extreme thermophile *Thermus thermophilus* (TtPFK) using thermodynamic linkage analysis revealed several peculiarities. Inhibition and activation of Fru-6-P binding by the allosteric effectors phosphoenolpyruvate (PEP) and MgADP are entropically-driven in TtPFK. It is also curious that PEP binding affinity is unusually strong in TtPFK when compared to PFKs from *Escherichia coli*, *Bacillus stearothermophilus*, and *Lactobacillus delbrueckii*, while the magnitude of the allosteric inhibition by PEP is much smaller in TtPFK. In an effort to understand the source of weak inhibition, a putative network of residues between the allosteric site and the nearest active site was identified from the three-dimensional structures of BsPFK. Three of the residues in this network, D59, T158, and H215, are not conserved in TtPFK, and, due to their nature (N59, A158, S215), are unlikely to be involved in the same non-covalent interactions seen in BsPFK. The triple chimeric substitution N59D/A158T/S215H, results in a 2.5 kcal mol^{-1} increase in the coupling free energy, suggesting that the region containing

these residues may be important for propagation of inhibitory response. The individual substitutions at each position resulted in an increase in the coupling free energy, and the double substitutions displayed additivity of these changes.

The chimeric substitution made at N59 suggests that the polar nature of the asparagine at position 59 is key for the enhanced binding of PEP. The non-conserved R55 was found to be particularly important for the enhanced binding of PEP in TtPFK, as chimeric substitutions R55G and R55E resulted in a 3.5 kcal mol^{-1} and 4.5 kcal mol^{-1} decrease in the binding affinity for PEP, respectively. Our results also confirm the observations previously made in PFKs from *E. coli* and *B. stearothermophilus*, that the ability of the effector to bind is independent of its ability to produce allosteric response. We show that several substitutions result in a decrease in binding affinity of PEP to TtPFK, while dramatically enhancing its ability to inhibit (N59D, R55G, R55E). Similarly, some substitutions, like S215H and A158T show an enhanced inhibition by PEP, while having no effect on its binding affinity.

DEDICATION

To my loving family:

Дорогие мама и бабушка, спасибо вам за любовь, поддержку и неподдельный интерес к моей науке. My sweet sister Ksenia, thank you for our hilarious late night conversations, for telling me how smart I am and for looking up to me. It's been a great motivation that kept me going when times got tough. My dear husband, thank you for listening to my numerous rants about failed experiments and sharing in the excitements of the ones that worked. Thank you for trying your best to understand what I do, cooking dinners 95% of the time, and being a wonderful dad. My sweet baby Sophia, thank you for always putting a smile on my face, for your hugs and kisses, and for simply being. You have all made this possible.

ACKNOWLEDGEMENTS

I would like to thank my Boss, Dr. Reinhart, for taking me under his wing. I really appreciate having the opportunity to learn and grow under his guidance and I will fondly remember all the stories about the time when men were men and the word processors were nonexistent. I also hope to retain at least some of the complicated words I've learned over the past few years and, maybe, one day, even use them in a sentence.

I want to thank Dr. Igumenova, Dr. Musser, and Dr. Cruz-Reyes for serving on my committee, asking a lot of questions, and providing the much-needed guidance. Thank you to the members of the Sacchettinni lab Dr. Manchi Reddy and Jennifer Tsai for help with crystallization trials. I also want to thank all the members of the Reinhart lab, past and present, for the inspiration from the frequent discussions of our projects and for the random-topic conversations during lunchtime.

NOMENCLATURE

A	Substrate
[A]	Concentration of substrate
BsPFK	Phosphofructokinase from *Bacillus stearothermophilus*
ΔG_{ax}	Coupling free energy between the binding of the substrate and activator
ΔG_{ay}	Coupling free energy between the binding of the substrate and inhibitor
ΔH_{ax}	Coupling enthalpy for the binding of the substrate and activator
ΔH_{ay}	Coupling enthalpy for the binding of the substrate and inhibitor
ΔS_{ax}	Coupling entropy for the binding of the substrate and activator
ΔS_{ay}	Coupling entropy for the binding of the substrate and inhibitor
ΔC_p	Change in the heat capacity
EcPFK	Phosphofructokinase from *Escherichia coli*
EDTA	Ethylenediamine Tetraacetic Acid
EPPS	N- [2-Hydroxyethyl] Piperazine--3-Propanesulfonic Acid
Fru-6-P	Fructose-6-Phosphate
K_a	Apparent dissociation constant for substrate A
K_{ia}°	Dissociation constant for A in the absence of effector
K_{ia}^{∞}	Dissociation constant for A in the presence of saturating effector
K_{ix}°	Dissociation constant for activator in the absence of substrate

K_{iy}°	Dissociation constant for inhibitor in the absence of substrate
K_m	Michaelis constant
K_y	Apparent dissociation constant for inhibitor Y
LbPFK	Phosphofructokinase from *Lactobacillus delbrueckii ssp. bulgaricus*
MOPS	3-[N-Morpholino] Propanesulfonic acid
NADH	Nicotinamide Adenine Dinucleotide, reduced form
n_H	Hill number
PEP	Phosphoenolpyruvate
PFK	Phosphofructokinase
PG	Phosphoglycolate
Q_{ax}	Coupling constant between the binding of the substrate and activator
Q_{ay}	Coupling constant between the binding of the substrate and inhibitor
Tris	Tris [Hyroxymethyl] Aminomethane
v°	Initial velocity
V	Maximal velocity
X	Activator
[X]	Concentration of activator
Y	Inhibitor
[Y]	Concentration of inhibitor

TABLE OF CONTENTS

CHAPTER Page

LIST OF FIGURES

FIGURE Page

LIST OF TABLES

CHAPTER I

INTRODUCTION: ADAPTATIONS TO HIGH TEMPERATURE

The chapters following the introduction discuss various aspects of the allosteric regulation of a phosphofructokinase (PFK) from the extreme thermophile *Thermus thermophilus* in comparison to that of the PFKs from mesophilic *E. coli* and moderately thermophilic *Bacillus stearothermophilus*. Since our interest in this enzyme stems from the thermophilic nature of the organism it came from, the following review is aimed to gain a better appreciation of the differences between thermophiles and mesophiles, as well as to provide a brief overview of the field of extremophile research as a whole.

Part 1: Extremophiles

As difficult as it is to imagine, life has been discovered in such harsh environments as desiccating soils of the Atacama Desert (*1*), radiation-plagued Chernobyl (*2*), and the boiling waters of the Yellowstone hot springs (*3*). By the late 20th century, more and more of these discoveries were made all over the world resulting in a number of landmark publications, which were followed by a colossal effort to uncover more extreme-loving organisms and study the nature of their adaptations. In 1974, R.D. MacElroy coined the term extremophile, from Latin *extremus* meaning "extreme" and Greek φιλία meaning "love", to describe the wide variety of organisms that possess the remarkable ability to survive and function well in the most extreme conditions on our planet, which would be deadly to most life forms (*4*). A distinction should be made between extremophiles and extremotrophs. The latter describes

---

This dissertation follows the style of *Biochemistry*.

organisms that are tolerant of extreme temperature, pH, salinity, pressure, etc., but function optimally under normal conditions, while the former applies to the organisms that thrive in the harsh environments (*5*).

Among an abundance of new organisms identified in the search for extremophiles, a large number belong to what we know now as the Archaea domain. However, at the time these organisms were being discovered, the phylogenetic system, while having come a long way from the "plant or animal" classification, still existed as yet another dichotomy dividing all organisms into prokaryotes (bacteria) and eukaryotes (plants, animals, fungi, & protists). And while the eukaryotes were defined by their complex properties, the prokaryotes were for a long time defined by the lack of properties characteristic of the eukaryotes. By the 1950's, the increased understanding of inner workings of the cellular machinery allowed scientists to actually define the prokaryotes based on shared cellular characteristics. However, since this high level of understanding was only reached in a limited number of model systems, this definition was based in its entirety on the characteristics of a single organism, *E. coli*, which became the model prokaryote.

Because at first glance they appeared similar to bacteria, the newly discovered archaeans were initially classified as bacteria along with the rest of the prokaryotes. However, the detailed molecular studies of these organisms revealed significant differences in their rRNA, DNA and biochemical pathways compared with those of known prokaryotes. As a matter of fact, in many aspects, such as RNA polymerase

sequences (*6*) and ribosomal protein sequences (*7*), these new organisms appeared to be more closely related to the eukaryotes. Carl Woese and colleagues recognized that these differences (mostly based on rRNA structure) were too meaningful to overlook and concluded that the known prokaryotes in the bacteria kingdom and the recently discovered ones must have evolved from a distant ancestor containing very rudimentary replication machinery. This led Woese to propose a new phylogenetic system, which recognized three domains: Eucarya, Bacteria, which contained the known prokaryotes, and Archaea, which encompassed the methanogens, extreme halophiles, and sulfate-reducing species all of which shared the thermophilic phenotype (*8, 9*).

Over the past several decades, the existence of extremophiles went from fiction to reality, and in 1997 the Extremophile Journal was originated to bring together the latest developments in the field. In 2002, the editors of the Extremophile Journal created the International Society for Extremophiles (ISE), which supports the researchers in the extremophile field and organizes a biannual conference to showcase the cutting edge research. The discovery of these extreme-loving organisms gave us more than enough reasons to reevaluate our theories on the origins and limits of life on Earth and the existence of life on other planets. But our interest in the life in extreme environments is not purely scientific; it is also fueled by its economic potential. There are several multimillion-dollar industries, which already utilize the unique properties of the biomolecules isolated from these organisms in a wide variety of applications such as paper bleaching (xylanases from thermophiles), detergents (proteases, lipases *etc.* from psychrophiles, alkaliphiles and acidophiles), drug delivery, and cosmetics (lipids from

halophiles) (*10, 11*). And the search for other potentially useful biomolecules produced by extremophiles continues today.

Diversity of extremophiles, history of discoveries and landmark publications

The examples of extremophile groups described below are by no means exhaustive, as a variety of other extremophiles have been characterized. These and other extremophiles, including the remarkable case of *Deinococcus radiodurans*, which is able to withstand extreme doses of ionizing radiation, are discussed in depth in the *Extremophiles Handbook* (*12*), as well as other sources. The brief descriptions of a few groups of extremophiles are included in this review to demonstrate the relative newness of the field of extremophile research, juxtaposed with the fact that these organisms have been around us all along, and to appreciate the complexity and diversity of life that exists in the most extreme environments on our planet. This section of the review is also intended to exemplify how the serendipitous events in our lives as scientists can lead to the discovery of new frontiers and become our life's work.

Piezophiles

The reports identifying the organisms found in the environments previously thought to be void of any life date back to late the 19th century. Among the first were the reports of Certes who found bacteria living at the ocean depth of over 5000 meters and showed that these organisms were able to tolerate pressures of 500 atm. In 1948 Claude ZoBell, considered by many the founder of modern marine microbiology, collected samples of bacteria from depth of the oceans and analyzed their growths at varying pressures and temperatures. ZoBell was the first to coin the term barophile (this term

was later changed to piezophile) to describe organisms that prefer high hydrostatic pressure (*13*); he was also the first to show that the effect of temperature is modulated by pressure (*14*). In a book review, one of ZoBell's students Richard Morita noted that, due to a large degree of disbelief, it often took years for the manuscripts reporting these findings to be accepted by reviewers (*15*).

Alkaliphiles

While the organisms that prefer higher than normal pH have been reported since the early 1900's, the man who is widely recognized for the discovery and naming of alkaliphiles is Koki Horikoshi (*16*). His first encounter with bacteria that preferred alkaline conditions happened in 1956 when he was a graduate student at University of Tokyo studying the autolysis of *Aspergillus oryzae* (*12*). One day he found his flask of mold was completely cleared and contained strong endo-1,3-β-glucanase activity. From the flask Horikoshi isolated *Bacillus circulans,* the bacterium that was responsible for producing the enzyme that lysed his mold culture. When he attempted to grow *B. circulans* in the absence of the mold spores, the bacterium showed poor growth and very low endo-1,3-β-glucanase activity. Horikoshi concluded that the endo-1,3-β-glucanase activity can only be obtained from growing on mold spores. This was the first example of a bacterium lysing the mold cells, and the results were published in Nature (*17*). It wasn't until some years later that Horikoshi realized that the autolysis of the mold increased the pH of his culture allowing the growth of *B. circulans* and he was able to grow it in conventional media at higher pH. This finding opened his mind to the possibility that there may be a whole unexplored world of life at higher pH. Inspired,

Horikoshi inoculated alkaline cultures with a variety of soil samples, and, to his great surprise, identified a large number of alkaliphilic organisms and studied their enzymes. The results of these experiments were described in his landmark publications in 1971 (*16, 18, 19*). Over the following several decades Horikoshi and colleagues studied the enzymology, physiology, and genetics of these organisms in an attempt to understand the nature of their adaptations to high pH.

Psychrophiles

A large portion of our biosphere belongs to permanently cold environments with temperatures below 5°C, which, until quite recently, have been thought to be devoid of life. That was changed with a series of discoveries of cold-adapted organisms in glacial ice, deep in the oceans and in the permafrost that were made in 1990's and early 2000's (*12, 20*). The organisms, which can tolerate cold environments, have been isolated and characterized since the early 1900's, however, there is little agreement on whether these organisms are truly psychrophilic, since most of them grow much better at mesophilic temperatures (*20*). This issue has been further exacerbated by the lack of consensus on what the definition of the term "psychrophile" should be.

The term "psychrophile" was first used by Schmidt-Nielsen in 1902 to describe an organism that was able to survive and multiply at 0°C (*21*). Morita argues that the majority of the organisms described by the scientists before 1960s as psychrophilic based on their ability to grow at 0°C were mislabeled, because they grew even better at mesophilic temperatures (*20*). Hucker proposed that the organisms that are able to grow at 0°C be divided into obligate (grow at 0°C, but not at 32°C) and facultative (can grow

at 0°C and 32°C) psychrophiles (*22*). Eddy argued that organisms that are capable of growing at 5°C and below should be termed psychrotrophic, irrespective of their optimum growth temperature, and that the term psychrophilic should be reserved for those organisms that have the optimum growth temperatures below 35°C (*23*). Many other definitions have been suggested over the years, including the widely accepted definition, proposed in the 1975 landmark publication by Morita, where he defines psychrophiles as organisms with the optimal growth temperature below 15°C that are unable to grow above 20°C (*12, 20*). In the same publication Morita also pointed out, that in order to identify true psychrophiles, it is crucial that the "source material" never reaches warm temperatures for an extended period of time, which explains why several attempts to isolate psychrophiles from environments which were exposed to higher temperatures for a few months a year have failed. Morita also noted that it is extremely important that the bacteria are never exposed to the temperatures much higher than their environment, so the growth media and anything that is used to handle the bacteria must be cooled, since the heat shock may be enough to lyse the cells.

The psychrophiles continue to be subject of rigorous research in several areas of science ranging from understanding how the various components of the cellular machinery are able to work at subzero temperatures to how the metabolic processes of these previously unaccounted for organisms affect the flux of the green house gasses (*12*). The cold-loving organisms are also of much interest because of their potential for biomedical industries (*24*).

Halophiles

Possibly the longest and most remarkable is the history of the discovery of halophiles. The studies aimed at isolating and characterizing the organisms capable of living in the extremely salty environments began in the late 19th century, but the evidence of their existence has been witnessed by mankind for several millennia (*25*). One of the earliest references, which dates back to around 2700 B.C., describes the salt production from sea water in one of the Chinese provinces and reports the occurrence of the red brines. The red brines may also be behind what was described as the first Plague of Egypt, where the waters of the Nile turned into blood. Aharon Oren describes many more accounts of the halophilic bacteria throughout history as well as first key discoveries in the field of halophile research in the first chapter of *Halophilic microorganisms and their environments* (*25*). It is curious that the modern era of halophile research originated in the Northern countries, which were heavily dependent on fishing and where spoilage of salted fish was becoming a big economical problem and the first halophilic bacteria to be isolated and studied in depth were obtained from salted fish.

Halophiles include a variety of organisms, both prokaryotic and eukaryotic, which are adapted to various levels of salt concentrations ranging from 0.2-5 M (*26*). Since biological membranes are water-permeable, halophilic organisms must keep their intracellular environment isoosmotic to the outside to avoid rapid loss of water. To do so, the halophiles adapted to use one of the two strategies (*27*). The salt-in strategy, used by *Halobacteriales* and *Haloanaerobiales*, is to maintain a high concentration of

intracellular (potassium) salt, and requires all of the cell components to be adapted to high salt concentration. The other strategy is to maintain low salt concentrations and synthesize or import organic solutes to maintain the osmotic pressure. While there is quite a bit of interest in the unique properties of the enzymes and solutes of halophiles and their potential uses in the industry, the majority of the efforts in the field of halophile research has been directed to better characterize the microbial diversity of the saline environments (*28*).

Thermophiles

The era of thermophiles began in 1969 with the discovery of *Thermus aquaticus* at the Yellowstone National Park (*3*). While other moderately thermophilic species (such as *Bacillus stearothermophilus*) had been described previous to this publication, this report was the first to point out that the usual enrichment of growth conditions to 55°C was not enough to find the more extreme thermophiles, which exhibit the optimal growth at above 70°C. The point was well made since, once discovered at Yellowstone, the strains of *Thermus* were isolated from a variety of natural (hot springs) and man-made (tap water) environments. The DNA polymerase from *Thermus aquaticus* was the first thermostable DNA polymerase to be purified, characterized and applied in the polymerase chain reaction (PCR), eliminating the need to add polymerase after each denaturation step (*29*). Since then a variety of DNA polymerases from other thermophilic organisms have been studied and are now being widely used in molecular biology (*Pyrococcus furiosis*-*pfu*, *Thermatoga maritima*-ULTima).

A few years later, the discovery of hyperthermophiles followed when Karl Stetter discovered *Methanothermus fervidus* from the boiling springs in Iceland. This obligate anaerobe was able to grow at temperatures up to 97°C. This finding inspired Stetter to look in hotter places and in 1981 he collected samples from the hot sea floor of Vulcano Island (Italy), where due to high pressure the water stayed liquid at temperatures above 100C. There he discovered yet another gem for his collection-*Pyrodictium*, a novel obligate anaerobe capable of living in temperatures up to 110°C. Another interesting discovery was that of a virus-sized archaeon, *Nanoarchaeum equitans,* which has one of the smallest genomes of 490,885 base pairs, 95% of which are predicted to code for proteins and stable RNA's. Surprisingly, *N. equitans*'s genome contains no information for the synthesis of amino acids, cofactors, nucleotides, or lipids, suggesting that its life cycle is completely dependent on that of its host, another archaean *Ignicoccus hospitalis*, thus making it the first example of a parasitic archaean. All in all, Stetter and colleagues discovered over 50 new species of hyperthermophiles, the majority of which belong to base branches of Bacteria and Archaea (*30*).

Part 2: Thermophiles: Challenges and Adaptations

Extremophiles embody a very diverse group of organisms that adapted to life in a variety of extreme conditions such as extreme pressure, extreme pH, high salt concentrations, and extreme temperatures, among others. These conditions present challenges to every aspect of the organism's existence, such as obtaining nutrients and oxygen, maintaining selective permeability of the cell membrane, the structural integrity of nucleic acids and proteins, and achieving the enzyme activities necessary to maintain

flux along metabolic pathways. To complicate matters further, many of these organisms, such as those living in deep-sea environments (with low temperature and high pressure) or hot springs (acidic pH and high temperatures), are confronted with the challenges of dealing with multiple extremes at once. The remainder of this review will address the challenges faced by thermophilic organisms and discuss the various adaptations the thermophiles employ to function in high temperature environments.

Membranes

One of the fundamental challenges faced by an organism growing at extremely high temperatures is how to maintain the normal fluidity of the membrane and retain its selective permeability. Biological membranes at their native growth temperature exist in a liquid crystalline state. The transition of the membrane into either the gel or the liquid state results in the disruption of many fundamental biochemical processes that occur within the membrane and, eventually, cell death. It has been proposed that the cells may be able to adjust certain properties of their membranes in order to increase or decrease the phase transition temperatures thus maintaining the liquid crystalline state over a wider temperature range (*31*). This part of the review will address the possible mechanisms used by the cells to regulate the fluidity of their membranes in response to temperature stress.

Lipids

Since lipids are responsible for maintaining the fluid mosaic of the membranes (*32*), their properties are obviously of importance to the stability of the membrane. It is interesting to note that the key difference in the membranes of the bacteria and the

archaeans, which are comprised to a large degree by various extremophiles, is in the nature of the lipids found in their membranes. The main component of the bacterial bilayer are the 14-18 carbon fatty acyl chains connected to the glycerol via an ester linkage, where the tails form the core of the membrane while the heads face the hydrophilic surface. The acyl chains may contain some combination of unsaturated bonds, methyl chains, and cyclohexane groups (*33*). In contrast to bacteria, the core of the archaean membrane bilayer is formed by the diether lipids consisting of two phytanyl chains connected to glycerol via an ether linkage. There are several advantages of the diether phytanyl chains compared to the ester fatty acyl chains in terms of stability. For one, the fully saturated phytanyl tails provide a much stiffer core and are thought to aid in packing, which also aids in decreasing the permeability of the membrane at high temperatures (*34*). Another benefit is the ether linkage, which is much more stable than an ester linkage, and that is crucial considering the additional challenges of extreme pH faced by many archaean hyperthermophiles. In the archaean acidothermophiles, the membrane is formed by a monolayer of tetraether lipids, formed by two fused diether lipids, which span the entire bilayer, thus providing additional stability and reducing the permeability of the membrane to protons (*35*). It was shown that liposomes containing archaean ether lipids are much more stable than those formed with ester lipids at high temperatures. They are also resistant to oxidation and hydrolysis, the effects of which are more pronounced at higher temperatures (*33, 36*). With that being said, there are psychrophilic archaeans like *Methanococcoides burtonii* (*37*), that are unable to function at high temperatures, even though their membranes contain diether phytanyls. There are

also multiple examples of extreme thermophiles among the bacteria that function just fine with the less stable ester fatty acyl membranes. This means that while the diether (and tetraether) lipids may add stabilization to the membranes of organisms at high (and low) temperatures, their existence alone does not explain the thermostability of the membrane of the extreme thermophiles.

There are some common mechanisms used by bacteria and archaeans to stabilize their membranes. For instance, when comparing thermophilic bacteria and archaeans to their mesophilic and psychrophilic counterparts, there is an increase in the ratio of the glycolipid over phospholipid. This may serve to increase the hydrogen bonding capacity on the surface of the membrane. A study of the effect of temperature on lipid composition in *Thermus aquaticus* reports that with the increase of growth temperature from 50°C to 75°C the cells responded with a 2.6-fold increase of the total lipid, strikingly, the increase in glycolipids was 4-fold (*38*). Similar results are reported by Adams *et al.* in the study of the lipid composition of the thermophilic alga *Cyanidium caldarium*: upon an increase of growth temperature from 20°C to 40°C, the total lipids increased by 33%, while the glycolipids increased by 90% (*39*). Oshima and Yamakawa report a novel glycolipid in *Thermus thermophilus,* which accounts for 70% of the total lipid. This number is much higher than the few percent reported for mesophilic bacteria (*40*) but corresponds well with numbers obtained for other thermophilic bacteria such as 64% for *Bacillus acidocaldarius* and 68% for *Sulfolobus acidocaldarius* (*41, 42*).

Elongation and various modifications of fatty acid tails are also believed to be important ways to control the fluidity of the cell membrane at higher temperatures. A

study of temperature variants of *Bacillus megaterium* reported an increase in the relative amounts of long-chain fatty acids compared to short-chain fatty acids as well in the ration of iso to anteiso fatty acids with the increase of growth temperatures (*43*). Another approach to regulate the fluidity of the membrane is to introduce cyclic molecules. In eukaryotes, this is achieved by varying the concentration of cholesterol in the membrane (*44*). However, bacteria and archeans do not produce cholesterols. Instead, they introduce cyclization into their fatty acyl (cyclohexane) or di- and tetraether lipids (cyclopentane). For instance, when comparing the ratios of acyclic: monocyclic: bicyclic C40 components in the *Thermoplasma*, grown at 59°C, and *Sulfolobus*, grown at 70°C, the proportions were found to be 65: 32: 2 and 30: 32: 38, respectively (*45*).

Souza *et al*. compared the effects of temperature on the wild type *Bacillus stearothermophilus* and a heat sensitive mutant, which was unable to maintain the integrity of its membrane (*46*). They showed that an increase in temperature resulted in an increase in the proportion of saturated fatty acids in the wild type *B. stearothermophilus*, while the mutant was unable to produce these changes. A study comparing the fatty acid composition of thermophilic, mesophilic, and psychrophilic chlostridia showed that the thermophilic bacteria produces more of the saturated straight-chain and branched fatty acids, while the mesophilic and psychrophilic bacteria contained larger portions of the unsaturated fatty acids (*47*). It is important to note that a series of studies that aimed to determine the effect of growth temperature on fatty acid composition agree that there is a variety of factors besides temperature that can influence

the lipid composition of the membrane. A study of *E. coli* lipid composition as a function of temperature showed that an increase in temperature resulted in an increase in proportions of saturated fatty acids. However, upon closer examination, it was found that the growth rate, growth phase and the composition of growth media had a significant effect on the lipid composition independent of the growth temperature (*48*). Similar conclusions were reached in the study interrogating the effects of temperature on the lipid composition of *Pseudomonas fluorescens* (*49*). Gill and Suisted, when comparing the effects of temperature on the proportion of the unsaturated fatty acids, reported that a number of bacterial species showed no significant alterations in the fatty acid composition with changes in temperature (*50*). They concluded that since these alterations are not necessary for the viability of these organisms, any changes that are seen in some species may be nothing more than a reflection of temperature effects on the activity of the enzymes responsible for fatty acid synthesis and degradation.

Membrane-associated proteins

When discussing the elements that allow the cell to maintain the integrity of its membrane at elevated temperatures it is easy to overlook the fact that lipid, while being an essential constituent of the bilayer, is by no means the only factor contributing to its thermal stability. In fact, 60-80% of the bacterial membrane is accounted for by integral and peripheral proteins, including a variety of ion channels and enzymes responsible for electron transport (the numbers are similar for archaean membranes as well) (*51, 52*). Thus, the stability of the membrane is, to a large degree, a consequence of the thermostability of its protein components.

While the sources of protein thermostability will be discussed later in the review, it is important to emphasize the potential importance of the membrane-associated proteins in coping with the thermal stress, and the role of the membrane lipids on the structure and function of these proteins. A multitude of studies have been done to elucidate the nature of the interactions between the lipids and the integral proteins in the membrane (*53, 54*). From electron spin resonance (ESR) experiments we know that the proteins in the membranes are surrounded by a fast-exchanging shell, or annulus, of lipids, similar to the way the soluble proteins are surrounded by solvent. There are also more specific non-annular interactions, which occur when the lipids bind between the α-helices of the transmembrane domains as well as at the protein-protein interfaces. The evidence of these interactions is seen in the multiple crystal structures of the transmembrane domains of proteins such as bacteriorhodopsin and cytochrome c oxidase, which show well-resolved lipid molecules (*54*).

The lipids interacting with the proteins as well as the proteins themselves undergo certain adjustments to maintain the integrity of the membrane, so it seems logical that certain properties of the membrane lipids, such as the level of unsaturation or the length of the tail (which determines membrane thickness) and nature of the head group, would have a significant effect on the protein structure and function. For example, Wisdom and Welker showed that the thermostability of an integral enzyme NADH oxidase and a peripheral enzyme alkaline phosphatase of *Bacillus stearothermophilus* increased with an increase in temperature (*55*). For alkaline phosphatase, this increase in thermostability was shown to be the result of its association

with the membrane, since the growth temperature did not affect the intrinsic thermostability of the enzyme (which is lower than the highest growth temperature). At the same time, the proteins can influence the stability of the membrane by restricting the mobility of the lipids, as well as, to some extent, dictate the thickness of the membrane around them. For instance, if the thickness of the protein is greater than the thickness of the membrane, the membrane lipids will attempt to match it by stretching their tails. On the other hand, if the membrane is thicker than the inserted protein, the tails may splay or tilt to accommodate the protein. The study of the temperature effect on the membrane of *Bacillus stearothermophilus* showed that an increase in temperature resulted in formation of more stable protoplasts and, notably, it also resulted in an increase in the protein to lipid ratio (*55*). It is possible that the higher stability was due to the increase in the proportion of the proteins that have a stabilizing effect on the membrane (potentially via thickening of the membrane and improving the lipid packing). Toman *et al*., upon examining different fractions of the cytoplasmic membrane of *Bacillus subtilus*, reported that one of the fractions possessed higher fluidity compared to that of the crude membrane. Since the two fractions had an identical fatty acid composition, the authors attributed the increase in fluidity to the decrease in protein content (*56*). In contrast, Rilfors *et al*. reported a 3-fold decrease in protein to lipid ratio as a function of the increase of growth temperature in *Bacillus megaterium* temperature variants (*43*). Curiously, there were large variations in the amounts of certain proteins when comparing the psychrophilic, mesophilic, and facultative and obligate thermophilic variants. A study of the growth temperature effects on the membrane components of *Pseudomonas*

aeruginosa revealed that upon increasing the temperature, some outer membrane proteins increased or decreased in concentration, while others remained unchanged (*57*). It was noted that one of the proteins to increase at higher growth temperatures was protein H1, which when associated with the lipopolysaccharides, stabilizes the outer membrane.

The results of the above studies suggest that there is no general correlation between the proportion of the total membrane protein and the stability of the membrane. It is, however, entirely possible that in the cases where we see a large increase in the protein content with an increase in temperature, it is due to the increase of the proportion of proteins that act to stabilize the membrane. Similarly, in the cases such as that of *B. megaterium*, the large decrease in protein content with the increase in temperature may correspond with the large decrease in the amount of the membrane-destabilizing proteins. And, since some proteins have a requirement for specific fatty acids, it is also possible that some changes in the lipid composition seen upon the increase in the growth temperature are a function of changes in the protein composition and have no intrinsic effect on the membrane stability.

Nucleic acids

Intrinsic stabilization

It is essential for any living organism to ensure the integrity of its genetic information. Thus, stabilization of the DNA against denaturation and degradation (depurination and hydrolysis of the phosphodiester linkage) is critical for organisms living in high temperature environments. Since GC base pairing provides an additional

hydrogen bond that could aid in stabilizing the DNA, it is easy to assume that the stability of nucleic acids necessary for thermophilic organisms is achieved through the high GC content. This idea was supported by studies that reported unusually high GC content in the genomes of some thermophiles, for instance the GC content in *Thermus thermophilus* genome is 69% (*58*). Elevated GC content is also found when comparing some genomes of thermophiles and mesophiles from the same genus. McDonald *et al*. found that *B. stearothermophilus* has a 9% higher GC content than *B. subtilis* (*59*). However, the authors also noted, that the high GC content strongly correlates to the amino acids that are prevalent in the thermophilic protein, thus it is not clear whether the GC-rich codons were evolutionary beneficial because they afforded better stability to the DNA or because they resulted in a higher stability of the encoded protein. It also appears that the abnormally high GC content is not common for the majority of thermophiles. For instance, after analyzing the genome sequences of 15 thermophilic archaeans and bacteria, Grogan concluded that there is no correlation of the GC content with the growth temperature and that none of the thermophiles appear to have unusually high GC contents (*60*). Galtier and Lobry reached the same conclusion after analyzing the GC content in the genomes of 764 prokaryotic species as a function of the optimal growth temperature (*61*).

Since the high GC content cannot explain the enhanced stability required for the DNA of thermophiles, the question still remains whether the thermophilic DNA possesses any additional intrinsic stability or whether it is stabilized entirely by the extrinsic factors. Kawashima *et al.* found that it is not the nature of the individual

nucleotides in terms of the GC content, but the purine (R) /pyrimidine (Y) content of the dinucleotides that may speak to the degree of the DNA stability in thermophiles (*62*). The authors showed that the increase in optimal growth temperature correlates with a shift from the predominance of the YR and RY dinucleotides to the YY and RR dinucleotides. It is thought that the DNA is most flexible at the YR and RY positions, because of clashing of the tilted bases of different size, while the RR and YY afford more stability to the DNA through better base stacking (*63*). Nakashima *et al.* showed that not only the nature of the dinucleotide as a RY/YR or RR/YY, but also which purine or pyrimidine is used at each position determines the stability of the DNA (*64*). And while the high overall GC content is not the answer for the DNA stability problem in thermophiles, the GC content of the non-coding functional RNA from thermophiles is higher than that of mesophiles, suggesting that the GC base pairing may play an important role in stabilizing the stems in the three-dimensional structures of tRNA and rRNA (*61*).

Another curious observation about the genomes of thermophiles is that they show a large enrichment in purines, which has little to do with the thermostability of RNA, but is thought to reduce the interactions between mRNA molecules (*65*). These interactions are likely to initiate by the "kissing" between the loops of the two mRNA molecules and would impede mRNA-tRNA interactions and result in less efficient protein synthesis. The formation of double-stranded RNA may also trigger an unwanted immune response, such as gene silencing (*66*). Since "kissing" involves a release of water molecules, which are ordered around the exposed bases, it is associated with a large favorable

change in entropy. At higher temperature, the effect of the entropic component contribution becomes more pronounced, making the mRNA loops even more sticky, which may explain the evolutionary pressure to select for the purine-loading of the mRNA loops in thermophiles.

There are several studies that address the role of posttranscriptional modifications in the thermostability of tRNA of thermophiles. The posttranscriptional modifications of tRNA nucleosides are common to all organisms and play important roles in a variety of processes associated with the regulation of protein synthesis, such as fine-tuning the efficiency of tRNA decoding, maintaining the reading frame, and improving the fidelity of protein synthesis (*67*). However, there is evidence that thermophiles also evolved certain modifications, which result in thermal stabilization of their tRNAs. One of the earlier reports by Agris *et al*. showed that the methylation of tRNA in *B. stearothermophilus* increased by 40% when the cells were grown at 70°C compared to 50°C (*68*). Several years later, Watanabe *et al*. reported that the thermal stability of the tRNA from *T. thermophilus* increased with the growth temperature (*69*). The increase in thermostability corresponded with the increase in 5-methyl-2-thiouridine that replaced ribothymidine in the TψC loop of tRNA, which is thought to stabilize the interaction between TψC and DHU loops, thus stabilizing the tRNA molecule. A more recent study by Kowalak *et al*. showed that the thermostability of the tRNA from an archaeon *Pyrococcus furiosus* is roughly 15-20°C higher than what can be predicted from the GC content, and attributed this phenomenon to the posttranscriptional modification of the tRNA (*70*). The authors reported that the levels of modification

increased with the increase in growth temperature and identified twenty-three modified nucleotides, some of them unique to the archaeal hyperthermophiles. One of modified nucleosides, 5-methyl-2-thiouridine, is found preferentially at tRNA position 54, which was also shown to be an important site for thermal stabilization of tRNA by modified nucleosides in *T. thermophilus* and *E. coli* (*71, 72*).

Extrinsic stabilization

After discussing the possible modes of stabilization of DNA and RNA in thermophiles, it appears that unlike tRNA, which can be stabilized via posttranscriptional modifications, the thermostabilizaton of the DNA and other RNAs depends on extrinsic factors. For instance, it's been suggested that the integrity of the nucleic acids in thermophiles may be maintained by various cations, such as sodium, potassium and magnesium salts and polyamines (*60*). Marmur and Doty showed that the melting temperature of DNA can be increased by upwards of 20°C by increasing the concentration of potassium chloride to 1M (*73*). Hensel and König found that the concentration of potassium in the mesophilic compared to the thermophilic members of *Methanobacteriales* increased from 0.4 to 1M with the increase of the optimal growth temperature and showed that high salt concentrations aid in the stabilization of thermoliable proteins from thermophilic methanobacteria (*74*). The authors also determined that the potassium salt had a large effect on the stability of the DNA, which is important considering the very low GC content of the methenobacterial genome. However, the most dramatic increase in DNA stability was seen only up to 300 mM salt, which means that the thermophiles containing close to 1M salt concentrations would

have no measurable advantage in terms of DNA stability over the mesophiles containing 0.4 M salt. It was also noted that even at high potassium salt concentrations the melting temperature of the DNA was still below the upper growth temperature limit of the thermophiles, suggesting that other means of extrinsic DNA stabilization must also be employed.

Nazar *et al*. showed that the structural stability of the 5-S rRNA of *Thermus aquaticus* is highly dependent on the presence of native salt concentrations (*75*). The authors showed that at 10mM K^+, the 5S rRNA from *T. aquaticus* and *E. coli* showed roughly the same melting temperature, however, at the native *T. aquaticus* salt concentrations of 91mM Na^+, 130mM K^+ and 59mM Mg^{2+}, the T_m for *T. aquaticus* 5-S rRNA increased by 20°C, while the T_m for *E. coli* 5-S rRNA increased only by 10°C, suggesting that the salts may play a more significant role in the stabilization of the nucleic acids of the thermophiles compared with mesophiles. The authors also noted that the stability of the 5-S rRNA from *B. stearothermophilus*, when assayed under the same conditions (in the presence of Mg ions), was significantly greater than that of *E. coli*, which is contrary to what was reported for these molecules in the absence of magnesium (T_m difference of 1.5°C) (*76*), suggesting that Mg^{2+} plays a particularly important role in stabilizing rRNA from thermophiles. Similarly to the results described above concerning the salt stabilization of methanobacterial DNA, Nazar *et al.* concluded that although the native salt concentrations significantly increase the melting temperature of the 5-S rRNA, this increase is not enough for the 5-S rRNA to be stable on its own at the optimal growth temperature and suggested that it may be further

stabilized by other extrinsic factors or the rRNA's, proteins, and cations within the ribosomes. Marguet and Forterre conducted a study on covalently closed circular DNA and its susceptibility to thermodenaturation and thermodegradation and found that the supercoiled DNA does not denature up to 107°C, as long as the backbone remains intact. The authors found that heat-induced hydrolysis of the phosphodiester bonds is a bigger issue for thermophiles. However, they determined that thermodegradation can be greatly inhibited in the presence of physiological concentrations of potassium and magnesium salts (*77*).

Reverse DNA gyrases may provide another means for protecting the plasmids in hyperthermophiles. Reverse DNA gyrase was first isolated from *Sulfolobus acidocaldarius* and was later found to exist in all hyperthermophiles (*78, 79*). This enzyme was initially thought to stabilize the DNA by introducing positive supercoiling, which increases the number of links between the two strands of DNA. However, later studies found that the presence of reverse gyrase does not always correlate with the increase in the positive supercoiling (*80*). Other studies have shown that reverse gyrase was critical for optimal growth of the hyperthermophiles at their physiological temperatures (*81*). The results obtained by Kampmann and Stock suggest that the reverse DNA gyrase binds at the site of nicked DNA and acts as a DNA chaperone by preserving the structural integrity of the DNA at the site of the double strand breakage (*82*). Similar results were obtained by Napoli et al. who showed that the reverse gyrase was recruited to the site of the UV-induced DNA damage (*83*). These findings suggest

that the reverse DNA gyrase may indeed be important for the stabilization of the plasmid DNA via protection of the nicked DNA regions.

Friedman *et al.* showed that the ribosomes from *E. coli* and *B. stearothermophilus* were greatly stabilized (by 27 and 17°C, respectively) in the presence of 10mM Mg^{2+} (*84*). The authors also showed that various polyamines have different stabilizing effects on the ribosomes and rRNA of the thermophilic and mesophilic bacteria. For instance, spermidine is more effective in stabilizing the ribosomes of *E. coli*, while putrescine is more effective in stabilizing the ribosomes of *B. stearothermophilus*. With regard to rRNA, putrescine had no effect on rRNA from *E. coli*, and a modest stabilizing effect on the rRNA on *B. stearothermophilus*, while spermidine resulted in a roughly 10°C increase in the melting temperatures for both.

The polyamines, such as the first-discovered spermidine, spermine and putrescine, are ubiquitous to almost all living cells and play a variety of roles in the cellular regulation including control of macromolecule synthesis, cell division, and apoptosis (*85*). Polyamines are polycations (at physiological pH) and can interact electrostatically with polyanionic macromolecules, however they are unique in that the positive charge is distributed along the entire length of the molecule. It's been shown that the polyamines can interact with the DNA, induce structural changes and increase DNA stability (*85*). The majority of mesophilic organisms produce a number of standard polyamines, while the thermophilic organisms also produce a number of unusual polyamines which can be classified as branched or extremely long (*86*). Oshima outlined several observations concerning unusual polyamines in thermophiles

(particularly in the extreme thermophile *Thermus thermophilus*), such as an increase in ratio of the branched polyamines compared to spermidine in cells grown at higher temperatures, the enhancement in stability of DNA and RNA in the presence of unusual polyamines (proportional to the number of amino nitrogen atoms), and the requirement for unusual polyamines for the polypeptide synthesis at high temperatures (*86*). Oshima also noted that the polyamines are not essential in the extreme halophiles where the intracellular concentrations of magnesium and potassium are extremely high. These findings suggest that polyamines play a very important role in maintaining the integrity of both DNA and RNA (as well as proteins) in thermophiles, especially when the intracellular concentrations of the mono- and divalent cations are not abnormally high compared to that of mesophiles.

Small DNA binding proteins provide yet another way to stabilize the DNA in thermophilic organisms. Thermophilic, as well as mesophilic, prokaryotes contain histone-like proteins that share similarities to the eukaryotic histone proteins in that they are small in size and are positively charged at neutral pH. In 1975, Searcy described the purification of a histone-like protein from *Thermoplasma acidophilum*, which was highly basic and had an amino acid composition similar to that of eukaryotic histones (*87*). Stein and Searcy later showed that this protein was able to stabilize the DNA against thermal denaturation by about 40°C under physiological conditions and suggested that it acted to prevent the strand separation of the DNA under denaturing conditions (*88*). Reddy and Suryanarayana identified four histone-like proteins in *Sulfolobus acidocaldarius*, three of which stabilized the DNA against thermal

denaturation by 15-30°C (*89*). It is particularly interesting that these proteins occur in large numbers (90% by weight of the nucleoid) and their helix-stabilizing properties were DNA-specific, since they had no effect on the stability of the double-stranded RNA.

In addition to the stabilization of the DNA by salts, polyamines and DNA binding proteins, some thermophilic organisms have found yet other ways to protect their genetic information. For instance, Ohtani *et al*. reported that *Thermus thermophilus* is a polyploid bacterium and estimated that it contains 4-5 copies of its chromosome as well as a megaplasmid. The authors suggested that polyploidy may aid in the maintenance of the genetic information and repair through recombination in the event of thermal damage to the DNA molecules. It is interesting that polyploidy is also observed in the closely related bacterium *Deinococcus radiodurans*, whose extreme radioresistancy has been attributed to efficient repair machinery and interchromosomal recombination (*90, 91*). All in all, it appears that thermophiles have successfully developed various strategies to protect their DNA and RNA from thermal denaturation and degradation. The DNA helices of thermophiles are stabilized though the purine-purine and pyrimidine-pyrimidine dinucleotides, as well as by extrinsic factors like salts, polyamines and DNA binding proteins. The mRNAs are stabilized by higher GC contents of the stems as well as by salts and polyamines, while the thermostability of the tRNAs is achieved by introduction of modified nucleotides at key positions.

Proteins

Proteins perform a myriad of roles in a living cell: they are responsible for transport, signaling, and catalyzing numerous metabolic reactions, to name a few. And their ability to perform these roles is highly dependent on their ability to preserve their three-dimensional structure. Retaining protein structure and (enzyme) activity can be difficult even at normal temperatures due to proteolysis and deamination, and at high temperatures these processes occur at a more rapid rate. Since the discovery of thermophiles and hyperthermophiles, a large number of proteins from these organisms have been studied in an attempt to understand the basis of their thermostability. As a rule, the sequences of homologous proteins from mesophiles and thermophiles have a high degree of similarity and their three-dimensional structures are superimposable (*92*). Based on the observation that most of these proteins retain their intrinsic characteristics, including thermostability, when expressed in *E. coli*, we know that the sources of their thermostability must be encoded into their amino acid sequence (*93*). Although there are quite a few examples of proteins from thermophiles that are not intrinsically stable, these proteins can be stabilized by a variety of external factors such as high salt concentrations, various compounds like cyclic 2,3-diphosphoglycerate, and species-specific solutes (*94*). However, for the purposes of this review, we will only consider intrinsically stable proteins. We know that all proteins consist of the same 20 amino acid, so how do the proteins of thermophiles and extreme thermophiles retain function at near or above the boiling point of water, while the proteins from mesophiles irreversibly denature long before they reach those temperatures?

The stability of a protein can be illustrated by a stability curve (Figure 1-1A), which is derived from the variations in the entropy and enthalpy of unfolding as a function of temperature (47). The curve is described by the modified Gibbs-Helmholtz equation (Equation 1-1),

$$\Delta G(T)=\Delta H^\circ - T\Delta S^\circ + \Delta C_p(T-T^\circ-T\ln(T/T^\circ)) \quad (1\text{-}1)$$

where ΔG is the unfolding free energy, T° is the reference temperature, ΔS° and ΔH° are the changes in entropy and enthalpy at the temperature T°, and ΔC_p is the change in heat capacity associated with the unfolding. The curvature of the plot is defined by $(-\Delta C_p/T)$, which is negative at all temperatures, because ΔC_p is positive at all temperatures. The slope of the curve is defined by (-ΔS), and the curve has one maximum, ΔG_s, which occurs at T_s, where ΔS=0. T_m and T_m' designate the high and low melting temperatures at which ΔG=0.

If we consider the three parameters (ΔH°, ΔS° and ΔC_p) that define the unfolding free energy at any given temperature, we can see that there are three possible ways to achieve the thermostabilization of a protein (*95*). One is the consequence of reducing the change in entropy ΔS, which results in a higher value for T_s. This would in effect maintain the same maximum of the ΔG, but shift it to a higher temperature, which would translate into a higher value for the T_m (Figure 1-1 B in red). The second possibility is that the protein is stabilized over the entire temperature range through an increase in the change in enthalpy (ΔH), resulting in higher maximum for ΔG, as well as the higher melting temperature (Figure 1-1 B in green).

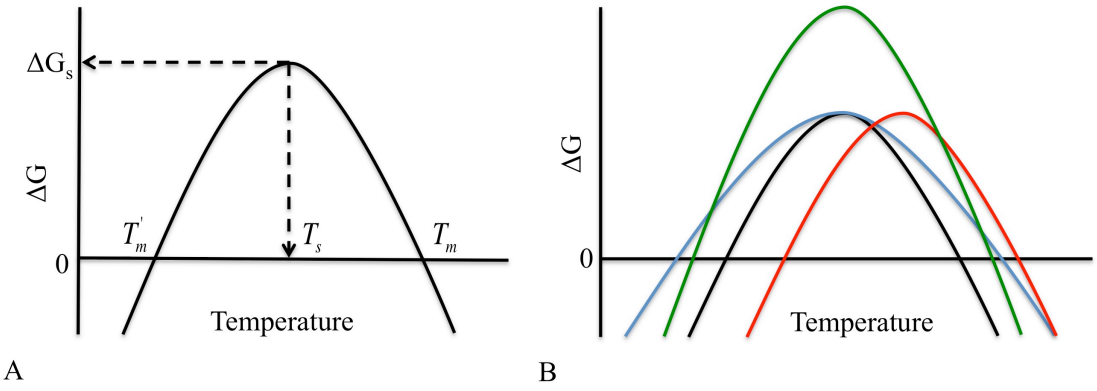

Figure 1-1. Stability curves for hypothetical proteins. (A) Stability curves for a hypothetical protein. T_m and T_m' designate the high and low melting temperatures at which $\Delta G=0$. The curve has one maximum, ΔG_s, which occurs at T_s. (B) Modes for increasing the thermostability of a protein. Black line represents a stability curve for a typical protein from a mesophile. In red, green and blue are the stability curves for a hypothetical protein from a thermophile.

Finally, a protein can be stabilized via a more shallow dependence of the unfolding free energy on the temperature due to a reduced ΔC_p (Figure 1-1 B in blue). In this case the ΔG maximum remains the same, but the T_m is increased.

There is evidence that all three methods in various combinations are seen in nature. In their review *Lessons in stability from thermophilic proteins*, Razvi and Scholtz compiled and analyzed the available data for 26 sets of homologous proteins from thermophiles and mesophiles to determine the thermodynamic mode of stabilization used in each case (*96*). They determined that 77% of the thermophilic proteins in the study achieve higher stability by increasing the intrinsic stability at all temperatures, alone and in combination with other stabilizing effects. The group of proteins (5/26) that are stabilized exclusively by the higher overall ΔG includes the HPr proteins from *Bacillus stearothermophilus* (BstHPr) and *Bacillus subtilus* (BsHPr). The two proteins share high sequence identity (72%), and their three-dimensional structures are highly superimposable (*97*). The values of the ΔC_p are the same for the both proteins, and those for T_s vary by less than one degree. There is, however, a 15°C difference in the melting temperatures between the two proteins which resulted from the 3 kcal/mol increase in the maximal stability (ΔG_s) value for the BstHPr compared to that of BsHPr (*98*). It is of interest to note that the stability at the physiological temperature is the same for these two proteins (4.8 and 5 kcal/mol).

The overall thermostability of a protein may be achieved via several different routes. Li *et al*. outlined several interesting differences in the amino acid sequences of archaeal histones from mesophile and thermophiles, which may be responsible for

higher melting temperature (*99*). After analyzing the sequences of 19 histones, the authors found that asparagine 14, which can suffer deamination at high temperatures, is not present in the histones from hyperthermophiles, with one exception, but occurs in the histones from a mesophile and a moderate thermophile. They also noted that the bulky aromatic residues (phenylalanine and tyrosine), which could potentially increase packing and reduce flexibility, are seen in histones from hyperthermophiles, but not in histones from mesophile and moderate thermophile. Another interesting insight comes from a comparison of the crystal structures of histones from hyperthermophile *Methanothermus fervidus* and mesophile *Methanobacterium formicicum*. An analysis of the hydrophobic cores of the two histones reveals a cavity, which is more solvent accessible in the mesophilic histone. The inside of the cavity is partially filled with three residues (31, 35, and 64), which exhibit a high variability in a sequence alignment. The histone from *M. formicicum* has two small hydrophobic (A31 and V64) and one polar (K35) residue in these positions, while the histone from *M. fervidus* contains V64, together with I31 and M35. The mutational analysis of A31I and K35M substitutions in the histone from the mesophile showed 11 and 14°C higher melting temperatures, while the reciprocal mutations, I21A and M35K in the thermostable histone reduced the melting temperatures by 4 and 17°C respectively. These results along with the observation that majority of the histones from hyperthermophiles have large hydrophobic residues at two of these three positions suggest that the size and hydrophobicity of these residues are important for the stabilization of these proteins.

Combining the increased ΔG with the reduced ΔC_p is the most common way for

the proteins from thermophiles to achieve a higher melting temperature (8 out of the 26 examples). An excellent example pair from this group are the ribosomal proteins L30e from *Saccharomyces cerevisiae* and *Thermococcus celer*. The two proteins are highly similar, but *T. celer* has a melting temperature that is higher than that of the yeast L30e by almost 50°C due to the overall increase in stability by 8.5 kcal mol^{-1} as well as a 1.2 kcal $K^{-1}mol^{-1}$ decrease in ΔC_p (*100*). Stabilization of the thermophilic proteins via the decrease in ΔC_p alone appears to be another commonly used strategy. Razvi and Scholtz found that in five out of the 26 pairs of homologous proteins in their study, the proteins from thermophiles showed broadened stability curves (*96*). This group contained examples of small DNA binding proteins as well as large enzymes.

There are different opinions as to the origins of the reduced of ΔC_p in proteins from thermophiles compared to proteins from mesophiles. Since we know that the hydration of the hydrophobic core contributes to ΔC_p, some attribute the change in ΔC_p to the change in the solvent-accessible surface area upon unfolding (ΔASA). For instance, Robic *et al*. believe that the differences in ΔC_p between a pair of homologous ribonuclease H enzymes from *E. coli* and *T. thermophilus* stem from the differences in ΔASA for the two enzymes (*101*). The authors designed and expressed two chimeras, one of which has the core of *T. thermophilus* RNase H and the outside shell of *E. coli* (TCEO) and the other that has an *E. coli* core and the outside of *T. thermophilus* (ECTO). TCEO displayed higher thermal stability and had the ΔC_p value comparable to that of the wild type *T. thermophilus* RNase H. Based on the parameters they obtained from the thermal and chemical denaturation profiles, the authors proposed that the core

of *T. thermophilus* RNase H may retain more structure compared to that of the *E. coli* enzyme, resulting in a lower ΔASA and thus a lower ΔC_p. The group followed up on this by obtaining the CD spectra of thermally denatured RNase H enzymes from *E. coli* and *T. thermophilus*, which suggested that unfolded *T. themophilus* RNase H retained more structure than *E. coli* RNase H (*102*).

However, some find that differences in ΔASA may not be the best explanation for the large differences in ΔCp seen between the homologous proteins from mesophiles and thermophiles, which have similar structures and are expected to have similar ΔASA. Lee *et al*. argue against this because if some residual structure were retained in the thermally unfolded state, it would in effect reduce the free energy difference between native and denatured states and make the thermophilic proteins appear less stable (*100*). Instead, the authors suggest that, according to the electrostatic model (*103*), stronger electrostatic interactions may be able to explain the decrease in ΔC_p seen in the L30e ribosomal proteins from yeast and the thermophile *T. celer*. They used the *T. celer* L30 protein as a model system to investigate the role of specific electrostatic interactions by engineering six charge-to-neutral mutants designed to disrupt the potentially important electrostatic network and found that in five out of six cases the mutations decreased the thermal stability of the protein and increased the ΔC_p values. The authors also found that the thermally denatured state retained more structure than that achieved with guanidine, suggesting that different proteins may react differently to various methods of denaturation. They also pointed out that the wild type and mutants showed the same level of structure in the denatured state (obtained by the same method), suggesting that

the increases in ΔC_p were indeed due to the disruption of electrostatic interactions, and not to the changes in ΔASA.

Razvi and Scholtz found no examples where the shift in T_s is used as the only means of stabilization, although there are several examples of proteins that use higher T_s in combination with higher overall stability and/or decrease in ΔC_p (*96*). An interesting pair of proteins where we see all three modes of stabilization are the archaeal histone proteins from *Methanobacterium formicium* and *Methanothermus fervidus*, which were discussed earlier *(99)*.

Although we can experimentally determine which components of the unfolding free energy (equation 1) are perturbed to yield an increase of the melting temperature, we still do not entirely understand how these perturbations are encoded into the amino acid sequences of thermostable proteins. The majority of our knowledge on this subject comes from the comparisons of three-dimensional structures of homologous pairs of proteins from mesophiles and thermophiles. The overall pattern that emerges from these comparisons is that in the thermostable proteins there is an increase in the number of non-covalent interactions (an increase in the number of hydrogen bonds and stronger networks of electrostatic interactions within the protein, as well as in the subunit interfaces for multimeric proteins), an increase in compactness (resulting from better hydrophobic packing and shortening and increase of proline content in the loops, less solvent-accessible cavities), and a reduced number of destabilizing features (a lower content of thermolabile amino acids (asn, gln, cys, met) as well as the replacement of amino acids that have unfavorable conformations) (*94*). It is likely, however, that many

of the changes in the sequence of the homologous proteins accumulated throughout the course of evolution are of little consequence for the thermostability of a protein. It is also important to remember that the amino acid content of the bulk protein is strongly dependent upon the GC content of the genome (*104*). Thus, when comparing two proteins from a mesophile and thermophile with drastically different genome CG content, the majority of the differences in amino acid composition is likely to reflect the differences in the genomic GC content, not the thermal adaptations of the protein. If this is the case, we are left trying to locate a handful of changes against a large background of neutral mutations. However, as we can see from the studies presented above, we can successfully identify some of the elements important for the thermostability of a particular protein pair through a thorough analysis of amino acid sequences and three-dimensional structures in combination with mutagenesis studies.

Enzymes

The temperature effect on the enzymes from thermophilic organisms is multifaceted, since in addition to thermostability we also have to consider the temperature dependence of the two fundamental properties of the enzymes: substrate affinity and catalytic activity. Yet another level of complexity is added for enzymes that are subject to allosteric regulation, since this process is also temperature-dependent (*105, 106*). Over the years, enzymes from thermophiles have been rigorously studied in an effort to understand the underlying principles of protein stability and thermoactivity, and for their potential application in various industrial processes.

It has been noted by Jaenicke and Somero, that the specific activities of the enzymes from thermophilic organisms are much lower at room temperature than those of the homologous enzymes from mesophiles, however, at their respective physiological temperatures, their activities are comparable (*107, 108*). These observations are curious, since, in most cases, the three-dimensional structures of homologous proteins from mesophiles and thermophiles are very similar, the catalytic residues, as well as other residues in the active site, are conserved, and the catalysis occurs via the same mechanism (*93*). What is also notable is that in many mesophilic/thermophilic enzyme pairs the enzyme from the thermophile displays higher rigidity at mesophilic temperatures, but becomes more flexible at higher temperatures, so that the flexibilities of the two homologous enzymes are comparable at their respective native temperatures (*109*). For instance Bonisch *et al.* showed by using FTIR spectroscopy and hydrogen/deuterium exchange experiments that the adenylate kinase from hyperthermophilic archaean *S. acidocaldarius* is more rigid compared to adenylate kinases from porcine and rabbit muscle at 20°C, as evidenced by narrow bandwidth in the FTIR spectra and low H/D exchange rate (*110*). However, as the temperature is increased to and above the native temperature of *S. acidocaldarius* (75-80°C), the enzyme attains similar flexibility to what is seen in the mesophilic enzymes at their native temperature. Similar results are described by Zavodszky *et al.* for the 3-isopropylmalate dehydrogenases (3IPMDH) from *Thermus thermophilus* and *E. coli* (*109*). The H/D exchange experiments show that *T. thermophilus* 3IPMDH is more rigid

than the *E. coli* enzyme at room temperature, however, at their respective native temperatures the two enzymes showed almost identical flexibilities.

Since it is accepted that a certain level of flexibility is required for catalysis, a popular approach to rationalize the observations discussed above is to conclude that the low activity observed in the enzymes from thermophiles at mesophilic temperatures is due to their higher overall rigidity. This rigidity appears to be a requirement for the thermostability of the enzyme and is alleviated at higher temperatures, allowing the enzyme to achieve the high catalytic activity that is seen in mesophilic enzymes at their native temperatures. For example D'Auria *et al*. showed that for β-glycosidase from *S. solfataricus* the addition of 1-butanol at low temperatures resulted in an increase in activity (*111*). The CD and FTIR spectra showed no disruption in the secondary or tertiary structure of the enzyme in the presence of the alcohol, while the time-resolved fluorescence data suggested that the enzyme became more flexible. The authors concluded that the increase in flexibility resulted in an increase in activity of the β-glycosidase at lower temperatures. Similar behavior was seen in triosephosphate isomerase from *Thermotoga maritima*, where at low temperatures the addition of guanidinium hydrochlodide results in a 180% increase in activity (*112*). As the temperature increases, this activating effect is gradually diminished until it disappears completely at the native temperature of the enzyme.

There are numerous examples where the enzymes from thermophiles exhibit higher rigidity compared to that of the enzymes from mesophiles. It has also been noted that what we see in nature, is that the activity of the enzyme is inversely proportional to

its thermostability and the native temperature of the organism (*93, 113*). However, is it reasonable to conclude that rigidity is synonymous with thermostability and that the thermostability of the enzyme is always increased at the expense of its activity? It appears that the answer is no on both accounts. The evidence that refutes the notion that the enzyme must be rigid to be stable comes from the amide hydrogen exchange experiments performed on the rubredoxin from *Pyrococcus furiosis*, one of the most stable proteins known to date (*114*). The data show that the exchange rates for all amide hydrogens at 28°C occur on a millisecond time scale and are similar to the rates observed in the mesophilic proteins. Lazaridis *et al.* found that the molecular dynamics simulations performed on the rubredoxins from *P. furiosis* and mesophilic *Desulfobrio vulgaris* exhibit similar dynamic behavior (*115*). While the RMS residue fluctuations are slightly smaller in the protein from the hyperthermophile, these minor differences do not provide a justification for the low activity seen in *P. furiosis* enzyme at room temperature. The authors also suggested that there is not a fundamental reason for the correlation of the thermostability with the rigidity. And at the same time, flexibility should not be considered detrimental to the stability of the protein, since the greater flexibility would imply an increase in the conformational entropy and would result in a more thermodynamically stable protein.

We can now argue, based on the example of rubredoxins, that the rigidity of the proteins is not absolutely required for their thermal stability, although there are numerous examples where the two correlate. However, we are still left with the question of whether or not the thermostability is achieved at the expense of the activity of the

enzyme, and on a more general note, whether the thermostability and the activity of the enzyme are co-dependent. Although the most prevalent trend in nature is that homologous enzymes display similar activities at their respective native temperatures, and the specific activities of the enzymes from thermophiles are much lower at mesophilic temperature compared to the those of the enzymes from mesophiles, there are some examples where the enzymes from thermophiles display low temperature activities that are similar or even higher than those of the mesophilic enzymes. Ichikawa and Clarke isolated and characterized a protein repair enzyme L-isoaspartyl methyltransferase from *Thermotoga maritima*, which is extremely thermostable and exhibits specific activity that is only 4-fold lower than that of the homologous mesophilic enzymes at lower temperature (*116*). At the native temperature, the specific activity of the enzyme from *T. maritima* is 18-fold higher than that of the mesophilic enzymes at their respective native temperatures. This increase in activity at native temperatures makes perfect sense considering the function of the enzyme in protein repair, since the elevated temperatures result in a higher rate of protein damage (in this case deamination of asparaginyl and isomerization of aspartyl residues). Similar results were obtained for indoleglycerol phosphate synthase and phosphoribosyl anthranilate isomerase from *T. maritima* (*117, 118*). Both enzymes are extremely thermostable and show higher k_{cat} values at native temperatures compared to the enzymes from *E. coli*. However, considering that both enzymes also show a much stronger substrate affinity at the native temperatures, the resulting k_{cat}/K_m values for *T. maritima* enzymes compared to the *E. coli* enzymes are not only an order of magnitude higher at the native

temperatures, but also several-fold higher when compared at 25°C.

The above examples suggest that the thermostability of the enzyme does not necessitate low activity at mesophilic temperatures. Furthermore, the results from numerous directed evolution experiments suggest that it is possible to independently enhance the stability of the enzyme and its activity at low temperatures, as well as obtain variants of the enzyme, that combine both features. But if thermostability and high activity are not mutually exclusive, why is it then, that in nature, we see the enzymes from thermophiles that are not super active at their native temperatures, and the enzymes from mesophiles, which display only marginal stability? Somero proposes that these phenomena are simply other examples of nature's ways of simplifying the regulation of metabolism in the living organisms (*108*). Providing that the concentrations of substrate and the enzyme in the cell are comparable for a given pair of enzymes, it makes little evolutionary sense for the enzyme from a thermophile to have extremely high activity at its native temperature, as the cell would be faced with the additional challenge of modulating that activity. Similarly, if the enzyme from the mesophile is extremely stable, the cell's protein degrading machinery would have to be that much more efficient in order to maintain the proper amount of the enzyme in the cell.

Although various enzymes from thermophiles have been characterized in much detail, it appears that most of the studies address the temperature dependence of the catalytic efficiency but overlook the effects of the temperature on substrate affinity. There are, however, a handful of studies, that include an analysis of both parameters and report a peculiar behavior of the Michaelis constant as a function of temperature.

Thomas and Scopes investigated the effects of increasing temperature on the kinetics of 3-phosphoglycerate kinase from two species of mesophiles with the optimum growth temperatures of 25-28°C and 30-35°C and one thermophile with the optimum growth temperature of 68-70°C (*119*). They found that in all three enzymes the K_m values for both substrates (PGA and ATP) change very little in the lower temperature range, but begin to increase substantially as the temperature approaches and passes the temperatures of the optimum k_{cat} for the respective enzymes. Similar results have been reported for the two forms of liver citrate synthase that occur in cold and warm acclimated trout (*120*). The form of the enzyme that appears in the trout acclimated to 2°C shows a stronger dependency of the K_m on temperature in the ranges of 0 to 40°C, while the form that appears in the 18°C acclimated trout shows a more gradual increase in K_m within the same temperature range. Another study looked at the kinetic adaptations of the cytoplasmic malate dehydrogenases (MDH) in abalone from different habitats (*121*). The authors found that while the K_m values for MDH isolated from both warm and cold species increased as a function of temperature, in the MDH isolated from the species found in warm environments the K_m values were less sensitive to the increase in temperature than those of the MDH isolated from the cold environment species in the same temperature range (5-45°C). Coppes and Somero report similar observations for the effect of temperature on the Michaelis constants for pyruvate in M_4-lactate dehydrogenase (M_4-LDH) isolated from eurythermal (acclimated to a wide temperature range) and stenothermal (acclimated to a narrow temperature range) fish (*122*). The K_m values for the M_4-LDH from the fish adapted to the narrow range of 14-18°C are

relatively unaffected in the 10-20°C range, but begin to increase steeply in the 20-30°C range. For the fish adapted to wider temperature ranges of 10-30°C, the M_4-LDH K_m values are unaffected in the 10-15°C range and show a slow increase in the 15-30°C range.

As a rule, the overall trend for the change in the Michaelis constant as a function of temperature is that the substrate affinity decreases with an increase in temperature. This increase is most pronounced in the temperature ranges where the enzyme approaches, reaches, or surpasses its maximum catalytic activity (*119*), although there are some examples where the K_m decreases slightly or substantially before the steep increase, as well as some examples where the K_m shows no steep increase within the sampled/expected temperature range (*123, 124*). The structural explanation for the dramatic decrease in the substrate affinity at high temperatures may possibly be temperature-induced deformations of the active site. Since some agree that the active site is not as structurally stable as the rest of the enzyme, the increase in temperature would result in serious distortion of the active site without leading to the complete unfolding of the protein, thus the deformation would be easily reversible as the temperature is decreased. Why would an enzyme evolve to produce such a large increase in K_m at temperatures the organism may encounter on somewhat regular basis? It's been suggested that the increase in K_m as a function of temperature may be a way to compensate for the increase in k_{cat} as the temperature is raised, so that the overall catalytic rates are not significantly perturbed with the fluctuations in temperature (*108*).

It is also conceivable that the dramatic increase in K_m may reflect an increase in the substrate concentrations at high temperatures.

The response of K_m to the increase in temperature preceding the temperature range of maximum catalytic activity varies from enzyme to enzyme (even within the same species). Scopes showed that glucokinase and glucose-6-phosphate dehydrogenase (G6PDH) from *Z. mobilis* display very different dependencies of K_m on temperature (*124*). For glucokinase, the K_m increased steadily in the 10-50°C range, showing a slightly steeper increase after 30°C, while in G6PDH the K_m increased very slowly from 10-44°C with a rapid increase from 44-50°C. Based on the results of the studies discussed above, the rapid increase in K_m will occur at much higher temperatures for the enzymes that are more thermostable compared to that for an average mesophilic enzyme. Thus, it is possible that in a narrow range of sampled temperatures the change in K_m in the mesophilic enzyme will be quite dramatic, while the enzyme from a thermophile may show no change in substrate affinity.

Another observation from these studies is that homologous enzymes from mesophiles and thermophiles display very comparable substrate affinities at their native temperatures, assuming, of course, that the organisms compared have similar cellular substrate concentrations. For instance the K_m for pyruvate for the muscle LDH's from rabbit and various species of fish at their native temperatures lie within a narrow range of 0.2-0.4 mM (*124, 125*). This observation goes hand in hand with the one made earlier, that the catalytic activities of the homologous enzymes from thermophiles and

mesophiles are comparable at their physiological temperatures. Can the same be said about the allosteric regulation of the enzymes?

Our understanding of the significance of elevated temperatures for the allosteric regulation of the enzymes from thermophiles is scarce. While there is a wealth of studies dedicated to understanding the allosteric regulation of various proteins and enzymes in general, the literature on the allostery of the enzymes from thermophiles is quite limited. Additionally, the main focus of these studies in terms of allosteric regulation is to determine whether the enzyme from a thermophile is activated and inhibited by the same compounds and with similar affinities as the homologous enzyme from the mesophile. Unfortunately, little attention has been paid to the thermodynamic parameters that define inhibition and activation and their dependence on temperature, although in some studies, discussed below, the attempt was made to analyze the allosteric response across a range of temperatures.

In order to appreciate the advancements and shortcomings of these studies, it is beneficial to consider them within the historical context. In the 1960's, when the first enzymes from thermophiles were isolated and studied, the concept of allostery itself was fairly new. The term "allosteric" was coined by Changeux in 1961 to describe the feedback inhibition between two non-overlapping sites (*126*). The famous Monod-Wyman-Changeux (MWC) model followed in 1965, as an attempt to rationalize the effect of the allosteric ligands on the protein (*127, 128*). At that time little was known about the structure of the regulatory proteins and the only three-dimensional structures available were the crystal structures of hemoglobin, which showed significant

differences in the quaternary structure between the oxygenated and reduced states (*129-131*). These observations influenced the authors of the MWC model to include the following into their discussion of the general properties of the allosteric proteins: "Allosteric interactions frequently appear to be correlated with alterations of the quaternary structure of the proteins" (*127*). The MWC model has been applied to several allosteric systems with the preconceived notion that the allosteric response is linked to the switch between two (or more) conformations (*132, 133*), even though Monod *et al*. specifically noted that the term "conformational", which they use to describe the allosteric transitions, should be taken in its "widest connotation", and that these transitions may not result in any significant alteration of the three-dimensional structure of the protein (*127*). The square model proposed by Koshland *et al*. to describe the behavior seen in hemoglobin further reinforced the idea of an allosteric switch between two conformations (*134*).

In view of the two-state models, Brock suggested that since a degree of flexibility is required for the allosteric regulation of the enzyme, the enzymes from thermophiles may not be able to undergo allosteric conformational changes due to their rigidity (*135*). However, this assumption was proved wrong shortly after, when several studies confirming the allosteric nature of enzymes from thermophiles were published. Ljungdahl and Sherod divided these enzymes into two groups: those, that display allosteric regulation at both low and high temperatures and those that only show allosteric regulation at the high (physiological) temperatures (*136*).

One of the representatives of the first group is the aspartokinase from *Bacillus stearothermophilus*. This enzyme was shown to be inhibited by lysine and threonine at both 23 and 55°C, although the effect of the inhibitors decreased with an increase in temperature (*137, 138*). Similar results were reported for the threonine deaminase from *B. stearothermophilus*, where isoleucine was found to reduce the binding affinity of the substrate (threonine). The inhibitory effect of isoleucine present in the reaction mix was diminished as the temperature increased from 30 to 80°C. However, it is important to note that the effect of temperature on isoleucine sensitivity of the enzyme was measured at 50 μM isoleucine, and the potential temperature-related changes of the binding affinity of isoleucine to the enzyme were not addressed (*139*). Yoshida *et al*. determined that phosphofructokinase from *Thermus thermophilus* is inhibited by phophoenolpyruvate (PEP) and activated by ADP at both 30 and 75°C (*140*). In a later publication it was noted that the effects of both PEP and ADP were stronger at 75°C (*141*). Yoshida and Oshima showed that the activity of fructose 1,6-diphosphatase (FDPase) from *T. thermophilus* was enhanced by the addition of PEP and decreased by AMP and ADP (*140*). The effect of PEP was seen throughout the temperature range of 25 to 65°C, and one could argue that the enhancement of FDPase activity was greater at higher temperatures.

The second group, according to Ljungdahl and Sherod, is represented by ribonucleotide reductase from Thermus X-1 and acetohydroxy-acid synthetases from *Thermus aquaticus* and *Bacillus* sp., where the addition of dGTP and valine respectively increase the activity of the enzymes (*142, 143*). In both cases, the effect of the activators

was more pronounced at higher temperatures. Another enzyme representing this group is pyrimidine ribonucleoside kinase from *B. stearothermophilus* (*144*). Orengo and Saunders showed that this enzyme is inhibited by CTP and its effect on the activity of the enzyme is small at low temperatures but becomes stronger at higher temperatures.

The more recent works by Johnson and Reinhart and Tlapak-Simmons and Reinhart addressed the temperature dependence of the allosteric regulation of bacterial type 1 ATP-dependent phosphofructokinase from *E. coli* (EcPFK) and a moderate thermophile *Bacillus stearothermophilus* (BsPFK) (*145, 146*). In EcPFK the allosteric response to the inhibitor PEP is diminished as a function of temperature (*145*). The van't Hoff analysis of the coupling coefficient for PEP shows that the inhibition is enthalpically-driven. In contrast, in BsPFK we see more inhibition by PEP at higher temperature because this process is entropically-driven (*146*). The results presented in the next chapter of this dissertation show that PFK 1 from *Thermus thermophilus* also displays entropically-driven inhibition by PEP, which raises the question whether all thermostable bacterial PFK 1 homologs have similar dominating entropic components of coupling free energy and how that may be beneficial to the organism as a whole. In the light of works by Weber and Reinhart, we know that activation and inhibition are thermodynamic processes and, as such, follow certain temperature dependence (*105, 147, 148*). Thus, it would be informative to categorize the allosterically regulated enzymes from thermophiles by whether the allosteric regulation is dominated by the entropy or enthalpy components of the free energy.

Our analysis of the allosteric inhibition of the Fru-6-P binding by PEP in TtPFK, revealed other interesting findings. One is that PEP binds to TtPFK with a very high affinity, compared to PEP binding affinities from PFKs from *E. coli* (EcPFK), *B. stearothermophilus* (BsPFK), and *L. delbrukii* (LbPFK). To understand this phenomenon, we analyzed the sequence alignments of TtPFK, BsPFK, and LbPFK and the crystal structures of BsPFK and LbPFK to identify the residues in the allosteric binding site, which may be responsible for the enhanced binding of PEP in TtPFK. The results of this investigation are discussed in Chapter IV. Another curious finding is that although the binding of the inhibitor to TtPFK is very tight, its ability to inhibit the binding of the substrate at 25°C is considerably weaker, compared to the magnitude of inhibition seen in PFK from the moderate thermophile *B. stearothermophilus.* From the sequence alignments and various three-dimensional structures of BsPFK, we identified a putative network of residues which lies directly between the two nearest allosteric and active sites. In Chapter III, we discuss our successful attempt to enhance the inhibitory response in TtPFK by introducing chimeric substations to the three non-conserved residues within this network.

CHAPTER II

ALLOSTERIC REGULATION IN PHOSPHOFRUCTOKINASE FROM AN EXTREME THERMOPHILE *THERMUS THERMOPHILUS*

Phosphofructokinase 1 (PFK 1) catalyzes the phosphoryl transfer from MgATP to fructose-6-phosphate (Fru-6-P) forming fructose-1,6-bisphosphate and MgADP. This is the first committed step of glycolysis and a critical control point of the glycolytic pathway, making PFK subject to rigorous allosteric regulation. The regulation of the PFKs from eukaryotic organisms is very complex, since they have distinct activator and inhibitor binding sites, are regulated by a variety of allosteric effectors including fructose-1,6-bisphosphate, fructose-2,6-bisphosphate, citrate, AMP, and ATP, and can exist in multiple active oligomeric states, (*149, 150*). In contrast, the bacterial PFKs provide a relatively simple paradigm for allosteric regulation (*151*). Generally, the bacterial type 1 ATP-dependent PFK is active as a homotetramer that contains 4 identical active sites and 4 identical allosteric sites, and is regulated by phosphoenolpyruvate (PEP) and MgADP, which compete for binding at the same effector sites. Both of these are K-type effectors, as they impact the binding affinity of the enzyme for the substrate Fru-6-P, while leaving the V_{max} unchanged.

The PFK's from *E. coli* (EcPFK) and *Bacillus stearothermophilus* (BsPFK) have been extensively studied resulting in a wealth of structural (*152-154*) and thermodynamic data (*145, 155-162*). The crystal structures of these two enzymes with various ligands show a high degree of similarity. However, substantial differences in the binding affinities for the substrate and the allosteric ligands, as well as in the magnitude

of the allosteric response are evident. Another difference is that both the inhibition by PEP and activation by MgADP in the PFK from mesophilic *E. coli* is enthalpically-driven (*145*), while in the PFK from the thermophile *Bacillus stearothermophilus* they are entropically-driven (*146*). This raises the question of whether entropy-dominated regulation might be due to the thermostability of BsPFK and therefore might be observed in the PFKs from other thermophiles. To further evaluate the potential relationship between thermal stability and the thermodynamic basis of allosteric regulation we have examined the allosteric regulation of PFK from the extreme thermophile, *Thermus thermophilus* (TtPFK).

TtPFK was partially purified (to a specific activity of 0.49 U/mg) by Yoshida (*140, 141*) and characterized as extremely thermostable with minimal loss of activity after incubation at 70°C for more than 30 hours. TtPFK followed simple Michaelis-Menten kinetics with respect to both Fru-6-P and MgATP with the respective Michaelis constants of 15 μM and 60 μM at 30°C and pH 8.4. The addition of 0.1 mM PEP resulted in a roughly 10-fold increase in the K_m for Fru-6-P and a change of the Fru-6-P binding curves from hyperbolic to sigmoidal yielding Hill number of 2. ADP was able to partially relieve the inhibition by PEP, and the effects of PEP and ADP were more pronounced at 75°C compared to 30°C.

In 1990, TtPFK was purified to homogeneity by Xu et al. and the specific activity was determined to be 57 U/mg at 25°C and pH 8.4 (*163*). TtPFK dissociation into dimers was observed when the enzyme was applied onto a gel filtration column that was equilibrated and eluted with buffer containing 0.1 mM PEP. This process could be

reversed by adding Fru-6-P or by removing PEP from the buffer. The authors suggested that this association-dissociation plays a role in the regulation of the activity of the enzyme.

Although these studies confirmed the allosteric regulation of TtPFK by PEP and ADP, the extent of PEP inhibition and ADP activation was not quantified. The present study offers a more comprehensive analysis of the allosteric effects of PEP and ADP on this enzyme using thermodynamic linkage analysis, a model-free approach that quantifies the magnitude of the allosteric response by comparing the difference in the substrate binding affinity for the enzyme in effector-free and effector-saturated forms.

Materials and Methods

Materials

All chemical reagents used in buffers, protein purifications, and enzymatic assays were of analytical grade, and were purchased from Sigma-Aldrich (St. Louis, MO) or Fisher Scientific (Fair Lawn, NJ). The EPPS buffer used for fluorescence was purchased from Acros Organics (Geel, Belgium). The sodium salt of Fru-6-P was purchased from Sigma-Aldrich or USB Corporation (Cleveland, OH). NADH and dithiothreitol were purchased from Research Products International (Mt. Prospect, IL). Creatine kinase and the ammonium sulfate suspension of glycerol-3-phosphate dehydrogenase were purchased from Roche Applied Sciences (Indianapolis, IN). The ammonium sulfate suspensions of aldolase and triosephosphate isomerase, as wells as, the sodium salts of phosphocreatine and PEP were purchased from Sigma-Aldrich. The sodium salt of ATP was purchased from Sigma-Aldrich and Roche Applied Sciences. The experiments

involving quantifying the allosteric response of TtPFK to MgADP were conducted using sodium salt of ATP purchased from Roche Applied. The coupling enzymes were dialyzed extensively against 50 mM MOPS-KOH, pH 7.0, 100 mM KCl, 5 mM $MgCl_2$, and 0.1 mM EDTA before use.

Mutagenesis

The pALTER plasmid with the wild type TtPFK gene was used as the starting template for mutagenesis (13). The L313W mutation was introduced using the QuikChange Site-Directed Mutagenesis protocol (Stratagene, La Jolla, CA). Two complementary oligonucleotides were used to produce the mutant genes, for which the template oligo is shown below. The underlined bases designate the site of the substitution

L313W: GGACATCAACCGGGCCTGGTTGCGCCTATCGC

The C111F/A273P substitutions were introduced via the Altered Sites in vitro Mutagenesis System protocol (Promega, Madison, Wisconsin) using the following primers (complementary to the coding strand):

C111F: GTGCTCCTCCACGAGAAAAAGCGCCCCGC

A273P: GGCCTCCACCGCGGGCGCCCCCAGGCG

The resulting sequences were verified via DNA sequencing at the Gene Technology Laboratory at Texas A&M University.

Protein expression and purification

Thermus thermophilus HB8 cells were purchased from ATCC (Manassas, VA). Cells were propagated in ATCC medium 697 (0.4% yeast extract, 0.8% polypepetone,

and 2% NaCl; pH 7.5). Genomic *T. thermophilus* DNA was purified using the Wizard Genomic DNA Purification Kit (Promega; Madison, WI). The isolated genomic DNA was digested with HindIII before subcloning. We first attempted to subclone the TtPFK gene into pLEAD4 (Ishida and Oshima (2002)). This vector is specially designed to express thermophilic bacterial genes containing high GC-content. While we were able to successfully subclone into pLEAD4 and see expression of TtPFK when using JM109 as the host strain, the plasmid was not compatible with our expression strain, RL257, which has the *E. coli* genes *pfkA* and *pfkB* deleted (*164*). Using PCR primers with the restriction enzymes appropriate for cloning into pALTER-1 (Promega), we amplified the TtPFK gene using the pLEAD4 construct as the template. The ligation products were screened via restriction enzyme digests and constructs containing the correct banding pattern were sequence verified.

In the process of cloning TtPFK from the genome, we found three single base differences in the sequence of the gene, relative to the published sequence of *T. thermophilus HB8* (Accession number M71213.1 (*165*)). One of the differences is inconsequential to the protein product. However, the other two result in differences in the amino acid sequence. Position 111 is reported to be a phenylalanine while our results show a cysteine and position 273 is reported to be proline while we see an alanine at that position. It should be noted that the sequence we determined is consistent with the more recent unpublished submission of the complete genome of *T. thermophilus HB8* (Accession number YP_145228).

The RL257 cells containing the plasmid with the TtPFK gene were induced with

IPTG at the beginning of growth and grown at 30°C for 18 hours in LB (Luria-Bertani media: 10 g/L tryptone, 5 g/L yeast extract, and 10 g/L sodium chloride) with 15 μg/mL tetracycline. The cells were harvested by centrifugation in a Beckman J6 at 4000 RPM and frozen at -80°C for at least 2 hours before lysis. The cells were resuspended in purification buffer (10 mM Tris-HCl, 1 mM EDTA; pH 8.0) and sonicated using the Fisher 550 Sonic Dismembrator at 0°C for 8-10 min using 15 second pulse/45 second rest sequence. The crude lysate was centrifuged using a Beckman J2-21 centrifuge at 22,500xg for 30 min at 4°C. The supernatant was heated at 70°C for 20 minutes, cooled, and centrifuged for 30 min at 4°C. The protein was then precipitated using 35% ammonium sulfate at 0°C and centrifuged. The pellet was dissolved in minimal volume of 20mM Tris-HCl, pH8 and dialyzed several times against the same buffer. The protein was then applied to a MonoQ column (GE Life Sciences), which was equilibrated with the purification buffer (20mM Tris-HCl, pH8) and eluted with a 0 to 1M NaCl gradient. Fractions containing PFK activity were analyzed for purity using SDS-PAGE, pooled and dialyzed against the same buffer and stored at 4°C. The protein concentration was determined using the BCA assay (Pierce), using bovine serum albumin (BSA) as the standard.

Kinetic assays

Initial velocity measurements were carried out in 600 μL of buffer containing 50 mM EPPS-KOH, pH 8, 100 mM KCl, 5 mM $MgCl_2$, 0.1 mM EDTA, 2 mM dithiothreitol, 0.2 mM NADH, 250 μg of aldolase, 50 μg of glycerol-3-phosphate dehydrogenase, 5 μg of triosephosphate isomerase, and 0.5 mM ATP. (To determine the

K_a for MgATP, the initial velocity measurements were carried out in 600 μL of buffer containing 50 mM EPPS-KOH, pH 8, 100 mM KCl, 5 mM $MgCl_2$, 0.1 mM EDTA, 2 mM dithiothreitol, 0.2 mM NADH, 250 μg of aldolase, 50 μg of glycerol-3-phosphate dehydrogenase, 5 μg of triosephosphate isomerase, 5 mM Fru-6-P, and varied concentrations of MgATP). 40 μg/mL of creatine kinase and 4 mM phosphocreatine were present in all assays performed in the absence of MgADP. The amount of Fru-6-P and PEP or MgADP used in any given assay varied. When measuring the activation by MgADP, phosphocreatine and creatine kinase were excluded from the assay mix, and equimolar concentrations of MgATP were added with MgADP to overcome competitive ADP product inhibition expected at the active site. The reaction was initiated by adding 10 μL of TtPFK appropriately diluted into 50 mM EPPS (KOH) pH 8, 100 mM KCl, 5 mM $MgCl_2$, 0.1 mM EDTA. The conversion of Fru-6-P to Fru-1,6-BP was coupled to the oxidation of NADH, which resulted in a decrease in absorbance at 340nm. The rate of the decrease in A_{340} was monitored using a Beckman Series 600 spectrophotometer.

Steady-state fluorescence assays

The fluorescence intensity measurements were performed using the ISS KOALA. The titrations were performed in buffer containing 50 mM EPPS (KOH) pH 8, 100 mM KCl, 5 mM $MgCl_2$, 0.1 mM EDTA. The enzyme concentration in the sample was 0.5 μM. Sample was excited at 295 nm and the fluorescence intensity was detected using the 2-mm 335 nm Schott cut-on filter. Change in the intrinsic tryptophan fluorescence at 25°C was measured as a function of PEP concentration at varying concentration of Fru-6-P.

Data analysis

Data were fit using the non-linear least-squares fitting analysis of Kaleidagraph software (Synergy). The initial velocity data were plotted against concentration of Fru-6-P and fit to the following equation:

$$v^{\circ} = \frac{V[A]^{n_H}}{K_a^{n_H} + [A]^{n_H}} \tag{2-1}$$

where v° is the initial velocity, [A] is the concentration of the substrate Fru-6-P (or ATP), V is the maximal velocity, n_H is the Hill coefficient, and K_a is the Michaelis constant defined as the concentration of substrate that gives one-half the maximal velocity. For the reaction in rapid equilibrium, K_a is equivalent to the dissociation constant for the substrate from the binary enzyme-substrate complex.

Data collected using steady-state fluorescence were plotted as the relative intensity as a function of the PEP concentration. The data were fit using the equation 2

$$F = \frac{(F - F_{\circ})[Y]^{n_H}}{K_y^{n_H} + [Y]^{n_H}} + F_{\circ} \tag{2-2}$$

where F is the relative intensity, $F_{\circ}$ is the relative intensity in the absence of PEP, [Y] is the concentration of PEP, K_y is the apparent dissociation constant for PEP, and n_H is Hill number. The resulting values for the apparent dissociation constants for PEP were then plotted as a function of the Fru-6-P concentration and fit to equation 2-3.

The K_a and K_y values obtained from the initial velocity and fluorescence experiments were plotted against effector or substrate concentrations and fit to equation

2-3 or 2-4:

$$K_a = K_{ia}^{\circ}\left(\frac{K_{iy}^{\circ} + [Y]}{K_{iy}^{\circ} + Q_{ay}[Y]}\right) \tag{2-3}$$

$$K_y = K_{iy}^{\circ}\left(\frac{K_{ia}^{\circ} + [A]}{K_{ia}^{\circ} + Q_{ay}[A]}\right) \tag{2-4}$$

where K_{ia}° is the dissociation constant for Fru-6-P in the absence of allosteric effector, Y is PEP, K_{iy}° is the dissociation constant for PEP in the absence of Fru-6-P, and Q_{ay} is the coupling coefficient (*148, 166, 167*). When equation 2-3 is applied to the allosteric action of MgADP, the subscripts are changed from "y" to "x", and MgADP is designated as "X", to be consistent with the notation we have used previously (*145*).

Q_{ay} is defined as the coupling constant, which describes the effect of allosteric effector on the binding of the substrate (and *vice versa*) and is defined by equation 2-5:

$$Q_{ay} = \frac{K_{ia}^{\circ}}{K_{ia}^{\infty}} = \frac{K_{iy}^{\circ}}{K_{iy}^{\infty}} \tag{2-5}$$

where K_{ia}° and K_{ia}^{∞} represent the dissociation constants for the substrate in the absence and presence of a saturating concentration of the allosteric effector, respectively, and K_{iy}° and K_{iy}^{∞} represent the dissociation constants for the allosteric effector in the absence and presence of a saturating concentration of the substrate, respectively.

Based on its definition, Q_{ay} represents the equilibrium constant for the following disproportionation equilibrium (Scheme 1):

The coupling constant Q_{ay} is related to the coupling free energy (ΔG_{ay}) and its

enthalpy (ΔH_{ay}) and entropy (ΔS_{ay}) components through the following relationship (*105*):

$$\Delta G_{ay} = -RT\ln(Q_{ay}) = \Delta H_{ay} - T\Delta S_{ay} \tag{2-6}$$

The coupling entropy and enthalpy components were determined by measuring the coupling constant as a function of temperature and the data were fit to equation 2-7:

$$\ln Q_{ay} = \frac{\Delta S_{ay}}{R} - \frac{\Delta H_{ay}}{R}\left(\frac{1}{T}\right) \tag{2-7}$$

where ΔG_{ay} is the coupling coefficient, ΔS_{ay} is the coupling entropy, ΔH_{ay} is coupling enthalpy, T is absolute temperature in Kelvin, and R is gas constant (R=1.99 cal K^{-1} mol^{-1})

The data, which display non-linearity were fit to the modified van't Hoff equation:

$$\ln Q_{ay} = \frac{\Delta S^{\circ}_{ay}}{R} - \frac{\Delta H^{\circ}_{ay}}{R}\left(\frac{1}{T}\right) - \frac{\Delta C_p\left(T - T^{\circ} - T\ln\left(\frac{T}{T^{\circ}}\right)\right)}{R}\left(\frac{1}{T}\right) \tag{2-8}$$

where T° is the reference temperature, in this case 298K, and ΔC_p is the change in the heat capacity.

Results

MgATP binding to TtPFK was measured to ensure that all measurements were done at saturating ATP, and the data were fit well by equation 2-1. At saturating Fru-6-P (5 mM), the Hill number for MgATP binding is 0.8±0.07 and the K_a for MgATP is 6.0±0.5 μM, with the specific activity equal to 41 units mg^{-1} at pH 8 (a unit of activity is defined as the amount of enzyme required to produce 1 μmol of fructose 1,6-bisphosphate/min) and a k_{cat} of 24.6 s^{-1} (Table 2-1). The subsequent assays were preformed at 0.5 mM MgATP. The K_a for Fru-6-P is 27.0±0.6 μM. The Fru-6-P binding showed a slight positive homotropic cooperativity resulting in a Hill number of 1.6. To address the possible consequences of the discrepancy between the sequence of TtPFK gene reported by Xu et al. (*165*) and the sequence obtained by us, we constructed the C111F/A273P variant and verified that the presence of these substitutions does not cause any dramatic changes in the properties of the enzyme (Table 2-2).

Table 2-1 Summary of kinetic and thermodynamic parameters for TtPFK, BsPFK and EcPFK, at pH 8 and 25°C[a].

	TtPFK	BsPFK	EcPFK
K_{ia}° (μM)	27± 1	31 ± 2	300 ± 10
K_{ix}° (μM)	0.4 ± 1	19 ± 2	48 ± 2
Q_{ax}	1.6 ± 0.1	1.70 ± 0.01	11.1 ± 0.2
ΔG_{ax} (kcal/mol)	-0.28 ± 0.04	-0.314±0.003	-1.42±0.01
K_{iy}° (μM)	1.6 ± 0.1	93 ± 6	300 ± 10
Q_{ay}	0.067 ± 0.002	0.0021 ± 0.0003	0.008 ± 0.0003
ΔG_{ay} (kcal/mol)	1.60 ± 0.02	3.67 ± 0.1	2.7 ± 0.1
SA (U/mg)	41	163	240
k_{cat} (s^{-1})	25	91	142
k_{cat}/K_m (M^{-1} s^{-1})	9.1e5	2.9e6	4.7e5

[a] Buffers used for TtPFK and BsPFK contained 100 mM potassium chloride, while buffers used for EcPFK contained 10 mM ammonium chloride. A represents Fru-6-P, X represents MgADP and Y represents PEP. The error given in the table represent the standard error calculated for the fit of the data to equation 2-3.

Table 2-2 Summary of the kinetic and thermodynamic properties of the wild type and C11F/A273P and L313W variants of TtPFK at pH 8 and 25°C[b].

	WT	C111F/A273P	L313W	L313W (fluor)
K_{ia}° (μM)	27.0 ± 0.6	36.5± 0.7	14.4±0.03	0.063±0.009
K_{iy}° (μM)	1.58 ± 0.07	4.5±0.2	1.15±0.07	0.66±0.06
Q_{ay}	0.067 ± 0.002	0.063± 0.001	0.072± 0.002	0.068±0.006
SA (U/mg)	41	34	54	n/a

[b] The error given in the table represent the standard error calculated for the fit of the data to equation 2-3.

To measure the allosteric effects of PEP and MgADP, the Fru-6-P titrations were performed at increasing concentrations of either effector and the individual titration curves were fit to equation 2-1 to obtain the Hill numbers (Figure 2-1), apparent specific activity (Figure 2-2) and apparent dissociation constants (Figure 2-3) for Fru-6-P binding. The fits of the apparent dissociation constant for Fru-6-P as a function of PEP or MgADP concentrations to equation 2-2 are shown in Figure 2-3. The resulting values of K_{ia}°, K_{ix}°, K_{iy}°, Q_{ay}, and Q_{ax} are presented in Table 2-1, along with the values for these parameters pertaining to PFK from other sources for comparison. Increasing concentrations of PEP, as expected, lead to a decrease in the Fru-6-P binding affinity as shown by the shift of the titration curves to the right. This shift continues until PEP saturation is reached, after which no additional inhibition of Fru-6-P binding can be achieved by further increasing the concentration of PEP. The addition of PEP also resulted in heterotropically induced homotropic cooperativity (*168*) in Fru-6-P binding as evidenced by the increase of the Hill numbers from 1.6 to above 2.5 as [PEP] approaches saturation (Figure 2-1). However, no effect on the apparent specific activity of the enzyme as a function of PEP concentration was evident (Figure 2-2).

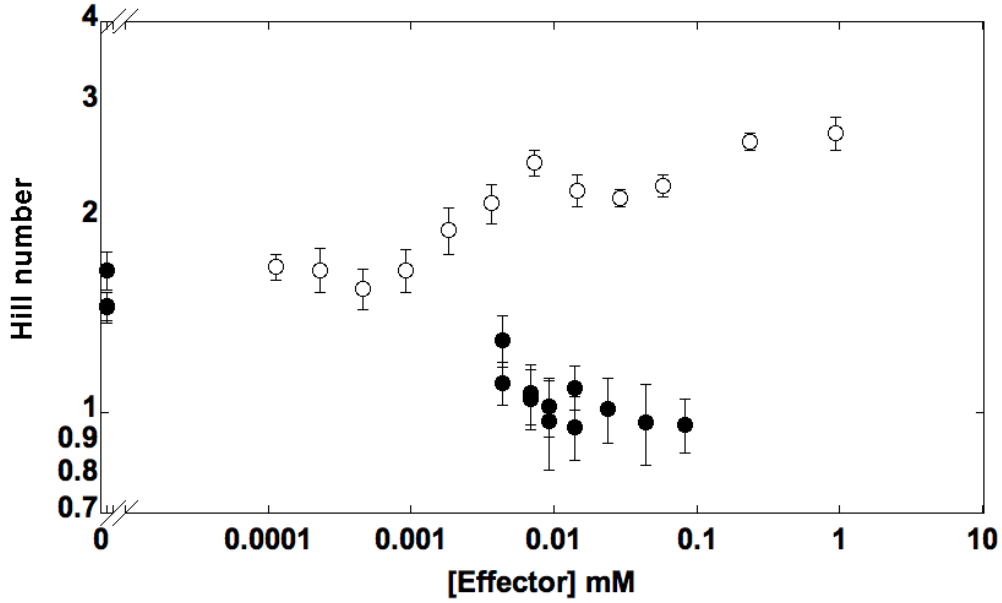

Figure 2-1. Variation in the Hill number as a function of effector concentration for wild type TtPFK. The data for the Hill number as a function of PEP concentration are shown in open circles. The data for the Hill number as a function or MgADP are shown in closed circles. The experiments were performed at pH 8 and 25°C. The error bars represent the standard error calculated for the fit of the data to equation 2-1.

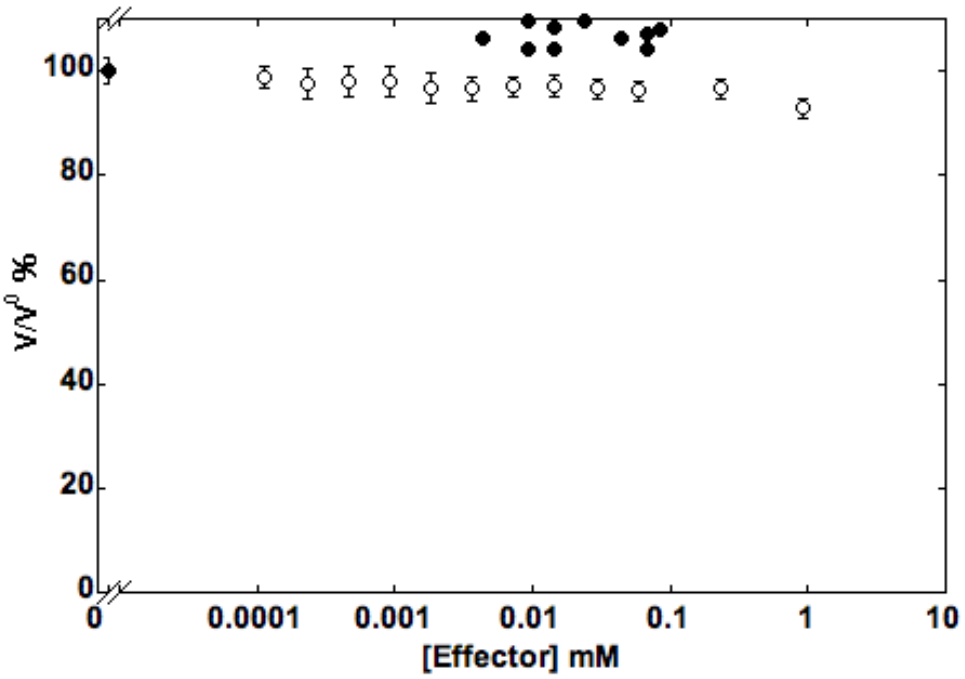

Figure 2-2. Variation in the apparent specific activity as a function of effector concentration for wild type TtPFK. The data for the relative maximal activity are shown as a function of PEP (open circles) or MgADP (closed circles) concentration. The experiments were performed at pH 8 and 25°C. The error bars represent the standard error calculated for the fit of the data to equation 2-1.

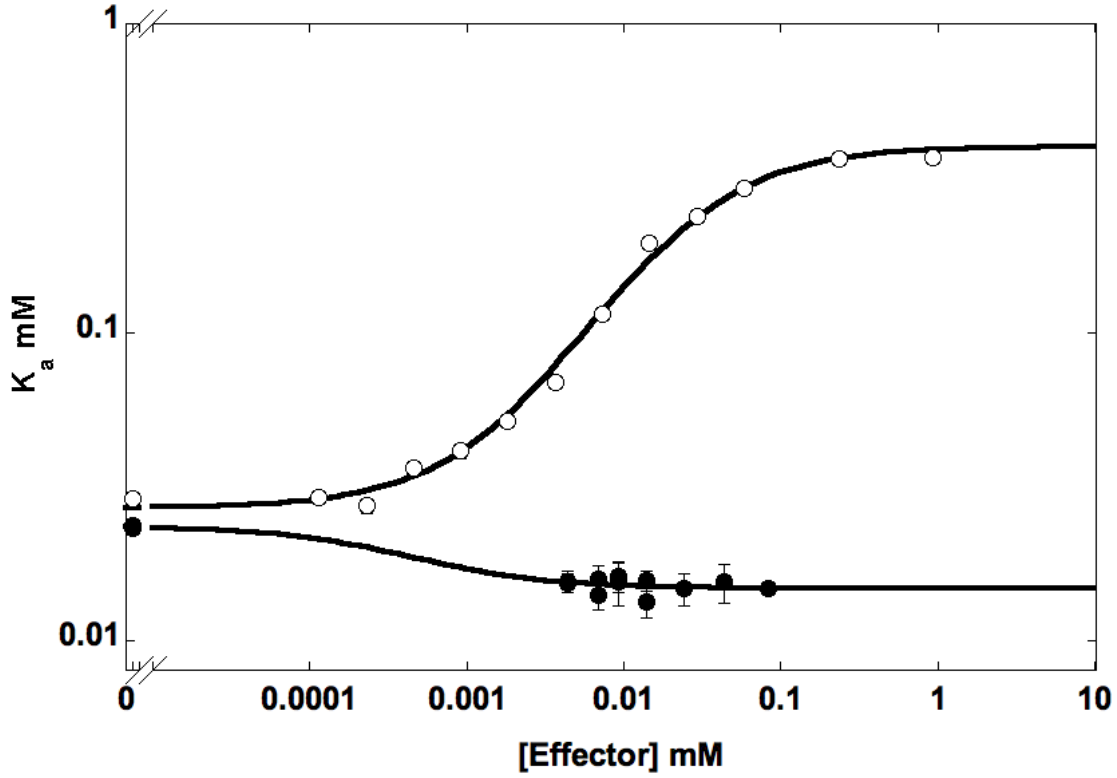

Figure 2-3. Change in the apparent dissociation constants for substrate as a function of effector concentration for wild type TtPFK. The data for apparent dissociation constants (K_a) for Fru-6-P as a function of PEP (open circles) or MgADP (closed circles) concentration. Experiments were performed at pH 8 and 25°C. The data were fit to equation 2-3 to obtain the dissociation constants for PEP (K_{iy}°) and MgADP (K_{ix}°) and the coupling constants Q_{ay} and Q_{ax}. The error bars represent the standard error calculated for the fit of the data to equation 2-1.

The rapid equilibrium assumption for the Fru-6-P binding in TtPFK was verified by comparing the value of Q_{ay} obtained by the method described above (Figure 2-4A in blue) to that obtained from PEP titrations described in (*169*) (Figure 2-4A in red). Since the binding of PEP cannot be measured at zero Fru-6-P using the initial velocity experiment, the data point for K_{iy}° shown in open circle is that shown in Table 2-1. The data for the apparent dissociation constant for PEP as a function of Fru-6-P concentration were not fit well by equation 2-4 due to the high degree of cooperativity in the Fru-6-P binding seen in the steepness of the slope in the transition region of the curve in red. However, the distance between the two plateaus is quite comparable. Figure 2-4B shows that there is no cooperativity in the binding of PEP to TtPFK.

The addition of MgADP had little effect the specific activity of the enzyme, but did diminish the homotropic cooperativity of Fru-6-P binding, reducing the Hill numbers from 1.6 to 1 (Figure 2-1, 2-2). The magnitude of the activation by MgADP is much smaller, compared to the magnitude of the inhibition by PEP (Figure 2-3). The large error in the value of K_{ix}° is a result of experimental limitation, because the lowest attainable concentration of MgADP used in the assay (that of the MgADP contamination in the MgATP) is well above the apparent dissociation constant of MgADP.

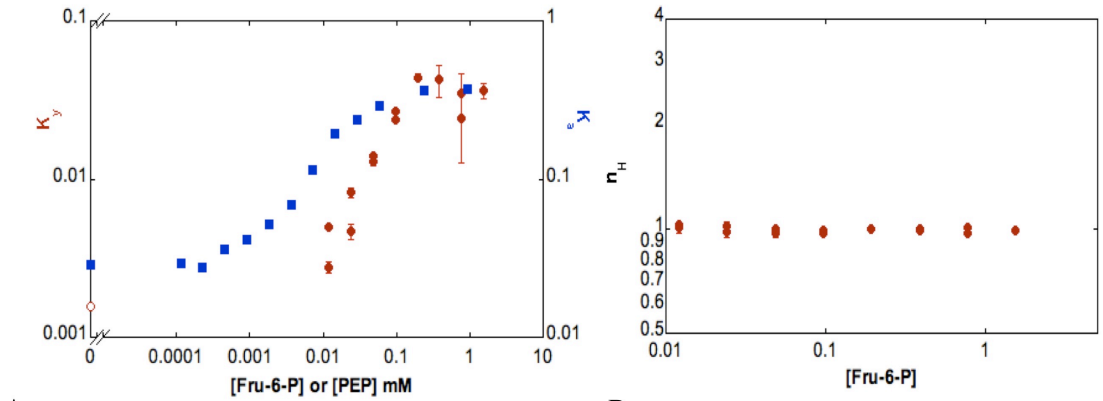

Figure 2-4. Verification of the rapid equilibrium assumption for the binding of Fru-6-P in TtPFK. (A) The plot of apparent dissociation constants for PEP (K_y) as a function of [Fru-6-P] (red circles) or apparent dissociation constants for Fru-6-P (K_a) as a function of [PEP] (blue squares) at pH 8 and 25°C. The zero point for the plot of (K_y) as a function of [Fru-6-P] is taken from Table 2-1 and shown in open circle for reference. (B) The Hill numbers for the binding of PEP as a function of [Fru-6-P].

To determine the entropic and enthalpic components of inhibition by PEP and activation by MgADP in TtPFK at room temperature, the coupling coefficients (Q_{ax} and Q_{ay}) were measured at temperatures ranging between 10 to 35°C (Figure 2-5). The plots of $\ln Q_{ax}$ or $\ln Q_{ay}$ as a function of inverse temperature were fit to equations 2-7 and 2-8. The values obtained from both the linear and non-linear fits are presented in Table 2-3. The data for the temperature dependence of $\ln Q_{ay}$ are well described by a straight line with a positive slope. In contrast, the data for the temperature dependence of $\ln Q_{ax}$ are fit better by the non-linear equation 2-8, suggesting that the entropy and enthalpy components vary as a function of temperature. It is interesting to note that the values of ΔH_{ay} and $T\Delta S_{ay}$ at 25°C obtained by the linear versus the non-linear fits are comparable (Table 2-2).

To establish the values for the binding of Fru-6-P and PEP, and coupling between PEP and Fru-6-P by tryptophan fluorescence in the absence of turnover, we introduced a tryptophan at position 313 (L313W). To ensure that this variant behaves similar to wild type protein, we measured the parameters for the binding and coupling of PEP and Fru-6-P using the initial velocity experiments described in the materials and methods section. The resulting values are presented in Table 2-2 and correlate well with the values for the wild type enzyme.

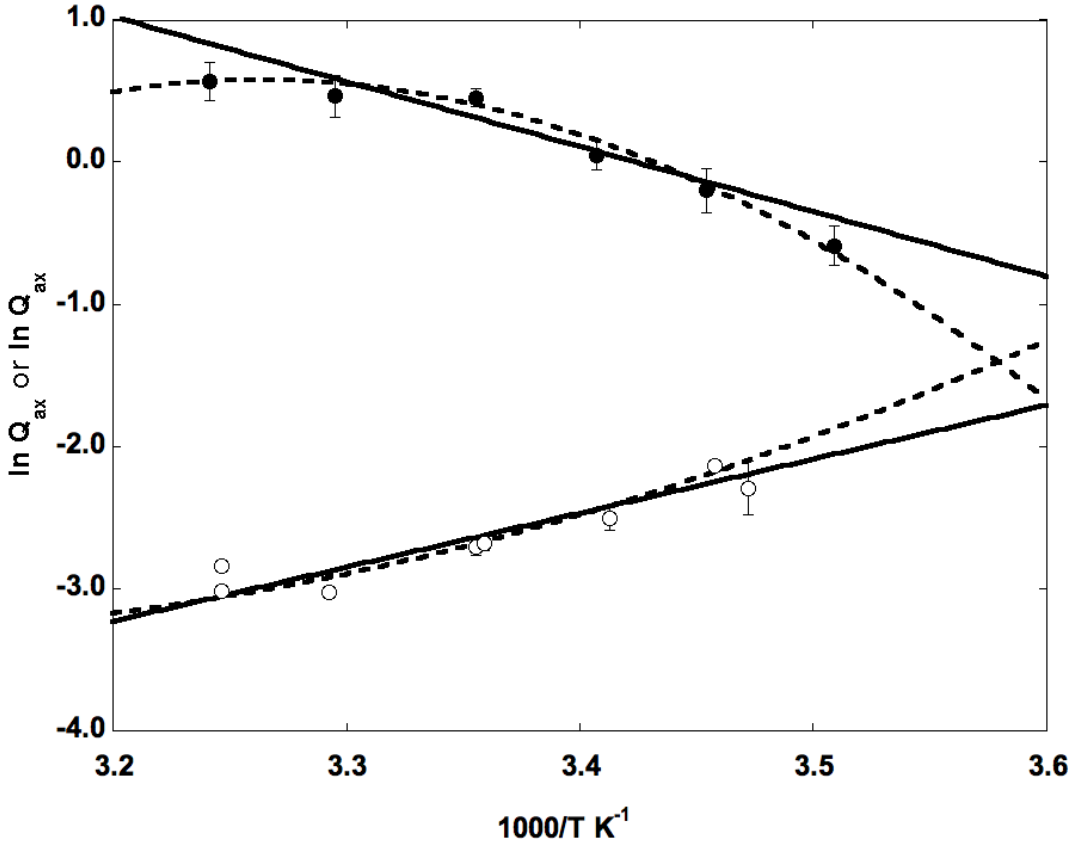

Figure 2-5. Van't Hoff analysis for coupling coefficients of activation and inhibition. The plots of $\ln Q_{ay}$ (open circle) and $\ln Q_{ax}$ (closed circles) are shown as a function of temperature. The data were fit to equation 2-7 (solid line) to obtain the enthalpy component of coupling free energy or to equation 2-8 (dashed line) to obtain the enthalpy and change in the heat capacity at 25°C. The error bars represent the standard error calculated for the fit of the data to equation 2-3

Table 2-3 Thermodynamic parameters for inhibition and activation of TtPFK[c].

	Linear Fit	Non-linear Fit
ΔH_{ax} (kcal/mol)	9 ± 1	8 ± 1
$T\Delta S_{ax}$ (kcal/K mol)	9.28 ± 1	8.28 ± 1
ΔC_p (kcal/K mol)	n/a	-0.7 ± 0.3
ΔH_{ay} (kcal/mol)	-7.5 ± 0.3	-8.4 ± 0.4
$T\Delta S_{ay}$ (kcal/K mol)	-9.1 ± 0.3	-10.0 ± 0.4
ΔC_p (kcal/K mol)	n/a	0.31± 0.08

[c] The values for the enthalpy and the change in heat capacity are obtained from the linear or non-linear fits of the temperature dependency of $\ln Q_{ay}$ and $\ln Q_{ax}$ to Equations 7 and 8. The values for the entropy and change in heat capacity were determined directly from the fit to the data. The values for $T\Delta S_{ay}$ and $T\Delta S_{ax}$ were calculated using the values for the coupling free energy obtained from the initial velocity experiments at 25° and the values for the enthalpy calculated from the slope on the van't Hoff plots. The error bars represent the standard error calculated for the fit of the data to equation 2-7 or 2-8.

The change in the intrinsic tryptophan fluorescence as a function of PEP concentration was measured at increasing concentrations of Fru-6-P (Figure 2-6A) and fit to equation 2-4. The Hill number for the binding of PEP to TtPFK is equal to 1, suggesting that there is no homotropic cooperativity in the PEP binding. The Hill number was not changed with the addition of Fru-6-P. The values for the dissociation constants for PEP were plotted as a function of Fru-6-P concentration (Figure 2-6B) and fit to equation 4 to obtain the values for the dissociation constant for Fru-6-P and the coupling constant (Table 2-2). The values for the dissociation constant for PEP and the coupling constant obtained from the tryptophan fluorescence experiments agree well with the values obtained from the initial velocity experiments. The dissociation constant for Fru-6-P binding obtained using tryptophan fluorescence experiments is over 200-fold lower compared to the value determined from the initial velocity experiments.

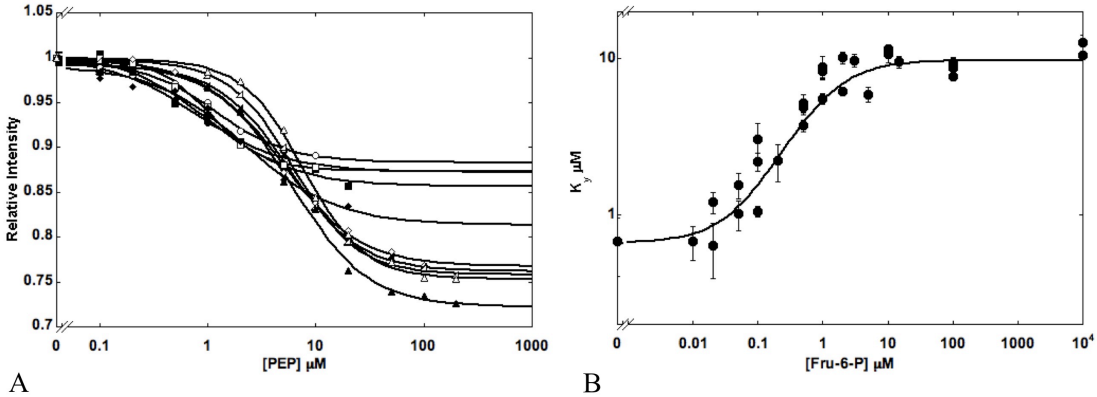

Figure 2-6. Binding of PEP as a function of substrate concentration in the L313W variant monitored by changes in intrinsic tryptophan fluorescence. (A) The plot of relative fluorescence intensity of the L313W variant at 25°C as a function of PEP concentration at Fru-6-P varying from zero to 10mM. The sample was excited at 295 nm and the fluorescence intensity was detected using the 2-mm 335 nm Schott cut-off filter. (B) The plot of apparent dissociation constants (K_y) for PEP as a function of [Fru-6-P] at pH 8 and 25°C. The data were fit to equation 2-4 to obtain the dissociation constants for Fru-6-P (K_{ia}°) and the coupling constants Q_{ay}. The error bars in 2-6 B represent the standard error calculated for the fit of the data to equation 2-2.

Discussion

The Michaelis constants for Fru-6-P of 27 μM and the specific activity of 40 Units/mg reported here correlate relatively well with the values reported by Yoshida and Xu *et al*. (K_m of 15 μM and specific activity of 57 Units/mg). The lower specific activity we report may be attributed to the difference in buffer pH (EPPS pH8 vs Tris-HCl pH8.4), since the specific activity increases with pH (*141*). The specific activity of TtPFK at 25°C is significantly lower than that of EcPFK and BsPFK (Table 2-1). The low activity at room temperature is not surprising since it has been noted that in nature the activities of the thermophilic enzymes at their native temperatures are comparable to that of the enzymes from mesophiles (*107, 108, 170*). As a consequence, at mesophilic temperatures the activity of the enzyme from the thermophile is expected to be low.

The binding of Fru-6-P in the absence of PEP is weakly cooperative, resulting in a Hill number of 1.6. Binding of PEP to TtPFK results in a decrease in apparent binding affinity for Fru-6-P, however, it also induces further homotropic cooperativity in Fru-6-P binding, increasing the Hill number to 2.5, thus the homotropic cooperativity of Fru-6-P binding is different for the free enzyme compared to the PEP-bound enzyme (Figure 2-2). The specific activity of the enzyme is not changed in the presence of PEP, confirming that PEP is a K-type effector (Figure 2-3). This finding is important because we were able to show that there is no V_{max} effect at the saturating concentrations of the inhibitor. Previously, the lack of the V_{max} effect of PEP was only inferred from the experiments done at subsaturating inhibitor concentrations. However, in order to understand the effect of the inhibitor in the turnover of the enzyme, it is necessary to

measure the turnover of the enzyme species that is bound to the inhibitor. Because of the antagonism between the inhibitor and substrate binding, both the substrate and the inhibitor will bind preferentially to the free enzyme, forming either YE or EA species. Because the population of the enzyme in the ternary complex YEA is very small, the turnover that is seen under these conditions comes mostly from the inhibitor-free form (EA), and cannot report on the effect of the inhibitor on the catalytic activity of the enzyme. In contrast, when the inhibitor is saturating, and the enzyme exists in the YE form, the binding of substrate will result in the formation of the ternary complex YEA and in the turnover of the inhibitor-bound species. In the present study we are able to show that the turnover seen for the EA form of the enzyme is the same as that seen for the YEA form, suggesting that the binding of PEP does not affect the catalytic activity of the TtPFK.

It is interesting to note that TtPFK exhibits very tight PEP binding compared to the PFK's from *Bacillus stearothermophilus* (*146*) and *E. coli* (*145*) while having a considerably weaker coupling between PEP and Fru-6-P binding (Table 2-1). This suggests that the binding affinity of the allosteric effector does not correlate with the magnitude of the allosteric effect it is able to produce. There are other examples that support this observation. For instance, the E187A substitution in EcPFK leads to the loss of activating effect of MgADP, although the binding of MgADP persists in this variant (*171*). Similar observations were made for the R252 variant of EcPFK, which can bind both allosteric effectors, but shows neither inhibition by PEP, nor activation by MgADP (*172*).

The coupling between PEP and Fru-6-P binding was also measured using intrinsic tryptophan fluorescence. The advantage of this method is that it gives us the ability to directly measure the dissociation constants for the substrate and the inhibitor in the absence of the coupling enzymes and the second substrate, MgATP. Since the wild type TtPFK does not have a native tryptophan, a tryptophan was introduced at position 313, the position of the native tryptophan in *E. coli* PFK. Using the initial velocity experiments, we verified that the binding and coupling parameters for PEP and Fru-6-P of the L313W variant are similar to those of the wild type enzyme and concluded that this variant is a suitable alternative to the wild type enzyme for the fluorescence studies (Table 2-2). The values of the coupling constant obtained by both methods agree very well (Table 2-2) and suggest that MgATP has no effect on the coupling between Fru-6-P and PEP. The dissociation constants for PEP obtained from the tryptophan fluorescence and the initial velocity experiments are also in good agreement. The only large discrepancy between the fluorescence and initial velocity experimental outcomes is the dissociation constant for Fru-6-P, which is roughly 200-fold lower when determined in the absence of MgATP. This comes as no surprise, as the antagonistic effect of ATP on Fru-6-P binding is also seen in PFK's from *E. coli* and *B. stearothermophilus* (*159, 173*). The results of this experiment also demonstrate the concept of reciprocity inferred from the thermodynamic linkage analysis, in that the binding of the allosteric effector elicits the same response on the binding of the substrate, as the substrate does on the allosteric effector.

The analysis of PEP coupling as a function of temperature using the initial velocity measurements shows, that the inhibition by PEP is entropically-driven in TtPFK, so that the strength of inhibition increases with increase in temperature (Figure 2-5). It is intriguing that the change in the enthalpy of inhibition is negative. This may suggest that any rearrangements in the three-dimensional static structures of the species on the right side of the disproportionation equilibrium compared to those on the left side would in fact reflect the activating effect of PEP on the enzyme. It is the change in the entropy between the two sides of the equilibrium that determines the positive sign of the coupling free energy. The linearity of the data (open circle) in Figure 2-5 within the sampled temperature range indicates that there is little if any change in the heat capacity associated with the inter-conversion among the free and liganded enzyme species represented in the disproportionation equilibrium. This indicates that the entropy associated with the inhibition by PEP stems mostly from the differences in the dynamic properties of the individual enzyme species as opposed to the differences in solvation of the different liganded states (*174*).

It is interesting to note that entropically-driven inhibition is also seen in the PFK from the moderate thermophile *B. stearothermophilus* (*146*), while the PFK from mesophilic *E. coli* displays enthalpically-driven inhibition by PEP (*145*). Although the analysis of the coupling parameter as a function of temperature has not been done in bacterial PFK's from other mesophiles and thermophiles, it is tempting to consider the possibility that the entropically-driven allosteric regulation is a common feature of the thermophilic PFK's. It is also worth noting that while the magnitude of the coupling

free energy of inhibition in TtPFK is relatively small at 25°C, at the physiologically relevant temperatures it may be comparable to that of EcPFK.

The binding of MgADP to TtPFK had little effect on the specific activity of the enzyme, but, interestingly, diminished the positive homotropic cooperativity in Fru-6-P binding, as evidenced by a reduction in the Hill numbers from 1.6 down to 1 (Figure 2-1). In contrast to the substantial inhibition by PEP, the magnitude of the activation of TtPFK by MgADP was quite small (Figure 2-3, Table 2-1). These finding are especially interesting in light of the results obtained by Yoshizaki (*175*), who measured the changes in the levels of metabolites in *T. thermophilus* under conditions of glycolysis and gluconeogenesis and reported that while the concentration of hexose phosphates and PEP varied inversely, the concentrations of adenylates (ATP, ADP, AMP) stayed consistent. It is possible that TtPFK has evolved the ability to maintain a slight basal level of activation due to the 30-40 μM ADP present in the cell. However, since the levels of ADP do not change appreciably, it may not play a central role in the regulation of this enzyme. In contrast, the PEP concentrations changed from negligible under the conditions of glycolysis to 0.17 mM under the conditions of gluconeogenesis, which, given the strong binding affinity of PEP and a substantial coupling free energy of inhibition, would afford PEP a central role in regulating the PFK in *T. thermophilus*.

The analysis of the coupling coefficient of activation as a function of temperature revealed several interesting findings. First is that the activation of TtPFK by MgADP is entropically driven, as is the inhibition by PEP. Second is that unlike in the case of inhibition by PEP, where the temperature dependence of the coupling coefficient is

described well by a straight line, the variation of $\ln Q_{ax}$ as a function of temperature exhibits curvature in the same temperature range. This non-linearity implies that there is a change in the heat capacity associated with the activation of TtPFK by MgADP. The negative change in heat capacity is conventionally linked to the removal of the non-polar surfaces from water (*174*), which suggests that there may be differences in the solvation states of the four species of the enzyme (E, XE, EA, and XEA). The third observation is that at temperatures below 20°C, MgADP loses its activating effects and becomes an inhibitor. While the existence of such a crossover temperature is implicit in the dependence of the coupling free energy on entropy, enthalpy and temperature, this crossover phenomenon is rarely observed at experimentally attainable temperatures. The few examples that have been reported include the allosteric effect of MgADP on the binding of Fru-6-P in BsPFK (at pH 6) and of IMP on the MgADP in *E. coli* carbamyl-phosphate synthetase, which switch from activation at temperatures above 16°C and 37°C, respectively, to inhibition below these temperatures (*106*). Similar phenomenon is observed for the effect of PEP on the binding of MgATP, which is slightly activating at room temperature, but becomes inhibitory at temperatures above 37°C (*145*).

CHAPTER III

ENHANCING THE ALLOSTERIC INHIBITION IN *THERMUS THERMOPHILUS* PHOSPHOFRUCTOKINASE

Phosphofructokinase (PFK) from the extreme thermophile *Thermus thermophilus* exhibits a much weaker coupling between the binding of phosphoenolpyruvate and Fru-6-P when compared to the PFK from another thermophile *Bacillus stearothermophilus* (BsPFK) at 25°C. In an attempt to pinpoint the source of the weaker coupling, we analyzed the available crystal structures of BsPFK in the apo form, as well as in the inhibitor (phosphoglycolate) and substrate and activator-bound forms (Fru-6-P and ADP) (*132, 152, 176*). Figure 3-1 shows a series of residues involved in an extensive hydrogen bonding network, which extends from the allosteric to the closest active site. We have previously shown this interaction to have the strongest contribution to the overall coupling free energy (*162*). This network includes residues D59, and, across the effector site interface, residues H215, T156, and T158, which in turn connect through D12 across the active site interface to R252, which binds Fru-6-P and was shown to be crucial for allosteric response in *E. coli* PFK (*172*). In either of the ligand-bound forms (PG or MgADP), the backbone of D59 interacts with the allosteric ligand and the side chain carboxyl forms a hydrogen bond with R154 (Figure 3-2). The backbone of R154 forms a hydrogen bond with the T158 in apo and Fru-6-P and ADP-bound form. In the Fru-6-P and ADP-bound structure, T158 interacts with H215 and connects though a water molecule to the side chain of the D59 hydroxyl. In the inhibitor-bound structure, T158 undergoes a large displacement due to the unwinding of the helix containing it and

forms a hydrogen bond with D12 across the active site interface. T156 located on the same helix is moved closer to the allosteric site and replaces T158 as a hydrogen bond partner for H215.

In TtPFK these interactions are not possible due to the nature of amino acids at these positions: N59, S215 and A158. It has been proposed that the lack of interactions between D59 and S215 would lead to destabilization of the effector site interface, and the lack of interaction between 158 and D12 would weaken the allosteric site interface (*165*). We hypothesized that, given the location of these residues between the nearest allosteric and active sites and the importance of R252 in the propagation of the allosteric response, this deficiency in interactions disrupts the path of allosteric communication between the two sites resulting in a weaker coupling between PEP and Fru-6-P binding, and that recreating this network would result in an increase in coupling. To test this hypothesis, we made single, double and triple chimeric substitutions at positions 59, 215, and 158 to the corresponding amino acids in BsPFK and measured the coupling between PEP and Fru-6-P using thermodynamic linkage analysis.

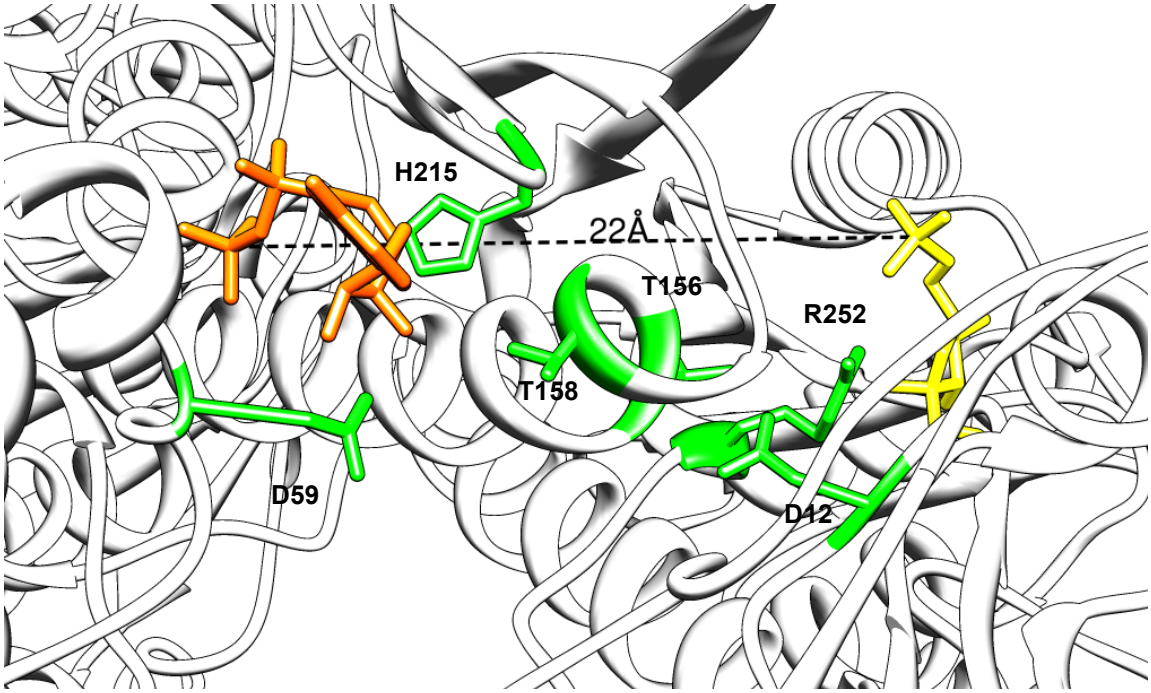

Figure 3-1 Residues located between the closest allosteric and active sites of BsPFK. The 22Å interaction in the Fru-6-P and ADP-bound BsPFK (*152*) is shown by the dotted line and is defined by the distance between the active and the allosteric site, measured from the gamma phosphate of ADP (orange) to the phosphate of Fru-6-P (yellow). Residues D59, H215, T158, T156, R252, and D12 (left to right) are highlighted in green.

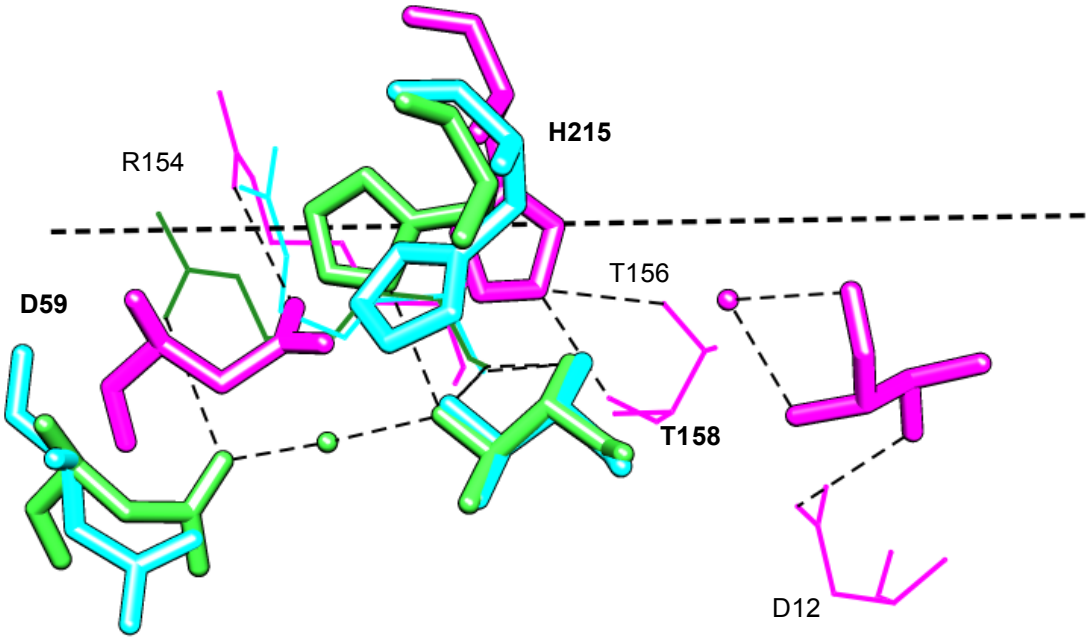

Figure 3-2 Hydrogen-bonding network involving residues D59, A158, and H215 in BsPFK. The crystal structure alignment includes three forms of BsPFK in apo (cyan) (*176*), PG- (magenta) (*132*), and Fru-6-P and ADP-bound (green) states (*152*). Residues D59, H215, and T158 are shown in stick. Residues involved in hydrogen bond interactions with the side chains of 59, 215, and 158 are shown in wire. The dotted line represents the 22Å interaction, defined by the distance between the gamma phosphate of MgADP and the phosphate of Fru-6-P located in the closest allosteric and active sites.

Materials and Methods

Materials

All chemical reagents used in buffers, protein purifications, and enzymatic assays were of analytical grade, purchased from Sigma-Aldrich (St. Louis, MO) or Fisher Scientific (Fair Lawn, NJ). The sodium salt of Fru 6-P was purchased from Sigma-Aldrich or USB Corporation (Cleveland, OH). NADH and dithiothreitol were purchased from Research Products International (Mt. Prospect, IL). Creatine kinase and the ammonium sulfate suspension of glycerol-3-phosphate dehydrogenase were purchased from Roche Applied Sciences (Indianapolis, IN). The ammonium sulfate suspensions of aldolase and triosephosphate isomerase, as wells as, the sodium salts of phosphocreatine and PEP were purchased from Sigma-Aldrich. The sodium salt of ATP was purchased from Sigma-Aldrich and Roche Applied Sciences. The experiments involving quantifying the allosteric response of TtPFK to MgADP were conducted using sodium salt of ATP purchased from Roche Applied. The coupling enzymes were dialyzed extensively against 50 mM MOPS-KOH, pH 7.0, 100 mM KCl, 5 mM $MgCl_2$, and 0.1 mM EDTA before use.

Mutagenesis

The pALTER plasmid with the wild type TtPFK gene was used as the starting template for mutagenesis (13). For double and triple substitutions, the plasmid containing the gene with the single or double mutation was used as a template. The mutations were introduced using QuikChange (Stratagene, La Jolla, CA) using a pair of complementary primers. The template primer used to construct N59D was

GCGGGACGTGGCCGATATCATCCAGCGGGG; the template primer used to construct A158T was GGGACACCGCGACGAGCCACGAGCG; the template primer used to construct S215H was GAGGCGGGGGAAGAAGCATTCCATCGTGGTGGTGG; the location of the substitution is underlined. The resulting sequences were verified via DNA sequencing at the Gene Technology Laboratory at Texas A&M University.

Protein expression and purification

The RL257 cells containing the plasmid with the TtPFK gene were induced with IPTG at the beginning of growth and grown at 30°C for 18 hours in LB (Luria-Bertani media: 10 g/L tryptone, 5 g/L yeast extract, and 10 g/L sodium chloride) 15 μg/mL tetracycline. The cells were harvested by centrifugation in a Beckman J6 at 4000 RPM and frozen at -80°C for at least 2 hours before lysis. The cells were resuspended in purification buffer (10 mM Tris-HCl, 1 mM EDTA; pH 8.0) and sonicated using the Fisher 550 Sonic Dismembrator at 0°C for 8-10 min using 15 second pulse/45 second rest sequence. The crude lysate was centrifuged using a Beckman J2-21 centrifuge at 22,500xg for 30 min at 4°C. The supernatant was heated at 70°C for 20 minutes, cooled, and centrifuged for 30 min at 4°C. The protein was then precipitated using 35% ammonium sulfate at 0°C and centrifuged. The pellet was dissolved in a minimal volume of 20 mM Tris-HCl, pH8 and dialyzed several times against the same buffer. The protein was then applied to a MonoQ column (GE Life Sciences), which was equilibrated with the purification buffer (20mM Tris-HCl, pH8) and eluted with a 0 to 1M NaCl gradient. Fractions containing PFK activity were analyzed for purity using

SDS-PAGE, pooled and dialyzed against the same buffer and stored at 4°C. The protein concentration was determined using the BCA assay (Pierce) using bovine serum albumin (BSA) as the standard.

Kinetic assays

Initial velocity measurements were carried out in 600 μL of buffer containing 50 mM EPPS-KOH, pH 8, 100 mM KCl, 5 mM $MgCl_2$, 0.1 mM EDTA, 2 mM dithiothreitol, 0.2 mM NADH, 250 μg of aldolase, 50 μg of glycerol-3-phosphate dehydrogenase, 5 μg of triosephosphate isomerase, and 0.5 mM ATP. 40 μg/mL of creatine kinase and 4 mM phosphocreatine were present in all assays performed in the absence of MgADP. The amount of Fru-6-P and PEP or MgADP used in any given assay varied. When measuring the activation by MgADP, phosphocreatine and creatine kinase were excluded from the assay mix, and equimolar MgATP was added with MgADP to avoid competition at the active site. The reaction was initiated by adding 10 μL of TtPFK appropriately diluted into 50 mM EPPS (KOH) pH 8, 100 mM KCl, 5 mM $MgCl_2$, 0.1 mM EDTA. The conversion of Fru-6-P to fructose-1,6-bisphosphate was coupled to the oxidation of NADH, which resulted in a decrease in absorbance at 340nm. The rate of the decrease in A_{340} was monitored using a Beckman Series 600 spectrophotometer.

Data analysis

Data were fit using the non-linear least-squares fitting analysis of Kaleidagraph software (Synergy). The initial velocity data were plotted against concentration of Fru-6-P and fit to the following equation:

$$v^{\circ} = \frac{V[A]^{n_H}}{K_a^{n_H} + [A]^{n_H}} \tag{3-1}$$

where v° is the initial velocity, [A] is the concentration of the substrate Fru-6-P (or ATP), V is the maximal velocity, n_H is the Hill coefficient, and K_a is the Michaelis constant defined as the concentration of substrate that gives one-half the maximal velocity. For the reaction in rapid equilibrium, K_a is equivalent to the dissociation constant for the substrate from the binary enzyme-substrate complex.

The K_a and K_y values obtained from the initial velocity and fluorescence experiments were plotted against effector or substrate concentrations and fit to Equation 3-2:

$$K_a = K_{ia}^{\circ}\left(\frac{K_{iy}^{\circ} + [Y]}{K_{iy}^{\circ} + Q_{ay}[Y]}\right) \tag{3-2}$$

where K_{ia}° is the dissociation constant for Fru-6-P in the absence of allosteric effector, Y is PEP, K_{iy}° is the dissociation constant for PEP in the absence of Fru-6-P, and Q_{ay} is the coupling coefficient (*148, 166, 167*). When equation 3-3 is applied to the allosteric action of MgADP, the subscripts are changed from "y" to "x", and MgADP is designated as "X", to be consistent with the notation we have used previously (*145*).

Q_{ay} is defined as the coupling constant, which describes the effect of allosteric effector on the binding of the substrate (and *vice versa*) and is defined by Equation 3-3:

$$Q_{ay} = \frac{K_{ia}^{\circ}}{K_{ia}^{\infty}} = \frac{K_{iy}^{\circ}}{K_{iy}^{\infty}} \tag{3-3}$$

where K_{ia}° and K_{ia}^{∞} represent the dissociation constants for the substrate in the absence and saturating presence of the allosteric effector, respectively, and K_{iy}° and K_{iy}^{∞} represent the dissociation constants for the allosteric effector in the absence and saturating presence of the substrate, respectively.

The coupling constant Q_{ay} is related to the coupling free energy (ΔG_{ay}) and its enthalpy (ΔH_{ay}) and entropy (ΔS_{ay}) components through the following relationship (*105*):

$$\Delta G_{ay} = -RT\ln(Q_{ay}) = \Delta H_{ay} - T\Delta S_{ay} \quad (3\text{-}4)$$

The coupling entropy and enthalpy components were determined by measuring the coupling constant as a function of temperature and the data were fit to Equation 3-5:

$$\ln Q_{ay} = \frac{\Delta S_{ay}}{R} - \frac{\Delta H_{ay}}{R}\left(\frac{1}{T}\right) \quad (3\text{-}5)$$

where ΔG_{ay} is the coupling coefficient, ΔS_{ay} is the coupling entropy, ΔH_{ay} is coupling enthalpy, T is absolute temperature in K, and R is gas constant (R=1.99 cal K^{-1} mol^{-1})

Crystal structure analysis

The analysis of crystal structures of apo (*176*), phosphoglycolate- (*132*) and Fru-6-P and ADP-bound (*152*) BsPFK was done using the UCSF CHIMERA software.

Results

To establish the magnitude of PEP inhibition in the single, double and triple variants of TtPFK, the apparent dissociation constants for Fru-6-P were determined as a function of PEP concentrations. The individual titration curves were fit to Equation 3-1 to obtain the dissociation constant for Fru-6-P as well as the specific activity and the Hill number. The specific activities and the Hill numbers for the single, double, and triple variants are presented in Table 3-1.

The data for the apparent dissociation constants as a function of PEP concentration were fit to Equation 3-2 to obtain the coupling parameter (Q_{ay}) and the dissociation constant for PEP (K_{iy}°), which were used to calculate the binding and coupling free energies reported in Figure 3-3 A-C. It is interesting to note that each of the mutations produced roughly 1 kcal mol^{-1} increase in the coupling free energy. The substitution of N59D also resulted in a large decrease in PEP binding affinity without a major effect on the Fru-6-P binding affinity. A158T resulted in a slight increase in F6P binding and a slight decrease in PEP binding. S215H did not have a significant effect on PEP or Fru-6-P binding. The fact that N59D produced an increase in coupling while making the PEP binding weaker, and A158T and S215H produced a similar increase while having very modest or no effect on the PEP binding, suggests that the binding of the inhibitor and the actual inhibition are achieved through somewhat independent routes.

Table 3-1 Specific activities and Hill numbers for single, double, and triple variants of TtPFK. Data were collected at pH 8, 25°C[d]

	SA (U/mg)	Hill number
N59D	33	1.2±0.1
A158T	40	1.6±0.2
S215H	36	1.8±0.3
N59D/A158T	23	0.95±0.07
N59D/S215H	41	1.8±0.2
A158T/S215H	26	1.1±0.1
N59D/A158T/S215H	46	1.0±0.1

[d] The error represents the standard error calculated for the fit of the data to equation 3-1.

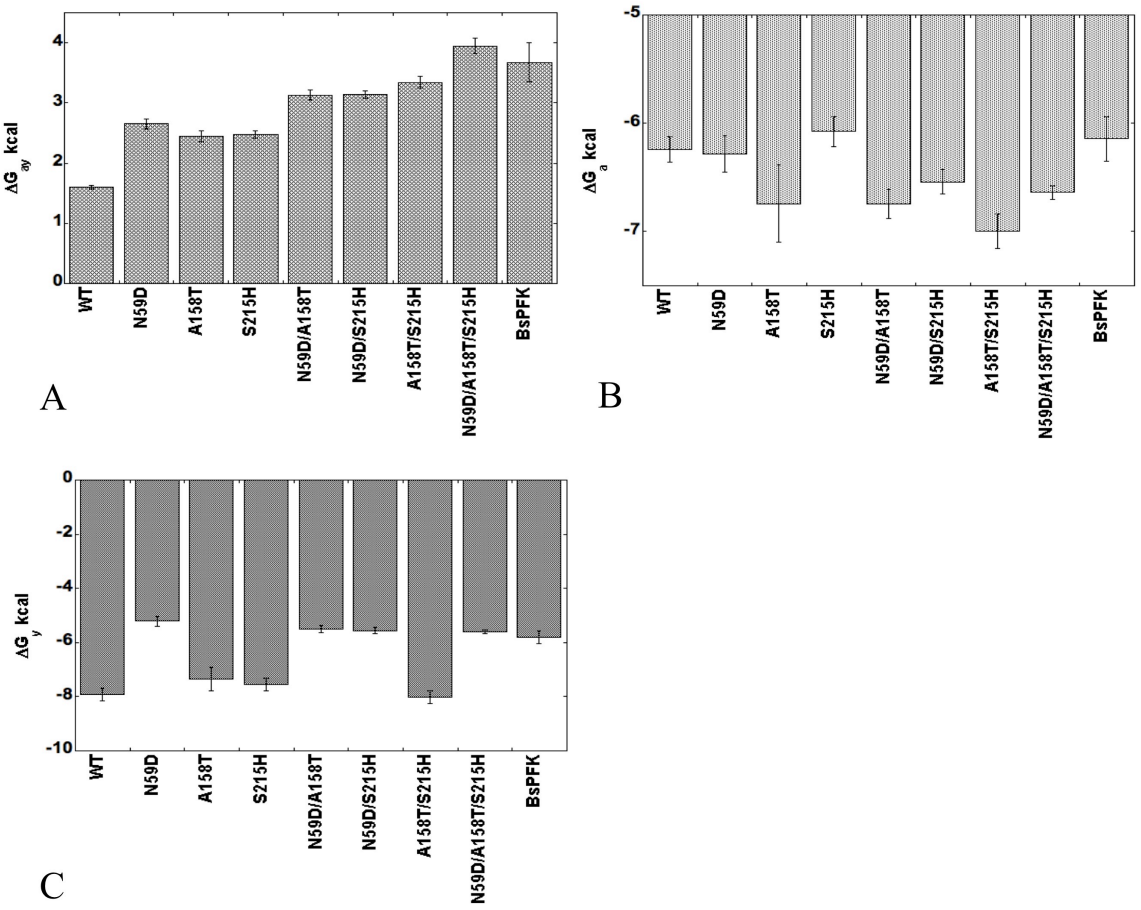

Figure 3-3. Diagram summarizing the binding free energies and the coupling free energies for the binding of Fru-6-P and PEP in wild type TtPFK and BsPFK and the chimeric variants of TtPFK. (A) Coupling free energies for the binding of Fru-6-P and PEP. (B) Binding free energies for Fru-6-P. (C) Binding free energies for PEP. Data were collected at pH 8, 25°C. Error bars represent the standard error calculated for the fit of the data to equation 3-2.

Each combination of the double substitutions N59D/A158T, N59D/S215H, and A158T/S215H produced a further increase in coupling free energy (Figure 3-3C). The overall changes in the coupling free energy for the double mutants appeared to be roughly a sum of those resulting from the individual mutations, suggesting once again that these residues may act independently in increasing the inhibitory response of the enzyme. Each of the double substitutions also retains the ligand binding features of the single mutations it contains, for instance, both combinations containing N59D show a much weaker PEP binding, while those containing A158T show a slightly improved Fru-6-P binding (Figure 3-3). The TtPFK variant containing the N59D/A158T/S215H substitution shows an even further increase of the coupling free energy between PEP and Fru-6-P and produced the inhibition on the level similar to what is seen in BsPFK (Figure 3-3C, Table 3-2). This variant also shows weaker PEP binding similar to what is seen in N59D variant and a slightly stronger Fru-6-P binding, seen in the A158T variant (Figure 3A and B).

Table 3-2 The summary of kinetic and thermodynamic parameters for wild type TtPFK, BsPFK and TtPFK N59D/A158T/S215H chimeric variant, at pH 8 and 25°C[e].

	TtPFK	TtPFK N59D/A158T/S215H	BsPFK
K_{ia}° (μM)	27.0 ± 0.6	0.013± 0.0002	31 ± 2
K_{ix}° (μM)	0.4 ± 1	ND	19 ± 2
Q_{ax}	1.6 ± 0.1	ND	1.70 ± 0.01
K_{iy}° (μM)	1.58 ± 0.07	0.079 ± 0.002	93 ± 6
Q_{ay}	0.067 ± 0.002	0.0012 ± 0.0007	0.0021 ± 0.0003
ΔG_{ay} (kcal mol^{-1})	1.60 ± 0.02	3.95 ± 0.03	3.67 ± 0.1
ΔH_{ay} (kcal mol^{-1})	-7.5 ± 0.3	-11.0± 0.5	-10 ± 1
$T\Delta S_{ay}$ (kcal mol^{-1})	-9.1 ± 0.3	-14.9± 0.5	-14 ± 1

[e] A represents Fru-6-P, X represents MgADP and Y represents PEP. The value for $T\Delta S_{ay}$ was calculated using the values for ΔG_{ay} and ΔH_{ay} at 25°C. Errors represent the standard error calculated for the fit of the data to equation 3-2 or 3-5.

Since the triple chimeric variant N59D/A158T/S215H produced such a significant increase in coupling free energy of inhibition, we wanted to evaluate which components of coupling free energy were affected and to what degree. To assess the dependence of coupling on temperature and establish the entropic and enthalpic components of PEP inhibition in N59D/A158T/S215H TtPFK, we analyzed the coupling coefficient as a function of temperature (Figure 3-4). The values for ΔH_{ay} and $T\Delta S_{ay}$ were determined to be -11.0±0.5 kcal mol^{-1} and -14.9±0.5 kcal mol^{-1}, respectively. It was surprising to see that both the entropy and enthalpy of PEP inhibition of the triple variant compared much better with wild type BsPFK than with wild type TtPFK (Table 3-2).

After achieving such a large increase in the coupling free energy of inhibition upon the introduction of the N59D/A158T/S215H revertant mutation, it was curious to see if this mutation would have a similar effect on the coupling free energy of activation by MgADP. To establish the effect of the N59D/A158T/S215H mutation on the binding and coupling of MgADP, the dissociation constants for F6P were measured as a function of concentration of MgADP. Equimolar MgATP was added to avoid competition at the active site. The data for the apparent dissociation constants as a function of MgADP concentration were fit to Equation 2, which yielded a coupling coefficient of 1 (Figure 3-5), suggesting that either MgADP does not bind to this variant, or it does bind, but elicits no allosteric response.

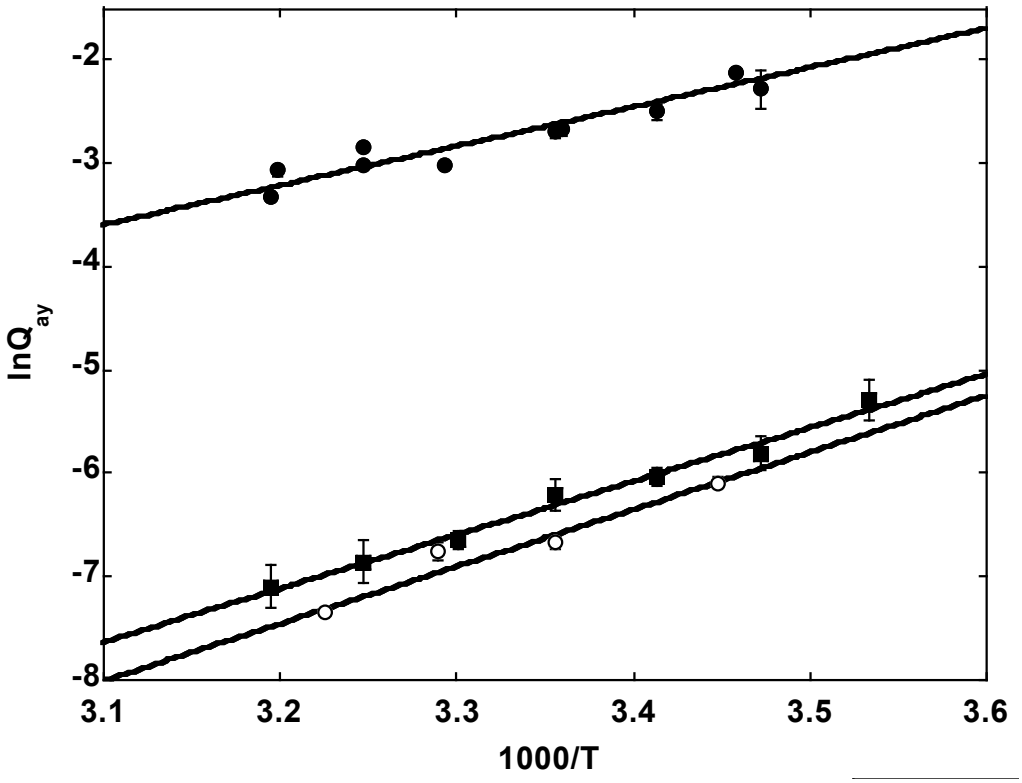

Figure 3-4 Van't Hoff analysis of $\ln Q_{ay}$ for wild type TtPFK, BsPFK, and the N59D/A158T/S215H variant of TtPFK. Data for $\ln Q_{ay}$ are shown as a function of temperature for wild type TtPFK (closed circles), the N59D/A158T/S215H variant of TtPFK (open circles), and wild type BsPFK (solid squares). The data were fit to equation 3-5 (solid line) to obtain the enthalpy component of the coupling free energy at 25°C. Data were collected at pH 8. Error bars represent the standard error calculated for the fit of the data to equation 3-2.

To verify whether the MgADP is able to bind to the allosteric site of this variant, the PEP binding was measured as a function of MgADP concentration. PEP binding was not affected when 0-1mM MgADP was added to the assays, suggesting that MgADP doesn't bind to the N59D/A158T/S215H variant of TtPFK at physiological concentrations (Figure 3-5 inset). To pinpoint which of the point mutations may be responsible for diminished MgADP binding, we measured the effect of the N59D, A158T and S215H on the binding and coupling of MgADP. Similarly to the triple variant, the S215H mutant showed no binding to MgADP, suggesting that the perturbations caused by introducing a histidine at position 215 greatly impair MgADP ability to bind to TtPFK (Figure 3-5). As shown in Figure 3-6, both N59D and A2158T variants yielded a slight increase in the magnitude of the coupling free energies compared to wild type TtPFK.

Discussion

It was exciting and surprising to see such a large increase in the coupling free energy for inhibition upon introducing the triple chimeric substitution N59D/A158T/S215H. It was even more surprising, in the context of our initial hypothesis, to see a large increase in coupling free energy resulting from each individual N59D, A158T, and S215H mutations. The simplest explanation of why we observed such an improvement in coupling in the absence of a completely reconstructed network is that N59, A158, and S215 are still able to partially fulfill their roles in conducting the allosteric signal, and substituting the chimeric mutants simply improves their efficiency.

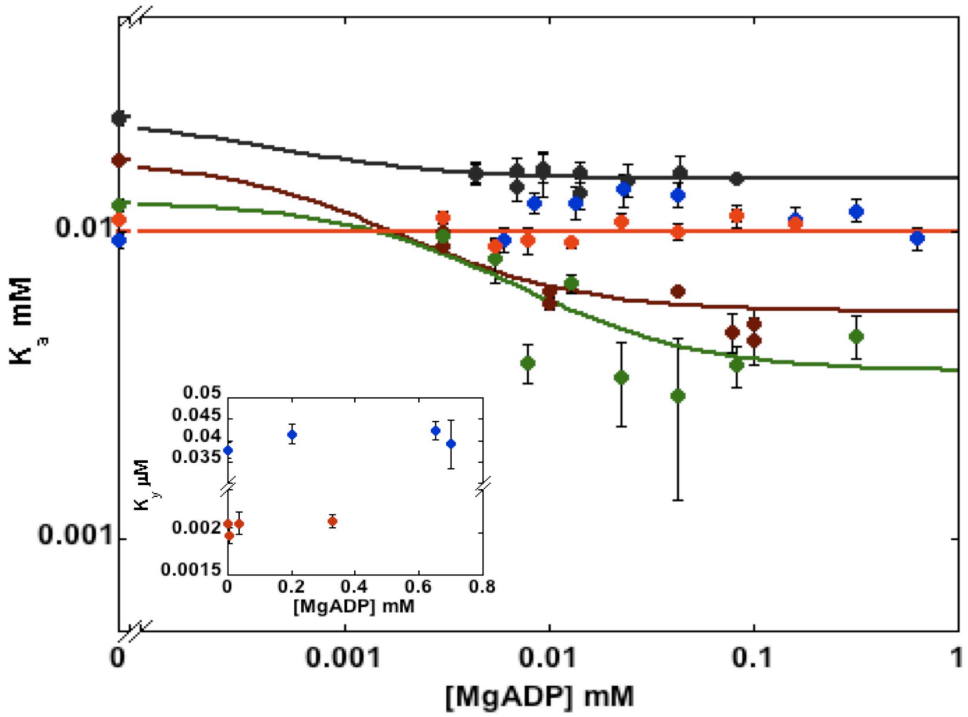

Figure 3-5 The change in the apparent dissociation constants for substrate as a function of MgADP concentration for wild type TtPFK. The apparent dissociation constants (K_a) for Fru-6-P as a function of MgADP are shown for wild type TtPFK (black), and the chimeric variants N59D (maroon), 158T (green), S215H (red), and N59D/A158T/S215H (blue). Experiments were performed at pH 8 and 25°C. The data were fit to equation 3-2 to obtain the dissociation constants for MgADP (K_{ix}°) and the coupling constant Q_{ax} . The inset is a plot of the apparent dissociation constants for PEP (K_{iy}°) as a function of the MgADP concentration for the S215H (red) and N59D/A158T/S215H (blue) variants. The error bars represent the standard error calculated for the fit of the data to equation 3-2.

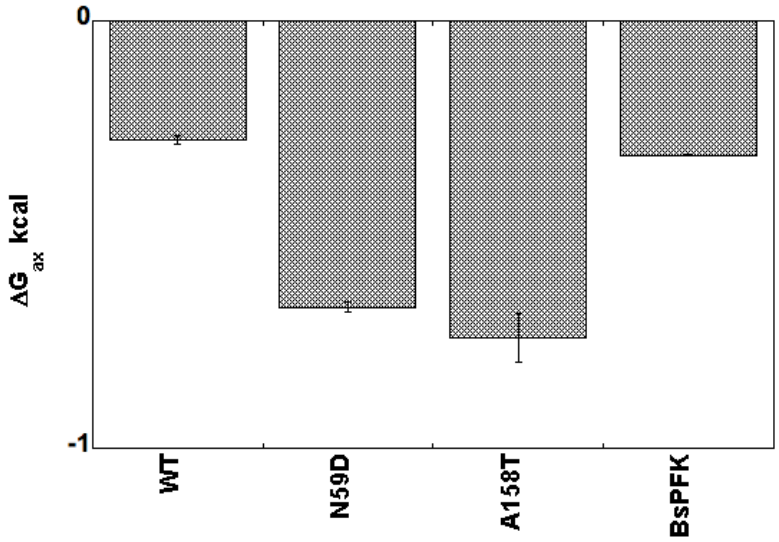

Figure 3-6 Diagram summarizing the coupling free energies for the binding of Fru-6-P and MgADP in wild type TtPFK, BsPFK and the N59D and A158T variants of TtPFK. The experiments were performed at pH 8, 25°C. The error bars represent the standard error calculated from the fit of the data to equation 3-2

Another possible explanation is that there is an independent contribution of each of these residues to the proliferation of allosteric response and the effect of these substitutions is seen not from the single closest heterotropic interaction, which contributes the most to the overall coupling free energy, but from the more distant interactions, whose contributions are smaller but still significant (*162, 177-179*). Figure 3-7 shows where these residues lie in reference to the four unique heterotropic interactions in a single subunit. We can see that A158T and S215 lie along the strongest 22Å interaction, while N59D is in about equal proximity to both 45Å and 30Å interactions. In this context, it would be possible to explain the independent contribution of N59D substitution to the increase in free energy of coupling since it is far removed from positions 158 and 215 within the single subunit. We cannot however use the same logic to explain the lack of synergism between positions 158 and 215. While it is clear that residues N59, A158, and S215 lie on the path of the inhibitory signal and play an important role in propagating that signal, without a crystal structure of TtPFK we cannot be sure that the contacts made by residues 59, 158 and 215 in TtPFK are the same as those predicted for BsPFK.

The analysis of PEP coupling as a function of temperature showed that the inhibition by PEP is still entropically driven in N59D/A158T/S215H TtPFK, just as it is the wild type enzyme, however, the entropy and enthalpy values more closely resemble those of BsPFK. The observed change in enthalpy of about 3.5 kcal mol^{-1} is quite modest and corresponds roughly to the formation of two new hydrogen bonds. It is interesting that with the introduction of N59D/A158T/S215H, we observed a decrease in

enthalpy, which means that the newly formed interactions actually favor activation. This decrease in enthalpy is offset with an even larger decrease in entropy resulting in a larger overall ΔG_{ay}.

What is also intriguing is that there is little change in the level of activation by MgADP displayed by the N59D and A158T variants, while the effect of these mutations on the magnitude of inhibition by PEP is quite large. This suggests that while N59 and A158 play an important role in the inhibition by PEP, they may be less involved in the path of allosteric activation by MgADP. It is also interesting that S215H greatly augmented the binding of MgADP, while having no effect on the binding of PEP. This indicates that the residue at position 215 plays a dual role in activator binding and in the propagation of the inhibitory signal.

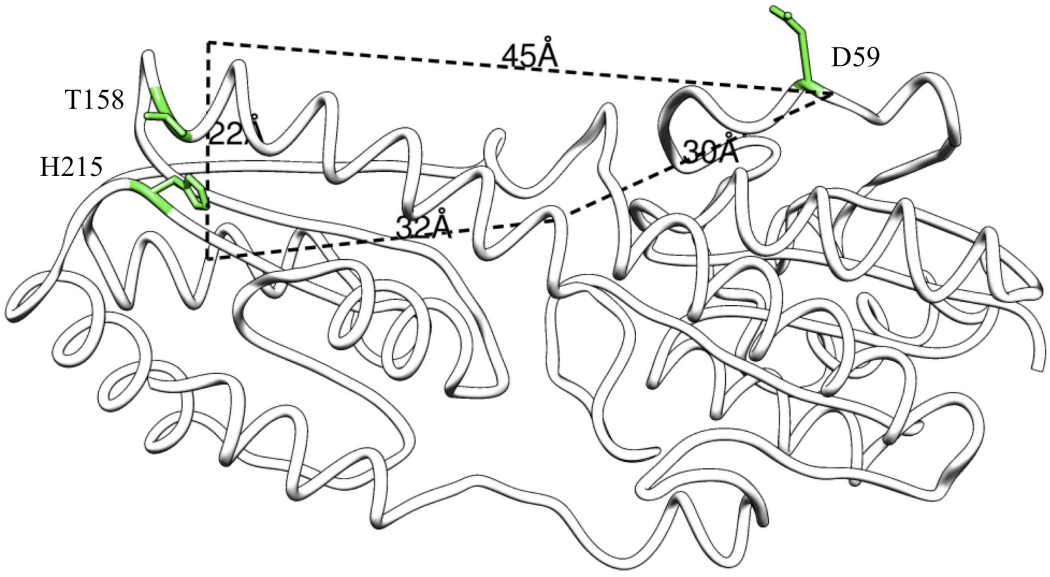

Figure 3-7 Location of residues 59, 158, and 215 in reference to the four unique heterotropic interactions within the single monomer. Residues D59, A158 and S215 are highlighted in green. The individual 22Å, 30Å, 32Å, and 45Å interactions are shown in dotted lines.

CHAPTER IV

THE ROLES OF THE NON-CONSERVED RESIDUES R55 AND N59 IN THE TIGHT BINDING OF PHOSPHOENOLPYRUVATE IN PHOSPHOFRUCTOKINASE FROM *THERMUS THERMOPHILUS*

Phosphofructokinase 1 (PFK 1) catalyzes the phosphoryl transfer from MgATP to fructose-6-phosphate (Fru-6-P) forming fructose-1, 6-bisphosphate and MgADP. Generally, bacterial PFK 1 is active as a homotetramer and contains four identical active sites and four identical allosteric sites, which are formed at the interface between the monomers, such that each monomer contributes one half of the binding site. Phosphofructokinase (PFK) from the extreme thermophile *Thermus thermophilus* has a much higher binding affinity for its allosteric inhibitor PEP when compared to PFK's from other organisms. To gain insight into the source of this tight binding, we analyzed the allosteric binding site using the crystal structures and sequence alignments of a PFK from another thermophile *Bacillus stearothermophilus* (BsPFK) as well as the weakly allosteric PFK from *Lactobacillus delbruekii ssp bulgaricus* (LbPFK), which has an extremely poor PEP binding affinity (*180*).

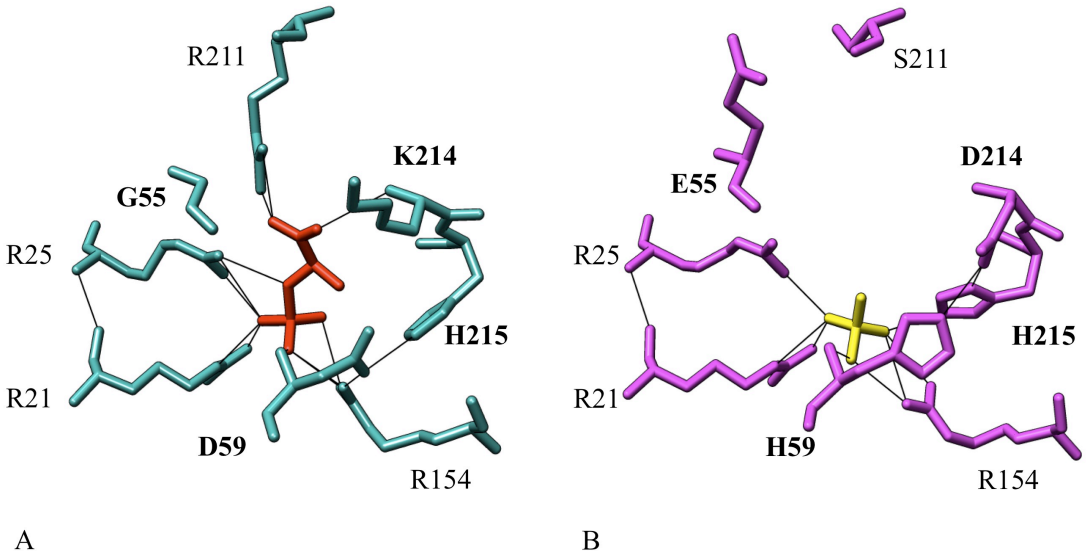

Figure 4-1 Allosteric site residues in BsPFK and LbPFK. (A) The allosteric site of D12A BsPFK in cyan with PEP shown in red. (B) The allosteric site of LbPFK in magenta with SO_4 shown in yellow. The hydrogen bonds shown in black were identified using UCSF CHIMERA.

While most of the residues in the allosteric site are conserved among the three enzymes, there are several residues that have amino acids unique to TtPFK (Figure 4-1). One of them is at position 55, which is an arginine in TtPFK, whereas it is a glycine in BsPFK and a glutamate in LbPFK. From the crystal structure of the LbPFK it can be seen that the side chain of glutamate 55 is pointed out from the allosteric binding pocket. It is possible that the positively charged side chain of the arginine in TtPFK may face into the allosteric site and potentially interact with the carboxyl of PEP. To investigate the consequence of removing the positive charge at this position as well as replacing it with a negative charge, we made mutations of R55 to glycine as well as glutamate.

Another region of interest contains the non-conserved residues at positions 59 and 214 and 215 (Figure 4-1). Our previous results obtained with the N59D variant of TtPFK show that this substitution results in a 100-fold decrease in the binding affinity of PEP, indicating that N59 is important for the binding of PEP. Residue 59 is an aspartate in BsPFK and a histidine in LbPFK. From the crystal structure of the D12A BsPFK bound to PEP, we can see that the backbone of D59 forms a hydrogen bond to the phosphate of PEP (also seen in *E. coli* PFK), while the sidechain forms hydrogen bonds across the interface to H215 and the conserved R154. In LbPFK the backbone nitrogen of the H59 coordinates the sulfate located at the same position as the phosphate of PEP in the BsPFK structure. The side chain of H59 forms a hydrogen bond to aspartate 214, thus forcing histidine 215 into the PEP binding pocket. In TtPFK, residue 59 is an asparagine, which, in contrast to BsPFK's D59, cannot be ionized. The interaction of N59 across the interface with the serine at position 215 is also unlikely, given the large

distance between the two residues. However, it is possible that N59 is still able to form a non-covalent interaction across the interface with K214. To test whether the absence of a charge and/or the deficiency in the network link across the interface in this region can explain the tighter PEP binding in TtPFK, we made a series of individual and combination mutations at positions 59, 214, and 215, to introduce the charge and to potentially recreate the interaction across the interface, which are seen in BsPFK and LbPFK.

Materials and Methods

Materials

All chemical reagents used in buffers, protein purifications, and enzymatic assays were of analytical grade, purchased from Sigma-Aldrich (St. Louis, MO) or Fisher Scientific (Fair Lawn, NJ). The sodium salt of Fru-6-P was purchased from Sigma-Aldrich or USB Corporation (Cleveland, OH). NADH and dithiothreitol were purchased from Research Products International (Mt. Prospect, IL). Creatine kinase and the ammonium sulfate suspension of glycerol-3-phosphate dehydrogenase were purchased from Roche Applied Sciences (Indianapolis, IN). The ammonium sulfate suspensions of aldolase and triosephosphate isomerase, as well as, the sodium salts of phosphocreatine and PEP were purchased from Sigma-Aldrich. The sodium salt of ATP was purchased from Sigma-Aldrich and Roche Applied Sciences. The coupling enzymes were dialyzed extensively against 50 mM MOPS-KOH, pH 7.0, 100 mM KCl, 5 mM $MgCl_2$, and 0.1 mM EDTA before use.

Mutagenesis

The pALTER plasmid with the wild type TtPFK gene was used as the starting template for mutagenesis (13). Mutagenesis was performed following the QuikChange Site-Directed Mutagenesis protocol (Stratagene, La Jolla, CA). Two complementary oligonucleotides were used to produce the mutant genes, for which the template oligos are shown in Table 4-1.

The resulting sequences were verified via DNA sequencing at the Gene Technology Laboratory at Texas A&M University.

Protein expression and purification

The RL257 (*164*) cells containing the plasmid with the TtPFK gene were induced with IPTG at the beginning of growth and grown at 30°C for 18 hours in LB (Luria-Bertani media: 10 g/L tryptone, 5 g/L yeast extract, and 10 g/L sodium chloride) with 15 μg/mL tetracycline. The cells were harvested by centrifugation in a Beckman J6 at 4000 RPM and frozen at -80°C for at least 2 hours before lysis. The cells were resuspended in purification buffer (10 mM Tris-HCl, 1 mM EDTA, pH 8.0) and sonicated using the Fisher 550 Sonic Dismembrator at 0°C for 8-10 min using a 15 second pulse/45 second rest sequence. The crude lysate was centrifuged using a Beckman J2-21 centrifuge at 22,500xg for 30 min at 4°C. The supernatant was heated at 70°C for 20 minutes, cooled, and centrifuged for 30 min at 4°C. The protein was then precipitated using 35% ammonium sulfate at 0°C and centrifuged. The pellet was dissolved in minimal volume of 20 mM Tris-HCl, pH 8.0 and dialyzed several times against the same buffer. The protein was then applied to a MonoQ column (GE Life Sciences), which was

Table 4-1 Template oligos used to introduce substitutions at positions 55, 59, 214, and 215.[f]

Substitution	Template oligo
R55G	CCCTTGGGGGTGGGCGACGTGGCCAAC
R55E	GTGCCCTTGGGGGTGGAAGACGTGGCCAACATC
N59A	GCGGGACGTGGCCGCCATCATCCAGCGGGG
N59D	GCGGGACGTGGCCGATATCATCCAGCGGGG
N59H	GCGGGACGTGGCCCATATCATCCAGCGGGG
N59K	GCGGGACGTGGCCAAAATCATCCAGCGGGG
K214A	GGCGGGGGAAGGCGAGCTCCATCGTGGTGG
K214D	GGCGGGGGAAGGATAGCTCCATCGTGGTGG
S215H	GAGGCGGGGGAAGAAGCATTCCATCGTGGTGGTGG
K214D/S215H	CCCAGAGGCGGGGGAAGGATCATTCCATCGTGGTGGTGGC

[f] The underlined bases designate the site of the substitution.

equilibrated with the purification buffer (20mM Tris-HCl, pH 8.0) and eluted with a 0 to 1 M NaCl gradient. Fractions containing PFK activity were analyzed for purity using sodium dodecyl sulfate polyacrylamide gel electrophoresis (SDS-PAGE), pooled and dialyzed against the same buffer and stored at 4°C. The protein concentration was determined using the BCA assay (Pierce) using bovine serum albumin (BSA) as the standard.

Kinetic assays

Initial velocity measurements were carried out in 600 μL of buffer containing 50 mM EPPS-KOH, pH 8, 100 mM KCl, 5 mM $MgCl_2$, 0.1 mM EDTA, 2 mM dithiothreitol, 0.2 mM NADH, 250 μg of aldolase, 50 μg of glycerol-3-phosphate dehydrogenase, 5 μg of triosephosphate isomerase, and 0.5 mM ATP. 40 μg/mL of creatine kinase and 4 mM phosphocreatine were present in all assays. The amount of Fru-6-P and PEP used in any given assay varied. The reaction was initiated by adding 10 μL of TtPFK appropriately diluted into 50 mM EPPS (KOH) pH 8, 100 mM KCl, 5 mM $MgCl_2$, 0.1 mM EDTA. The conversion of Fru-6-P to Fru-1, 6-bisphosphate was coupled to the oxidation of NADH, which resulted in a decrease in absorbance at 340 nm. The rate of the decrease in A_{340} was monitored using a Beckman Series 600 spectrophotometer.

Data analysis

Data were fit using the non-linear least-squares fitting analysis of Kaleidagraph software (Synergy). The initial velocity data were plotted against concentration of Fru-6-P and fit to the following equation:

$$v^{\circ} = \frac{V[A]^{n_H}}{K_a^{n_H} + [A]^{n_H}} \tag{4-1}$$

where v° is the initial velocity, [A] is the concentration of the substrate Fru-6-P (or ATP), V is the maximal velocity, n_H is the Hill coefficient, and K_a is the Michaelis constant defined as the concentration of substrate that gives one-half the maximal velocity. For the reaction in rapid equilibrium, K_a is equivalent to the dissociation constant for the substrate from the binary enzyme-substrate complex.

The nature and magnitude of allosteric response to the allosteric effector binding were measured by repeating the initial velocity experiments with the successive addition of zero to saturating concentrations of the effector. The K_a values obtained from these experiments were plotted against effector concentrations and fit to (*148, 166, 167*):

$$K_a = K_{ia}^{\circ}\left(\frac{K_{iy}^{\circ} + [Y]}{K_{iy}^{\circ} + Q_{ay}[Y]}\right) \tag{4-2}$$

where K_{ia}° is the dissociation constant for Fru-6-P in the absence of allosteric effector, Y is PEP, K_{iy}° is the dissociation constant for PEP in the absence of Fru-6-P, and Q_{ay} is the coupling coefficient.

In the cases when the upper plateau cannot be established, the data are fit the modified form of Equation 4-2, which assumes infinite coupling, i.e. $Q_{ay} = 0$

$$K_a = K_{ia}^{\circ}\left(\frac{K_{iy}^{\circ} + [Y]}{K_{iy}^{\circ}}\right) \tag{4-3}$$

Structure analysis

The analysis of crystal structures of sulfate-bound LbPFK (*180*) and PEP-bound D12A BsPFK was done using UCSF CHIMERA software.

Results

To understand the potential role of the arginine at position 55 we substituted the arginine at this position with either glycine or glutamine. The plots of initial velocity as a function of the Fru-6-P concentration were fit using Equation 4-1. The values for the specific activity and the Hill numbers for variants discussed in this chapter are given in Table 4-2. The plots of the apparent dissociation constants for Fru-6-P as a function of the PEP concentration are presented in Figure 4-2. The data in these plots are fit to Equation 4-2 for wild type and R55G variant or Equation 4-3 for the R55E variant. The binding affinity for PEP is strongly augmented in both R55G and R55E variants (Figure 4-3B). The Q_{ay} value for the R55E variants could not be determined because the upper plateau is not well defined. However, the data in Figure 4-2 suggest that the coupling between the binding of Fru-6-P and PEP is stronger in both R55G and R55E variants when compared to wild type TtPFK. The binding affinity for Fru-6-P is slightly higher for both variants (Figure 4-3A).

In addition to the N59D variant, described earlier in Chapter III, three different mutations were introduced at position 59 to assess the role of this residue in the binding of PEP: N59A, N59H (to LbPFK), and N59K. These mutations had little effect on the binding affinity for Fru-6-P (Figure 4-3A), but all resulted in diminished binding affinity for PEP (Figure 4-3B). The substitution N59D had the most dramatic effect on the

binding affinity for PEP, producing a 2.5 kcal mol^{-1} increase in the binding free energy for PEP, while the N59H substitution resulted in less than 1 kcal mol^{-1} increase in binding free energy. These substitutions also resulted in significant changes in the coupling free energy between PEP and Fru-6-P binding (Figure 4-3C). The N59D substitution resulted in an increase in the coupling free energy, while N59A, N59H, and N59K reduced the coupling free energy compared to that of the wild type TtPFK.

To recreate the interactions seen in BsPFK and LbPFK between residue N59 to residues 214 or 215 across the interface, variants N59D/S215H (to BsPFK) and N59D/K214D/S215H (to LbPFK) were constructed. Both of these variants showed an increase in the binding free energy for PEP (Figure 4-3B). However, when the individual mutations contained within these variants were analyzed, it became evident that the drop off in the PEP binding affinity was due largely to the K214D mutation (Figure 4-3B). K214A mutations did not dramatically augment the PEP binding affinity, suggesting that lysine 214 is not directly involved in the binding of PEP, however, introducing an aspartate at position 214 is detrimental to the binding of PEP (Figure 4-3B).

Table 4-2 Specific activities and Hill numbers for single, double, and triple variants of TtPFK[g].

	SA (U/mg)	Hill number
R55G	53	1.5±0.1
R55E	45	1.4±0.2
N59A	27	1.2±0.1
N59H	47	1.2±0.1
N59K	43	1.6±0.1
K214A	56	2.0±0.2
K214D	20	2.2±0.2
N59D/S215H	32	1.3±0.2
N59H/K214D/S215H	44	1.9±0.2

[g] Data were collected at pH 8, 25°C. The errors represent the standard errors calculated from the fit of the data to 4-1

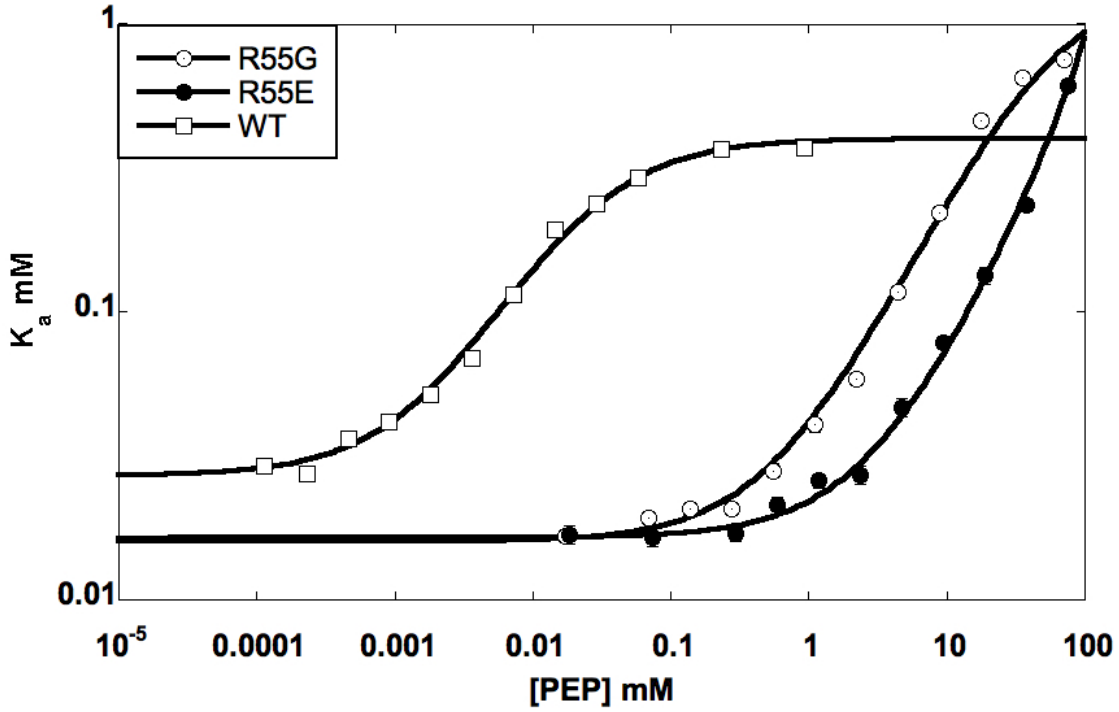

Figure 4-2 Apparent dissociation constants for Fru-6-P (K_a) as a function of PEP concentration for the wild type TtPFK and the R55G and R55E variants. The experiments were performed at pH 8 and 25°C. The data for wild type and R55G variant were fit to Equation 4-2 to obtain the dissociation constant for PEP (K_{iy}°) and the coupling constant (Q_{ay}). The data for the R55E variant were fit to Equation 4-3 to obtain the dissociation constant for PEP (K_{iy}°). The error bars represent the standard errors calculated from the fit of the data to Equation 4-1

Discussion

Replacing the non-conserved arginine 55 with glycine, as found in BsPFK, resulted in a 3.5 kcal mol^{-1} increase in binding free energy for PEP in TtPFK (Figure 4-3B). This suggests that the arginine 55 may be critical for the enhanced PEP binding seen in TtPFK. The substitution with a glutamate at position 55, as found in LbPFK, produced a 4.5 kcal mol^{-1} increase in the binding free energy for PEP. It is interesting to note that the binding of PEP to the R55G variant is 1.5 kcal mol^{-1} weaker than what is seen in wild type BsPFK and the binding of PEP to the R55E variant is about 1.5 kcal mol^{-1} stronger compared to wild type LbPFK (Figure 3B). Furthermore, when the E55R substitution was made in LbPFK in an attempt to enhance the binding of PEP, the resulting mutant produced PEP binding similar to wild type LbPFK (*181*). Together, these results suggest that the allosteric site of TtPFK and the residues important for PEP binding may differ from that of BsPFK and LbPFK.

In the absence of a three-dimensional structure of TtPFK, we can only speculate about the function of the arginine at position 55 in producing a tight PEP binding. Given the proximity of residue 55 to the carboxyl group of PEP, as judged from the three-dimensional structure of BsPFK, it is possible that the side chain of R55 is involved in a non-covalent interaction with PEP, which is unique to TtPFK (Figure 4-1). In that context, we would expect that breaking this interaction through the R55G mutation would result in a decrease in the binding affinity for PEP. It is intriguing that both R55G and R55E substitutions have such a profound effect on the coupling of PEP, resulting in over 1 kcal mol^{-1} increase in coupling free energy.

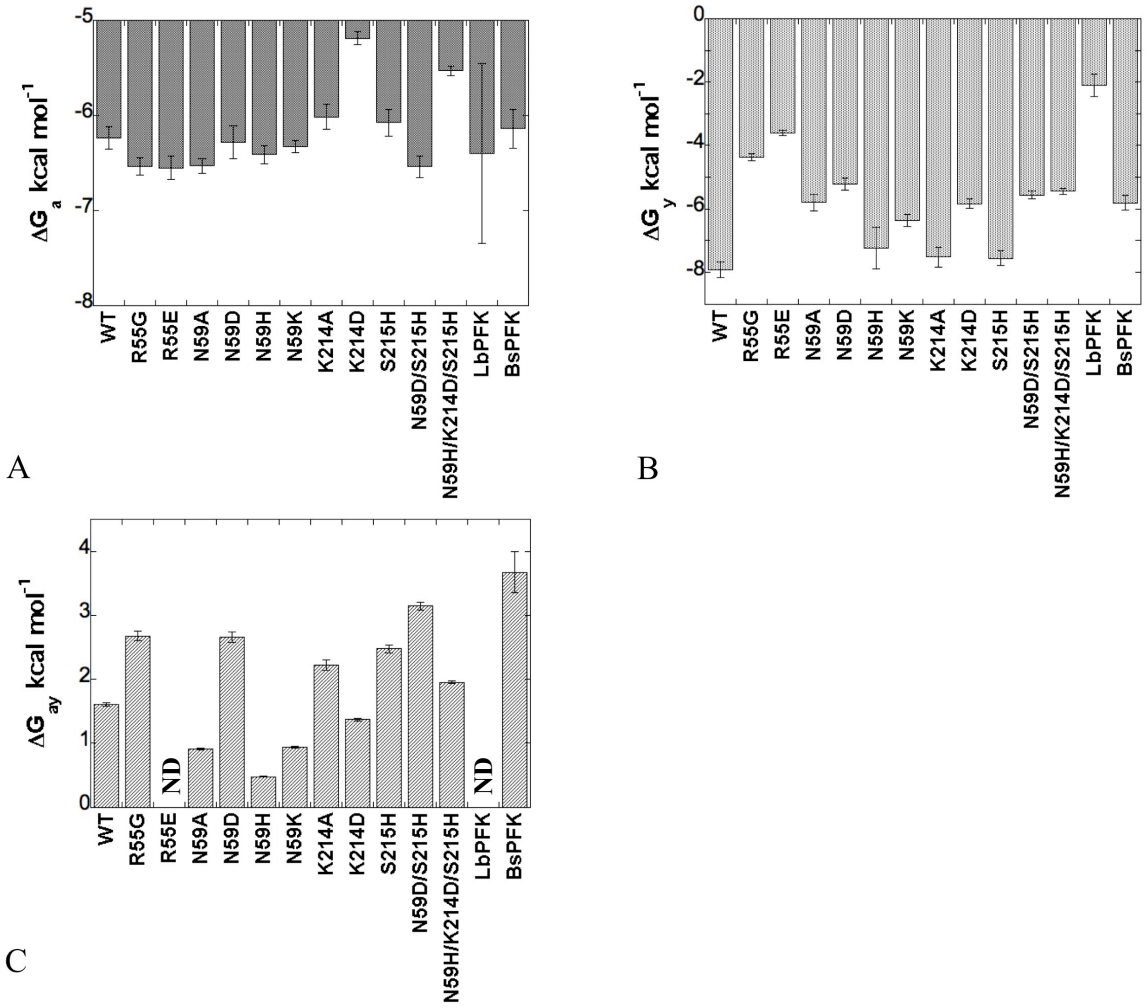

Figure 4-3 Summary of the binding and coupling free energies for the wild type TtPFK, BsPFK, and LbPFK, and for the TtPFK variants. (A) Diagram summarizing the binding free energies for Fru-6-P for the revertant variants of TtPFK, as well as for wild type TtPFK, BsPFK, and LbPFK. (B) Diagram summarizing the binding free energies for PEP for the revertant variants of TtPFK, as well as for wild type TtPFK, BsPFK, and LbPFK. (C) Diagram summarizing the coupling free energies for binding of PEP and Fru-6-P for the revertant variants of TtPFK, as well as for wild type TtPFK, BsPFK, and LbPFK. The data were collected at 25°C pH 8. The error bars represent the standard error calculated from the fit of the data to equation 4-2 or 4-3.

Asparagine 59 was substituted with several amino acids to assess whether the non-charged polar nature and potential interactions involving the side chain of N59 play a role in tight PEP binding in TtPFK. We previously showed that when N59 is changed to aspartate, the binding affinity of PEP to the resulting variant decreased by 100-fold. The N59K substitution results in a 15-fold decrease in PEP binding (Figure 4-3B). Thus, it appears that the presence of an ionizable side chain, whether negative or positive, at position 59 is detrimental to the binding of PEP. The N59A variant shows a 37-fold decrease in PEP binding affinity, while a substitution with histidine resulted in only a minor decrease in PEP binding. These results suggest that the polar nature of the side chain of residue 59 is important for the tight binding of PEP.

It is difficult to predict the potential interaction partners of N59 in TtPFK, since no structural data is available for this enzyme, however, interactions of residue 59 with residues 214 or 215 across the allosteric site interface were seen in PFK's from *Bacillus stearothermophilus* and *Lactobacillus delbruekii* (Figure 4-1). To evaluate whether these interaction take place in TtPFK and evaluate their importance for the binding of PEP, various combination substitutions were made with these residues.

To assess if potential interactions of asparagine 59 with lysine 214 are important for PEP binding, K214 was changed to alanine. K214A mutant showed a very small decrease in PEP binding, suggesting that K214 and its potential interactions were not crucial for PEP binding in TtPFK (Figure 4-3B). Figure 4-3B also shows that the double variant N59D/S215H, designed to mimic the interaction across the interface seen in BsPFK, displays PEP binding similar to that of the single N59D mutation (the single

S215H mutation had no significant effect on PEP binding). We also attempted to recreate the interaction seen in LbPFK by introducing the N59H/K214D/S215H triple substitution and saw diminished binding of PEP. However, the weak binging of PEP to the triple variant is likely due to the K214D mutation, which results in 2 kcal mol^{-1} increase in PEP binding free energy. Our results show that neither N59D/S215H, nor N59H/K214D/S215H variant alter the binding affinity of PEP beyond what is seen for the individual component substitutions. This lack of an effect may mean that the interaction of N59 across the interface with residues 214 or 215 is not important for PEP binding. Alternatively, it is possible that the relative positions of these residues are slightly altered in TtPFK such that the interactions produced by D59 and S215 in BsPFK or by H59 and K214 in LbPFK are not be possible in TtPFK due to the distance between or side chain orientation of these residues.

The results of our experiments suggest that, in the context of TtPFK structure, a charged residue at position 59 is detrimental to the binding of PEP (Figure 4-3B). The results obtained with the N59A mutant suggests that the interactions formed by the side chain of the residue at position 59 are important for the binding of PEP. Since the N59H variant is most comparable to the wild type TtPFK in terms of the binding affinity for PEP, we believe that the polar nature of the residue at position 59 is important for the binding of PEP. We saw no significant changes in PEP binding upon potentially breaking or creating the interactions of residue at position 59 with residues 214 or 215 by introducing K214A or N59D/S215H and N59H/K214D/S215H, which suggests that these particular interactions either do not exist or are not important for PEP binding. It is

possible that the side chain of N59 is displaced closer to R154 since it appears to the only available hydrogen bond partner.

What is also interesting is that none of the variants, with the exception of K214D changed the binding affinity of Fru-6-P, but most of them had quite large effects on the coupling between PEP and Fru-6-P binding. Substitutions at position 55 appeared to not only dramatically decrease the binding affinity of PEP, but also increase the coupling between the binding of Fru-6-P and PEP. The majority of the substitutions at position 59 resulted in a weaker coupling between PEP and Fru-6-P (Figure 4-3C). The only exception we saw was the BsPFK revertant substitution N59D, which increased the coupling free energy by roughly 1 kcal mol^{-1}. The most dramatic effect in the opposite direction was produced by the LbPFK revertant mutant N59H. This mutation had very little effect on the binding affinity of PEP, but the coupling between PEP and Fru-6-P binding was diminished by 1 kcal mol^{-1}. The substitution N59K resulted in a slightly less augmented coupling compared to N59H, although its effect on the PEP binding was more pronounced.

The roles of residues 55 and 59 in the binding of the allosteric ligands have been also investigated in other bacterial PFKs. In EcPFK, Y55F and Y55G variants were constructed to establish the importance of Y55 potential hydrophobic interaction with the adenine moiety as well as the possible hydrogen bond of its hydroxyl with the adenine of ADP (*182*). Y55F showed minimal augmentation of GDP binding, while Y55G reduced the binding of GDP several fold, suggesting that the hydroxyl group of Y55 has little impact on the binding of the activator, while the aromatic ring is likely to

be involved in the hydrophobic interaction with the adenine. Notably, the study reported no effects of Y55F or Y55G on the binding of the inhibitor PEP in *E. coli* PFK.

The role of residue 59 in the binding of the allosteric effectors has also been investigated previously. Valdez *et al*. probed the role of the side chain of D59 in the binding of PEP and GDP in BsPFK by constructing the D59A and D59M variants (*183*). The authors reported that the binding affinity for PEP in the D59A variant was the same as in wild type BsPFK, while the D59M mutation resulted in a 3-fold increase in the PEP binding affinity. It was also reported that GDP was able to reverse the inhibition by PEP. The authors concluded that the side chain of D59 is not directly involved in the binding of the allosteric effectors.

In a study done in our lab, BsPFK residue D59 was substituted with asparagine, which resulted in a large decrease in coupling between PEP and Fru-6-P, but the PEP binding affinity was not significantly affected (Stephanie Perez, personal communication). In contrast, the reverse N59D substitution in TtPFK results in both an increase in coupling and a 100-fold decrease in PEP binding, suggesting that the side chain of this residue may be involved in different interactions than what are seen in BsPFK.

Our results suggest that the side chains of the residues at positions 55 and 59 are crucial for the binding of PEP as well as for the propagation of the inhibitory signal to the active sites in TtPFK. These results differ from previous results pertaining to EcPFK and BsPFK, suggesting that the interactions in the allosteric site of TtPFK may be

different from those of the other PFKs due to the presence of the non-conserved arginine at position 55 and lack of an ionizable residue at position 59.

CHAPTER V

SUMMARY

The available crystal structures of type 1 ATP-dependent PFK-1 from several bacterial sources reveal a high overall structure conservation (Figure 5-1), and while no three-dimensional structure of TtPFK is available to date, we have no reason to believe that it is dramatically different. Given the high conservation of the structure, it is particularly interesting to see the extent of variation in the functional properties of these PFK's (Figure 5-2). As discussed in Chapter II, TtPFK displays a very high binding affinity for its allosteric inhibitor PEP. At the same time, the allosteric coupling between the substrate and the inhibitor is much weaker compared to other enzymes. We feel that these characteristics of TtPFK make it a very useful tool in our attempt to understand the phenomenon of allosteric regulation. Since the evidence of the allosteric effect is seen in the difference in the binding of the substrate in the absence versus saturating concentrations of the allosteric effector, it is necessary to consider all four species of the enzyme, including the ternary complex (*148*). The ternary complex consisting of the enzyme, substrate, and the activator is achieved quite easily, because the binding of one ligand improves the binding of the other ligand. In contrast, the ternary complex with the inhibitor is more difficult to form, because of the antagonism between the binding of substrate and inhibitor. The tight binding of PEP and Fru-6-P (in the absence of ATP) and the weaker coupling between the binding of the substrate and inhibitor mean that, in the case of TtPFK, the ternary complex with the inhibitor is more easily attainable, than in the case of PFK's from *E. coli* and *Bacillus stearothermophilus*.

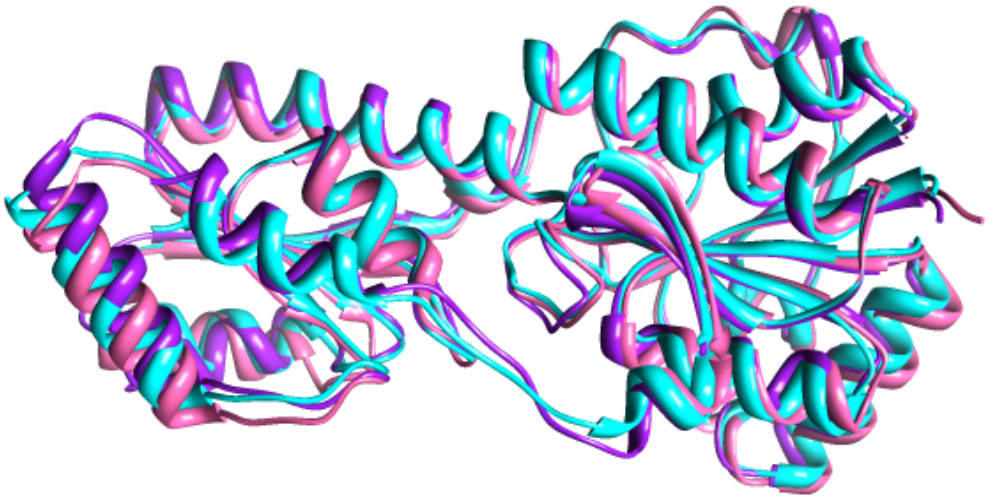

Figure 5-1 Comparison of the three-dimensional structures of bacterial PFK's. The alignment of the tetramers of PFK's from *E. coli* (pink) (*154*), *B. stearothermophilus* (cyan) (*176*), and *Lactobacillus delbrukii ssp. Bulgaricus* (purple) (*180*) was performed using the UCSF CHIMERA. Only one out of four subunits is shown above.

The strong binding affinity of TtPFK for its allosteric inhibitor PEP was explored in Chapter IV. Understanding the binding of PEP to TtPFK is of particular interest considering the extremely weak binding of PEP in the PFK from *Lactobacillus delbrukii ssp. bulgaricus*. Chapter IV outlined the effect of substituting the non-conserved residues in the allosteric pocket of TtPFK to the amino acids found in BsPFK and LbPFK. Our results indicate that the non-conserved R55 is crucial for the binding of PEP in TtPFK, as the glycine and glutamate substitutions at this position resulted in a dramatic decrease in the binding affinity of PEP. It is interesting to point out that the BsPFK revertant variant R55G produced a decrease in PEP binding affinity, which is weaker by an order of magnitude compared to that of BsPFK. It is possible that due to the presence of the arginine at position 55, the positioning of the PEP molecule in the allosteric pocket of TtPFK may differ from that of BsPFK (and other PFK's). This possibility is also supported by the fact that the E55R variant of LbPFK did not show any enhancement in the binding affinity of PEP (*181*).

Another interesting trait of the TtPFK is that the ability of PEP to antagonize the binding of Fru-6-P in this enzyme is weaker than that displayed by PFK's from *E. coli* and *B. stearothermophilus*. In an attempt to identify the source of the weaker coupling between the substrate and inhibitor, the region between the closest allosteric and active site was analyzed. As a result of our analysis of the sequence alignments of TtPFK and BsPFK and the three-dimensional structures of the BsPFK in various ligated states, we identified three non-conserved residues N59, A158, and S215. In BsPFK, the side chains of the complementary residues D59, T158, and H215 participate in a network of

interactions, which are not likely to be present in TtPFK, due to the nature of the amino acids at these positions. As described in Chapter III, we found that we are able to increase the coupling free energy of inhibition in TtPFK by 3 kcal mol^{-1} by introducing the N59D/A158T/S215H substitution. It is also of interest that each individual substitution contributed roughly equal amount to the overall increase in the coupling free energy. This result was somewhat unexpected since our initial hypothesis presumed that all the links in the chain must be restored to see an enhancement in the coupling. However, our observation may mean that the residues N59, A158 and S215 are already involved in the propagation of the inhibitory signal in TtPFK, and the N59D, A158T, and S215H substitutions simply make the inhibition by PEP more effective. This may be achieved by altering the flexibility of this region through the strengthening of the existing or the creation of alternative interactions for these residues. The steric effect may also be a factor, especially in the case of the S215H variant, where a small side chain is replaced by a large bulky one. It is also intriguing to consider the possibility that the effect of these substitutions is seen from the communication between the allosteric site and the other three active sites, which also contribute to the overall coupling free energy. These possibilities can be further investigated by measuring the effect of the individual mutations on each unique heterotropic interaction using the hybrid technology.

REFERENCES

1. Drees, K. P., Neilson, J. W., Betancourt, J. L., Quade, J., Henderson, D. A., Pryor, B. M., and Maier, R. M. (2006) Bacterial community structure in the hyperarid core of the Atacama Desert, Chile, *Appl. Environ. Microbiol. 72*, 7902-7908.

2. Dadachova, E., Bryan, R. A., Huang, X., Moadel, T., Schweitzer, A. D., Aisen, P., Nosanchuk, J. D., and Casadevall, A. (2007) Ionizing radiation changes the electronic properties of melanin and enhances the growth of melanized fungi, *PLoS One 2*, e457.

3. Brock, T. D., and Freeze, H. (1969) *Thermus aquaticus* gen. n. and sp. n., a nonsporulating extreme thermophile, *J. Bacteriol. 98*, 289-297.

4. Macelroy, R. (1974) Some comments on the evolution of extremophiles, *Biosystems 6*, 74-75.

5. Mueller, D. R., Vincent, W. F., Bonilla, S., and Laurion, I. (2005) Extremotrophs, extremophiles and broadband pigmentation strategies in a high arctic ice shelf ecosystem, *FEMS Microbiol. Ecol. 53*, 73-87.

6. Puhler, G., Leffers, H., Gropp, F., Palm, P., Klenk, H. P., Lottspeich, F., Garrett, R. A., and Zillig, W. (1989) Archaebacterial DNA-dependent RNA polymerases testify to the evolution of the eukaryotic nuclear genome, *Proc. Natl. Acad. of Sci. U.S.A. 86*, 4569-4573.

7. Kimura, M., Arndt, E., Hatakeyama, T., and Kimura, J. (1989) Ribosomal proteins in halobacteria, *Can. J. Microbiol. 35*, 195-199.

8. Woese, C. R., and Fox, G. E. (1977) Phylogenetic structure of the prokaryotic domain: the primary kingdoms, *Proc. Natl. Acad. Sci. U.S.A. 74*, 5088-5090.

9. Woese, C. R., Kandler, O., and Wheelis, M. L. (1990) Towards a natural system of organisms: proposal for the domains Archaea, Bacteria, and Eucarya, *Proc. Natl. Acad. Sci. U.S.A. 87*, 4576-4579.

10. Egorova, K., and Antranikian, G. (2005) Industrial relevance of thermophilic Archaea, *Curr. Opin. Microbiol. 8*, 649-655.

11. Bruins, M. E., Janssen, A. E. M., and Boom, R. M. (2001) Thermozymes and their applications - a review of recent literature and patents, *Appl. Biochem. Biotechnol. 90*, 155-186.

12. Horikoshi, K., and ebrary Inc. (2011) *Extremophiles handbook* with 238 figures and 120 tables, p 2 v. in 1, Springer, Tokyo.

13. Zobell, C. E., and Johnson, F. H. (1949) The influence of hydrostatic pressure on the growth and viability of terrestrial and marine bacteria, *J. Bacteriol. 57*, 179-189.

14. Johnson, F. H., and Zobell, C. E. (1949) The retardation of thermal disinfection of *Bacillus subtilis* spores by hydrostatic pressure, *J. Bacteriol. 57*, 353-358.

15. Morita, R. Y. (1999) Extremes of biodiversity, *BioScience 49*, 245-248.

16. Horikoshi, K. (1971) Production of alkaline enzymes by alkalophilic microorganisms. 1. Alkaline protease produced by *Bacillus* N-2210, *Agric. Biol. Chem. 35*, 1407-1414.

17. Horikoshi, K., and Iida, S. (1958) Lysis of fungal mycelia by bacterial enzymes, *Nature 181*, 917-918.

18. Horikoshi, K. (1971) Production of alkaline enzymes by alkalophilic microorganisms. 2. Alkaline amylase produced by *Bacillus* No a-40-2, *Agric. Biol. Chem. 35*, 1783-1791.

19. Horikoshi, K. (1972) Production of alkaline enzymes by alkalophilic microorganisms. 3. Alkaline pectinase of *Bacillus* No P-4-N, *Agric. Biol. Chem. 36*, 285-293.

20. Morita, R. Y. (1975) Psychrophilic bacteria, *Bacteriol. Rev. 39*, 144-167.

21. Schmidt-Nielsen. (1902) Über einige psychrophile Mikroorganismen und ihr Vorkommen, *Zbl. Bakt. (Abt. 2)*, 145-147.

22. Hucker, G. J. (1954) Low temperature organisms in frozen vegetables, *Food Technol. 8*, 79-82.

23. Eddy, B. P. (1960) The use and meaning of the term 'psychrophilic', *J. Appl. Microbiol. 23*, 189-190.

24. Margesin, R., and Feller, G. (2010) Biotechnological applications of psychrophiles, *Environ. Technol. 31*, 835-844.

25. Oren, A. (2002) Halophilic microorganisms in their natural environment and in culture — an historical introduction, In *Halophilic microorganisms and their environments*, pp 3-16, Springer Netherlands.

26. DasSarma, S., and DasSarma, P. (2001) Halophiles, In *eLS*, John Wiley & Sons, Ltd.

27. Oren, A. (1999) Bioenergetic aspects of halophilism, *Microbiol. Mol. Biol. Rev. 63*, 334-348.

28. Setati, M. E. (2010) Diversity and industrial potential of hydrolase-producing halophilic/halotolerant eubacteria, *Afr. J. Biotechnol. 9*, 1555-1560.

29. Chien, A., Edgar, D. B., and Trela, J. M. (1976) Deoxyribonucleic acid polymerase from the extreme thermophile Thermus aquaticus, *J. Bacteriol. 127*, 1550-1557.

30. Stetter, K. O. (2006) History of discovery of the first hyperthermophiles, *Extremophiles 10*, 357-362.

31. Sinensky, M. (1974) Homeoviscous adaptation - homeostatic process that regulates viscosity of membrane lipids in *Escherichia coli*, *Proc. Natl. Acad. Sci. U.S.A. 71*, 522-525.

32. Singer, S. J., and Nicolson, G. L. (1972) The fluid mosaic model of the structure of cell membranes, *Science 175*, 720-731.

33. Albers, S. V., Van de Vossenberg, J. L., Driessen, A. J., and Konings, W. N. (2001) Bioenergetics and solute uptake under extreme conditions, *Extremophiles 5*, 285-294.

34. Deamer, D. W., and Bramhall, J. (1986) Permeability of lipid bilayers to water and ionic solutes, *Chem. Phys. Lipids 40*, 167-188.

35. van de Vossenberg, J. L., Ubbink-Kok, T., Elferink, M. G., Driessen, A. J., and Konings, W. N. (1995) Ion permeability of the cytoplasmic membrane limits the

maximum growth temperature of bacteria and archaea, *Mol. Microbiol. 18*, 925-932.

36. Choquet, C. G., Patel, G. B., Beveridge, T. J., and Sprott, G. D. (1994) Stability of pressure-extruded liposomes made from archaeobacterial ether lipids, *Appl. Microbiol. Biotechnol. 42*, 375-384.

37. Nichols, D. S., Miller, M. R., Davies, N. W., Goodchild, A., Raftery, M., and Cavicchioli, R. (2004) Cold adaptation in the Antarctic archaeon *Methanococcoides burtonii* involves membrane lipid unsaturation, *J. Bacteriol. 186*, 8508-8515.

38. Ray, P. H., White, D. C., and Brock, T. D. (1971) Effect of growth temperature on the lipid composition of *Thermus aquaticus*, *J. Bacteriol. 108*, 227-235.

39. Adams, B. L., McMahon, V., and Seckbach, J. (1971) Fatty acids in the thermophilic alga, *Cyanidium caldarium*, *Biochem. Biophys. Res. Commun. 42*, 359-365.

40. Brundish, D. E., Shaw, N., and Baddiley, J. (1967) The structure and possible function of the glycolipid from *Staphylococcus lactis* I3, *Biochem. J. 105*, 885-889.

41. Langworthy, T. A., Mayberry, W. R., and Smith, P. F. (1976) A sulfonolipid and novel glucosamidyl glycolipids from the extreme thermoacidophile *Bacillus acidocaldarius*, *Biochim. Biophys. Acta 431*, 550-569.

42. Langworthy, T. A., Mayberry, W. R., and Smith, P. F. (1974) Long-chain glycerol diether and polyol dialkyl glycerol triether lipids of *Sulfolobus acidocaldarius*, *J. Bacteriol. 119*, 106-116.

43. Rilfors, L., Wieslander, A., and Stahl, S. (1978) Lipid and protein composition of membranes of *Bacillus megaterium* variants in the temperature range 5 to 70 degrees C, *J. Bacteriol. 135*, 1043-1052.

44. Sorensen, P. G. (1993) Changes of the composition of phospholipids, fatty-acids and cholesterol from the erythrocyte plasma-membrane from flounders (*Platichthys flesus* L) which were acclimated to high and low-temperatures in aquariums, *Comp. Biochem. Physiol. B Biochem. Mol. Biol. 106*, 907-912.

45. De Rosa, M., Gambacorta, A., and Bu'Lock, J. D. (1976) The caldariella group of extreme thermoacidophile bacteria: Direct comparison of lipids in *Sulfolobus*, *Thermoplasma*, and the MT strains, *Phytochemistry 15*, 143-145.

46. Souza, K. A., Kostiw, L. L., and Tyson, B. J. (1974) Alterations in normal fatty-acid composition in a temperature-sensitive mutant of a thermophilic *Bacillus*, *Arch. Microbiol. 97*, 89-102.

47. Chan, M., Himes, R. H., and Akagi, J. M. (1971) Fatty acid composition of thermophilic, mesophilic, and psychrophilic clostridia, *J. Bacteriol. 106*, 876-881.

48. Marr, A. G., and Ingraham, J. L. (1962) Effect of temperature on the composition of fatty acids in *Escherichia coli*, *J. Bacteriol. 84*, 1260-1267.

49. Gill, C. O. (1975) Effect of growth temperature on the lipids of *Pseudomonas fluorescens*, *J. Gen. Microbiol. 89*, 293-298.

50. Gill, C. O., and Suisted, J. R. (1978) The effects of temperature and growth rate on the proportion of unsaturated fatty acids in bacterial lipids, *J. Gen. Microbiol. 104*, 31-36.

51. Bishop, D. G., Rutberg, L., and Samuelsson, B. (1967) The chemical composition of the cytoplasmic membrane of *Bacillus subtilis*, *Eur. J. Biochem. 2*, 448-453.

52. Sprott, G. D., Shaw, K. M., and Jarrell, K. F. (1983) Isolation and chemical composition of the cytoplasmic membrane of the archaebacterium *Methanospirillum hungatei*, *J. Biol. Chem. 258*, 4026-4031.

53. Lee, A. G. (2004) How lipids affect the activities of integral membrane proteins, *Biochim. Biophys. Acta Biomembranes 1666*, 62-87.

54. Lee, A. G. (2003) Lipid-protein interactions in biological membranes: a structural perspective, *Biochim. Biophys. Acta 1612*, 1-40.

55. Wisdom, C., and Welker, N. E. (1973) Membranes of *Bacillus stearothermophilus*: factors affecting protoplast stability and thermostability of alkaline phosphatase and reduced nicotinamide adenine dinucleotide oxidase, *J. Bacteriol. 114*, 1336-1345.

56. Toman, O., Le Hegarat, F., and Svobodova, J. (2007) Detection of lateral heterogeneity in the cytoplasmic membrane of *Bacillus subtilis*, *Folia Microbiol. 52*, 339-345.

57. Kropinski, A. M., Lewis, V., and Berry, D. (1987) Effect of growth temperature on the lipids, outer membrane proteins, and lipopolysaccharides of *Pseudomonas aeruginosa* PAO, *J. Bacteriol. 169*, 1960-1966.

58. Henne, A., Bruggemann, H., Raasch, C., Wiezer, A., Hartsch, T., Liesegang, H., Johann, A., Lienard, T., Gohl, O., Martinez-Arias, R., Jacobi, C., Starkuviene, V., Schlenczeck, S., Dencker, S., Huber, R., Klenk, H. P., Kramer, W., Merkl, R., Gottschalk, G., and Fritz, H. J. (2004) The genome sequence of the extreme thermophile *Thermus thermophilus*, *Nature Biotechnol. 22*, 547-553.

59. McDonald, J. H., Grasso, A. M., and Rejto, L. K. (1999) Patterns of temperature adaptation in proteins from *Methanococcus* and *Bacillus*, *Mol. Biol. Evol. 16*, 1785-1790.

60. Grogan, D. W. (1998) Hyperthermophiles and the problem of DNA instability, *Mol. Microbiol. 28*, 1043-1049.

61. Galtier, N., and Lobry, J. R. (1997) Relationships between genomic G+C content, RNA secondary structures, and optimal growth temperature in prokaryotes, *J. Mol. Evol. 44*, 632-636.

62. Kawashima, T., Amano, N., Koike, H., Makino, S., Higuchi, S., Kawashima-Ohya, Y., Watanabe, K., Yamazaki, M., Kanehori, K., Kawamoto, T., Nunoshiba, T., Yamamoto, Y., Aramaki, H., Makino, K., and Suzuki, M. (2000) Archaeal adaptation to higher temperatures revealed by genomic sequence of *Thermoplasma volcanium*, *Proc. Nat. Acad. Sci. U.S.A. 97*, 14257-14262.

63. Dickerson, R. E. (1983) Base sequence and helix structure variation in B-DNA and A-DNA, *J. Mol. Biol. 166*, 419-441.

64. Nakashima, H., Fukuchi, S., and Nishikawa, K. (2003) Compositional changes in RNA, DNA and proteins for bacterial adaptation to higher and lower temperatures, *J Biochem 133*, 507-513.

65. Singer, G. A. C., and Hickey, D. A. (2003) Thermophilic prokaryotes have characteristic patterns of codon usage, amino acid composition and nucleotide content, *Gene 317*, 39-47.

66. Fire, A. (1999) RNA-triggered gene silencing, *Trends Genet. 15*, 358-363.

67. Bjork, G. R., Ericson, J. U., Gustafsson, C. E. D., Hagervall, T. G., Jonsson, Y. H., and Wikstrom, P. M. (1987) Transfer-RNA modification, *Annu. Rev. Biochem. 56*, 263-287.

68. Agris, P. F., Koh, H., and Soll, D. (1973) The effect of growth temperatures on the in vivo ribose methylation of *Bacillus stearothermophilus* transfer RNA, *Arch. Biochem. Biophys. 154*, 277-282.

69. Watanabe, K., Shinma, M., Oshima, T., and Nishimura, S. (1976) Heat-induced stability of tRNA from an extreme thermophile, *Thermus thermophilus*, *Biochem. Biophys. Res. Commun. 72*, 1137-1144.

70. Kowalak, J. A., Dalluge, J. J., McCloskey, J. A., and Stetter, K. O. (1994) The role of posttranscriptional modification in stabilization of transfer RNA from hyperthermophiles, *Biochemistry 33*, 7869-7876.

71. Horie, N., Hara-Yokoyama, M., Yokoyama, S., Watanabe, K., Kuchino, Y., Nishimura, S., and Miyazawa, T. (1985) Two tRNAIle1 species from an extreme thermophile, *Thermus thermophilus* HB8: effect of 2-thiolation of ribothymidine on the thermostability of tRNA, *Biochemistry 24*, 5711-5715.

72. Davanloo, P., Sprinzl, M., Watanabe, K., Albani, M., and Kersten, H. (1979) Role of ribothymidine in the thermal-stability of transfer-RNA as monitored by proton magnetic-resonance, *Nucleic Acids Res. 6*, 1571-1581.

73. Marmur, J., and Doty, P. (1962) Determination of the base composition of deoxyribonucleic acid from its thermal denaturation temperature, *J. Mol. Biol. 5*, 109-118.

74. Hensel, R., and Konig, H. (1988) Thermoadaptation of methanogenic bacteria by intracellular ion concentration, *FEMS Microbiol. Lett. 49*, 75-79.

75. Nazar, R. N., Sprott, G. D., Matheson, A. T., and Van, N. T. (1978) An enhanced thermostability in thermophilic 5-S ribonucleic acids under physiological salt conditions, *Biochim. Biophys. Acta 521*, 288-294.

76. Varricchio, F., and Marotta, C. A. (1976) Thermal denaturation of mesophilic and thermophilic 5S ribonucleic acids, *J. Bacteriol. 125*, 850-854.

77. Marguet, E., and Forterre, P. (1994) DNA stability at temperatures typical for hyperthermophiles, *Nucleic Acids Res. 22*, 1681-1686.

78. Kikuchi, A., and Asai, K. (1984) Reverse gyrase - a topoisomerase which introduces positive superhelical turns into DNA, *Nature 309*, 677-681.

79. Heine, M., and Chandra, S. B. C. (2009) The linkage between reverse gyrase and hyperthermophiles: A review of their invariable association, *J. Microbiol. 47*, 229-234.

80. Delatour, C. B., Portemer, C., Huber, R., Forterre, P., and Duguet, M. (1991) Reverse gyrase in thermophilic eubacteria, *J. Bacteriol. 173*, 3921-3923.

81. Atomi, H., Matsumi, R., and Imanaka, T. (2004) Reverse gyrase is not a prerequisite for hyperthermophilic life, *J. Bacteriol. 186*, 4829-4833.

82. Kampmann, M., and Stock, D. (2004) Reverse gyrase has heat-protective DNA chaperone activity independent of supercoiling, *Nucleic Acids Res. 32*, 3537-3545.

83. Napoli, A., Valenti, A., Salerno, V., Nadal, M., Garnier, F., Rossi, M., and Ciaramella, M. (2004) Reverse gyrase recruitment to DNA after UV light irradiation in *Sulfolobus solfataricus*, *J. Biol. Chem. 279*, 33192-33198.

84. Friedman, S. M., Axel, R., and Weinstein, I. B. (1967) Stability of ribosomes and ribosomal ribonucleic acid from *Bacillus stearothermophilus*, *J. Bacteriol. 93*, 1521-1526.

85. Wallace, H. M., Fraser, A. V., and Hughes, A. (2003) A perspective of polyamine metabolism, *Biochem. J. 376*, 1-14.

86. Oshima, T. (2010) Enigmas of biosyntheses of unusual polyamines in an extreme thermophile, *Thermus thermophilus*, *Plant Physiol. Biochem. 48*, 521-526.

87. Searcy, D. G. (1975) Histone-like protein in the prokaryote *Thermoplasma acidophilum*, *Biochim. Biophys. Acta 395*, 535-547.

88. Stein, D. B., and Searcy, D. G. (1978) Physiologically important stabilization of DNA by a prokaryotic histone-like protein, *Science 202*, 219-221.

89. Reddy, T. R., and Suryanarayana, T. (1989) Archaebacterial histone-like proteins. Purification and characterization of helix stabilizing DNA binding proteins from the acidothermophile *Sulfolobus acidocaldarius*, *J. Biol. Chem. 264*, 17298-17308.

90. Hansen, M. T. (1978) Multiplicity of genome equivalents in the radiation-resistant bacterium *Micrococcus radiodurans*, *J. Bacteriol. 134*, 71-75.

91. Daly, M. J., and Minton, K. W. (1995) Interchromosomal recombination in the extremely radioresistant bacterium *Deinococcus radiodurans*, *J. Bacteriol. 177*, 5495-5505.

92. Davlieva, M., and Shamoo, Y. (2010) Crystal structure of a trimeric archaeal adenylate kinase from the mesophile *Methanococcus maripaludis* with an unusually broad functional range and thermal stability, *Proteins 78*, 357-364.

93. Vieille, C., and Zeikus, G. J. (2001) Hyperthermophilic enzymes: sources, uses, and molecular mechanisms for thermostability, *Microbiol. Mol. Biol. Rev.: MMBR 65*, 1-43.

94. Sterner, R., and Liebl, W. (2001) Thermophilic adaptation of proteins, *Crit. Rev. Biochem. Mol. Biol. 36*, 39-106.

95. Nojima, H., Ikai, A., Oshima, T., and Noda, H. (1977) Reversible thermal unfolding of thermostable phosphoglycerate kinase - thermostability associated with mean zero enthalpy change, *J. Mol. Biol. 116*, 429-442.

96. Razvi, A., and Scholtz, J. M. (2006) Lessons in stability from thermophilic proteins, *Protein Sci. 15*, 1569-1578.

97. Sridharan, S., Razvi, A., Scholtz, J. M., and Sacchettini, J. C. (2005) The HPr proteins from the thermophile *Bacillus stearothermophilus* can form domain-swapped dimers, *J. Mol. Biol. 346*, 919-931.

98. Razvi, A., and Scholtz, J. M. (2006) A thermodynamic comparison of HPr proteins from extremophilic organisms, *Biochemistry 45*, 4084-4092.

99. Li, W. T., Grayling, R. A., Sandman, K., Edmondson, S., Shriver, J. W., and Reeve, J. N. (1998) Thermodynamic stability of archaeal histones, *Biochemistry 37*, 10563-10572.

100. Lee, C. F., Allen, M. D., Bycroft, M., and Wong, K. B. (2005) Electrostatic interactions contribute to reduced heat capacity change of unfolding in a thermophilic ribosomal protein l30e, *J. Mol. Biol. 348*, 419-431.

101. Robic, S., Berger, J. M., and Marqusee, S. (2002) Contributions of folding cores to the thermostabilities of two ribonucleases H, *Protein Sci. 11*, 381-389.

102. Robic, S., Guzman-Casado, M., Sanchez-Ruiz, J. M., and Marqusee, S. (2003) Role of residual structure in the unfolded state of a thermophilic protein, *Proc. Natl. Acad. Sci. U.S.A. 100*, 11345-11349.

103. Zhou, H. X. (2002) Toward the physical basis of thermophilic proteins: linking of enriched polar interactions and reduced heat capacity of unfolding, *Biophys. J. 83*, 3126-3133.

104. Lobry, J. R. (1997) Influence of genomic G+C content on average amino-acid composition of proteins from 59 bacterial species, *Gene 205*, 309-316.

105. Reinhart, G. D., Hartleip, S. B., and Symcox, M. M. (1989) Role of coupling entropy in establishing the nature and magnitude of allosteric response, *Proc. Natl. Acad. Sci. U.S.A. 86*, 4032-4036.

106. Braxton, B. L., Tlapak-Simmons, V. L., and Reinhart, G. D. (1994) Temperature-induced inversion of allosteric phenomena, *J. Biol. Chem. 269*, 47-50.

107. Jaenicke, R. (1991) Protein stability and molecular adaptation to extreme conditions, *Eur. J. Biochem. / FEBS 202*, 715-728.

108. Somero, G. N. (1978) Temperature adaptation of enzymes - biological optimization through structure-function compromises, *Annu. Rev. Ecol. Syst. 9*, 1-29.

109. Zavodszky, P., Kardos, J., Svingor, A., and Petsko, G. A. (1998) Adjustment of conformational flexibility is a key event in the thermal adaptation of proteins, *Proc. Natl. Acad. Sci. U.S.A. 95*, 7406-7411.

110. Bonisch, H., Backmann, J., Kath, T., Naumann, D., and Schafer, G. (1996) Adenylate kinase from *Sulfolobus acidocaldarius*: expression in *Escherichia coli* and characterization by Fourier transform infrared spectroscopy, *Arch. Biochem. Biophys. 333*, 75-84.

111. D'auria, S., Nucci, R., Rossi, M., Bertoli, E., Tanfani, F., Gryczynski, I., Malak, H., and Lakowicz, J. R. (1999) Beta-glycosidase from the hyperthermophilic

archaeon *Sulfolobus solfataricus*: structure and activity in the presence of alcohols, *J Biochem 126*, 545-552.

112. Beaucamp, N., Hofmann, A., Kellerer, B., and Jaenicke, R. (1997) Dissection of the gene of the bifunctional PGK-TIM fusion protein from the hyperthermophilic bacterium *Thermotoga maritima*: design and characterization of the separate triosephosphate isomerase, *Protein Sci. 6*, 2159-2165.

113. Somero, G. N. (1995) Proteins and temperature, *Annu. Rev. Physiol. 57*, 43-68.

114. Hernandez, G., Jenney, F. E., Adams, M. W. W., and LeMaster, D. M. (2000) Millisecond time scale conformational flexibility in a hyperthermophile protein at ambient temperature, *Proc. Natl. Acad. Sci. U.S.A. 97*, 3166-3170.

115. Lazaridis, T., Lee, I., and Karplus, M. (1997) Dynamics and unfolding pathways of a hyperthermophilic and a mesophilic rubredoxin, *Protein Sci. 6*, 2589-2605.

116. Ichikawa, J. K., and Clarke, S. (1998) A highly active protein repair enzyme from an extreme thermophile: the L-isoaspartyl methyltransferase from *Thermotoga maritima*, *Arch. Biochem. Biophys. 358*, 222-231.

117. Merz, A., Knochel, T., Jansonius, J. N., and Kirschner, K. (1999) The hyperthermostable indoleglycerol phosphate synthase from *Thermotoga maritima* is destabilized by mutational disruption of two solvent-exposed salt bridges, *J. Mol. Biol. 288*, 753-763.

118. Sterner, R., Kleemann, G. R., Szadkowski, H., Lustig, A., Hennig, M., and Kirschner, K. (1996) Phosphoribosyl anthranilate isomerase from *Thermotoga*

maritima is an extremely stable and active homodimer, *Protein Sci. 5*, 2000-2008.

119. Thomas, T. M., and Scopes, R. K. (1998) The effects of temperature on the kinetics and stability of mesophilic and thermophilic 3-phosphoglycerate kinases, *Biochem. J. 330 (Pt 3)*, 1087-1095.

120. Hochachka, P. W., and Lewis, J. K. (1970) Enzyme variants in thermal acclimation. Trout liver citrate synthases, *J. Biol. Chem. 245*, 6567-6573.

121. Dahlhoff, E., and Somero, G. N. (1993) Kinetic and structural adaptations of cytoplasmic malate-dehydrogenases of eastern Pacific abalone (genus *Haliotis*) from different thermal habitats - biochemical correlates of biogeographical patterning, *J. Exp. Biol. 185*, 137-150.

122. Coppes, Z. L., and Somero, G. N. (1990) Temperature-adaptive differences between the M4 lactate-dehydrogenases of stenothermal and eurythermal sciaenid fishes, *J. Exp. Zool. 254*, 127-131.

123. Baldwin, J. (1971) Adaptation of enzymes to temperature: acetylcholinesterases in the central nervous system of fishes, *Comp. Biochem. Physiol. B 40*, 181-187.

124. Scopes, R. K. (1995) The effect of temperature on enzymes used in diagnostics, *Clin. Chim. Acta 237*, 17-23.

125. Graves, J. E., Rosenblatt, R. H., and Somero, G. N. (1983) Kinetic and electrophoretic differentiation of lactate-dehydrogenases of teleost species-pairs from the Atlantic and Pacific coasts of Panama, *Evolution 37*, 30-37.

126. Changeux, J. P. (1961) The feedback control mechanisms of biosynthetic L-threonine deaminase by L-isoleucine, *Cold Spring Harbor Symp. Quant. Biol. 26*, 313-318.

127. Monod, J., Wyman, J., and Changeux, J. P. (1965) On the nature of allosteric transitions: a plausible model, *J. Mol. Biol. 12*, 88-118.

128. Changeux, J. P. (2011) Allostery and the Monod-Wyman-Changeux model after 50 years, *Annu. Rev. Biophys.*, 103-133.

129. Perutz, M. F., Rossmann, M. G., Cullis, A. F., Muirhead, H., Will, G., and North, A. C. (1960) Structure of haemoglobin: a three-dimensional Fourier synthesis at 5.5-A. resolution, obtained by X-ray analysis, *Nature 185*, 416-422.

130. Muirhead, H., and Perutz, M. F. (1963) Structure of haemoglobin. A three-dimensional Fourier synthesis of reduced human haemoglobin at 5-5 a resolution, *Nature 199*, 633-638.

131. Perutz, M. F., Bolton, W., Diamond, R., Muirhead, H., and Watson, H. C. (1964) Structure of haemoglobin. An X-ray examination of reduced horse haemoglobin, *Nature 203*, 687-690.

132. Schirmer, T., and Evans, P. R. (1990) Structural basis of the allosteric behaviour of phosphofructokinase, *Nature 343*, 140-145.

133. Kantrowitz, E. R., and Lipscomb, W. N. (1988) *Escherichia coli* aspartate-transcarbamylase - the relation between structure and function, *Science 241*, 669-674.

134. Koshland, D. E., Nemethy, G., and Filmer, D. (1966) Comparison of experimental binding data and theoretical models in proteins containing subunits, *Biochemistry 5*, 365-385.

135. Brock, T. D. (1988) Life at high-temperature, *Recherche 19*, 476-485.

136. Ljungdahl L. G., S. D. (1976) Proteins from thermophilic microorganisms, In *Extreme environments: mechanisms of microbial adaptation* (Heinrich, M. R., Ed.), pp 147-187, Academic Press, New York.

137. Kuramitsu, H. (1968) Concerted feedback inhibition of aspartokinase from *Bacillus stearothermophilus*, *Biochim. Biophys. Acta 167*, 643-645.

138. Kuramitsu, H. (1970) Concerted feedback inhibition of aspartokinase from *Bacillus stearothermophilus*. 1. Catalytic and regulatory properties, *J. Biol. Chem. 245*, 2991-2997.

139. Thomas, D. A., and Kuramits.Hk. (1971) Biosynthetic L-threonine deaminase from *Bacillus stearothermophilus*. 1. Catalytic and regulatory properties, *Arch. Biochem. Biophys. 145*, 96-104.

140. Yoshida, M., Oshima, T., and Imahori, K. (1971) The thermostable allosteric enzyme: phosphofructokinase from an extreme thermophile, *Biochem. Biophys. Res. Commun. 43*, 36-39.

141. Yoshida, M. (1972) Allosteric nature of thermostable phosphofructokinase from an extreme thermophilic bacterium, *Biochemistry 11*, 1087-1093.

142. Sando, G. N., and Hogenkamp, P. C. (1973) Ribonucleotide reductase from *Thermus X-1*, a thermophilic organism, *Biochemistry 12*, 3316-3322.

143. Chin, N. W., and Trela, J. M. (1973) Comparison of acetohydroxy-acid synthetases from two extreme thermophilic bacteria, *J. Bacteriol. 114*, 674-678.

144. Orengo, A., and Saunders, G. F. (1972) Regulation of a thermostable pyrimidine ribonucleoside kinase by cytidine triphosphate, *Biochemistry 11*, 1761-1767.

145. Johnson, J. L., and Reinhart, G. D. (1997) Failure of a two-state model to describe the influence of phospho(enol)pyruvate on phosphofructokinase from *Escherichia coli*, *Biochemistry 36*, 12814-12822.

146. Tlapak-Simmons, V. L., and Reinhart, G. D. (1998) Obfuscation of allosteric structure-function relationships by enthalpy-entropy compensation, *Biophys. J. 75*, 1010-1015.

147. Weber, G. (1972) Ligand binding and internal equilibria in proteins, *Biochemistry 11*, 864-878.

148. Reinhart, G. D. (2004) Quantitative analysis and interpretation of allosteric behavior, *Methods Enzymol. 380*, 187-203.

149. Kemp, R. G., and Gunasekera, D. (2002) Evolution of the allosteric ligand sites of mammalian phosphofructo-1-kinase, *Biochemistry 41*, 9426-9430.

150. Kemp, R. G., and Foe, L. G. (1983) Allosteric regulatory properties of muscle phosphofructokinase, *Mol. Cell. Biochem. 57*, 147-154.

151. Evans, P. R., Farrants, G. W., and Hudson, P. J. (1981) Phosphofructokinase: structure and control, *Philos. Trans. R. Soc. London Ser. B Biol. Sci. 293*, 53-62.

152. Evans, P. R., and Hudson, P. J. (1979) Structure and control of phosphofructokinase from *Bacillus stearothermophilus*, *Nature 279*, 500-504.

153. Shirakihara, Y., and Evans, P. R. (1988) Crystal structure of the complex of phosphofructokinase from *Escherichia coli* with its reaction products, *J. Mol. Biol. 204*, 973-994.

154. Rypniewski, W. R., and Evans, P. R. (1989) Crystal structure of unliganded phosphofructokinase from *Escherichia coli*, *J. Mol. Biol. 207*, 805-821.

155. Johnson, J. L., and Reinhart, G. D. (1992) MgATP and fructose 6-phosphate interactions with phosphofructokinase from *Escherichia coli*, *Biochemistry 31*, 11510-11518.

156. Johnson, J. L., and Reinhart, G. D. (1994) Influence of substrates and MgADP on the time-resolved intrinsic fluorescence of phosphofructokinase from *Escherichia coli*. Correlation of tryptophan dynamics to coupling entropy, *Biochemistry 33*, 2644-2650.

157. Johnson, J. L., and Reinhart, G. D. (1994) Influence of MgADP on phosphofructokinase from *Escherichia coli* - elucidation of coupling interactions with both substrates, *Biochemistry 33*, 2635-2643.

158. Tlapak-Simmons, V. L., and Reinhart, G. D. (1994) Comparison of the inhibition by phospho(enol)pyruvate and phosphoglycolate of phosphofructokinase from *B. stearothermophilus*, *Arch. Biochem. Biophys. 308*, 226-230.

159. Kimmel, J. L., and Reinhart, G. D. (2000) Reevaluation of the accepted allosteric mechanism of phosphofructokinase from *Bacillus stearothermophilus*, *Proc. Natl. Acad. Sci. U.S.A. 97*, 3844-3849.

160. Riley-Lovingshimer, M. R., and Reinhart, G. D. (2001) Equilibrium binding studies of a tryptophan-shifted mutant of phosphofructokinase from *Bacillus stearothermophilus*, *Biochemistry 40*, 3002-3008.

161. Fenton, A. W., Paricharttanakul, N. M., and Reinhart, G. D. (2004) Disentangling the web of allosteric communication in a homotetramer: heterotropic activation in phosphofructokinase from *Escherichia coli*, *Biochemistry 43*, 14104-14110.

162. Ortigosa, A. D., Kimmel, J. L., and Reinhart, G. D. (2004) Disentangling the web of allosteric communication in a homotetramer: heterotropic inhibition of phosphofructokinase from *Bacillus stearothermophilus*, *Biochemistry 43*, 577-586.

163. Xu, J., Oshima, T., and Yoshida, M. (1990) Tetramer-dimer conversion of phosphofructokinase from *Thermus thermophilus* induced by its allosteric effectors, *J. Mol. Biol. 215*, 597-606.

164. Lovingshimer, M. R., Siegele, D., and Reinhart, G. D. (2006) Construction of an inducible, pfkA and pfkB deficient strain of *Escherichia coli* for the expression and purification of phosphofructokinase from bacterial sources, *Protein Exp. Purif. 46*, 475-482.

165. Xu, J., Seki, M., Denda, K., and Yoshida, M. (1991) Molecular-cloning of phosphofructokinase-1 gene from a thermophilic bacterium, *Thermus-thermophilus*, *Biochem. Biophys. Res. Commun. 176*, 1313-1318.

166. Reinhart, G. D. (1983) The determination of thermodynamic allosteric parameters of an enzyme undergoing steady-state turnover, *Arch. Biochem. Biophys. 224*, 389-401.

167. Reinhart, G. D. (1985) Influence of pH on the regulatory kinetics of rat liver phosphofructokinase: a thermodynamic linked-function analysis, *Biochemistry 24*, 7166-7172.

168. Reinhart, G. D. (1988) Linked-function origins of cooperativity in a symmetrical dimer, *Biophys. Chem. 30*, 159-172.

169. Symcox, M. M., and Reinhart, G. D. (1992) A steady-state kinetic method for the verification of the rapid-equilibrium assumption in allosteric enzymes, *Anal. Biochem. 206*, 394-399.

170. Plou, F. J., and Ballesteros, A. (1999) Stability and stabilization of biocatalysts, *Trends Biotechnol. 17*, 304-306.

171. Pham, A. S., Janiak-Spens, F., and Reinhart, G. D. (2001) Persistent binding of MgADP to the E187A mutant of *Escherichia coli* phosphofructokinase in the absence of allosteric effects, *Biochemistry 40*, 4140-4149.

172. Fenton, A. W., Paricharttanakul, N. M., and Reinhart, G. D. (2003) Identification of substrate contact residues important for the allosteric regulation of phosphofructokinase from *Eschericia coli*, *Biochemistry 42*, 6453-6459.

173. Johnson, J. L., and Reinhart, G. D. (1992) MgATP and fructose 6-phosphate interactions with phosphofructokinase from Escherichia coli, *Biochemistry 31*, 11510-11518.

174. Sturtevant, J. M. (1977) Heat-capacity and entropy changes in processes involving proteins, *Proc. Natl. Acad. Sci. U.S.A. 74*, 2236-2240.

175. Yoshizaki, F., and Imahori, K. (1979) Key role of phosphoenolpyruvate in the regulation of glycolysis-gluconeogenesis in *Thermus thermophilus* HB-8, *Agric. Biol. Chem. 43*, 537-545.

176. Mosser, R., Reddy, M. C., Bruning, J. B., Sacchettini, J. C., and Reinhart, G. D. (2012) Structure of the apo form of *Bacillus stearothermophilus* phosphofructokinase, *Biochemistry 51*, 769-775.

177. Kimmel, J. L., and Reinhart, G. D. (2001) Isolation of an individual allosteric interaction in tetrameric phosphofructokinase from *Bacillus stearothermophilus*, *Biochemistry 40*, 11623-11629.

178. Fenton, A. W., and Reinhart, G. D. (2002) Isolation of a single activating allosteric interaction in phosphofructokinase from *Escherichia coli*, *Biochemistry 41*, 13410-13416.

179. Fenton, A. W., and Reinhart, G. D. (2009) Disentangling the web of allosteric communication in a homotetramer: heterotropic inhibition in phosphofructokinase from *Escherichia coli*, *Biochemistry 48*, 12323-12328.

180. Paricharttanakul, N. M., Ye, S., Menefee, A. L., Javid-Majd, F., Sacchettini, J. C., and Reinhart, G. D. (2005) Kinetic and structural characterization of phosphofructokinase from *Lactobacillus bulgaricus*, *Biochemistry 44*, 15280-15286.

181. Ferguson, S. B. (2011) Understanding weak binsing for phospho(enol)pyruvate to the allosteric site of phosphofructokinase from *Lactobacillus delbrueckii* subspecies *bulgaricus*, Texas A&M University, College Station.

182. Lau, F. T., Fersht, A. R., Hellinga, H. W., and Evans, P. R. (1987) Site-directed mutagenesis in the effector site of *Escherichia coli* phosphofructokinase, *Biochemistry 26*, 4143-4148.

183. Valdez, B. C., Chang, S. H., and Younathan, E. S. (1988) Site-directed mutagenesis at the regulatory site of fructose 6-phosphate-1-kinase from *Bacillus stearothermophilus*, *Biochem. Biophys. Res. Commun. 156*, 537-542.

APPENDIX A

Table of kinetic and thermodynamic parameters for the TtPFK variants not discussed in the chapters[h].

	V (U/mg)	n_H	K°_{ia} (μM)	K°_{iy} (μM)	Q_{ay}
D12A*	3.8	1.8±0.1	6.3e3±0.2e3	0.220±4E-3	0.0060±0.0005
D12A/F140W*	3.7	1.12±0.02	550±10	0.014±0.001	0.003±0.001
N59E*	ND	0.88±0.05	22±1	4.8e3±0.5e3	0.21±0.01
N59R*	ND	0.90±0.04	27±1	10e3±2e3	ND
F140W	31	1.4±0.2	6±0.3	2.7±0. 2	0.046±0.002
F176W	38	1.6±0.2	9±1	0.6±0.1	0.034±0.005
Y266W	58	2.5±0.3	15±1	1.9±0.1	0.019±0.001
N59H/K214D	33	3.1±0.3	81±1	44±3	0.29±0.01
N59H/S215H	45	1.3±0.2	10.0±0.6	13±1	0.025±0.001
R55G/N59H/S215H*	ND	1.1±0.2	20±1	1.5e3±0.3e3	0.05±0.01
R55E/N59H/S215H*	ND	1.6±0.2	17±1	5.1e3±0.8e3	0.058±0.001
TtPFK-His tag	48	1.4±0.2	23±1	2.6±0.2	0.603±0.002
TtPFK/BsPFK 2:2	ND	1.1±0.1	47±1	50±1	0.017±0.001

[h] * Denotes heat-sensitive variants

VITA

Name	Maria Shubina-McGresham
Address	Department of Biochemistry and Biophysics Texas A&M University 2128 TAMU College Station, TX 77843-2128
Education	B.S., Biology, University of Texas, Tyler, TX, 2004
Publications	Allosteric regulation in *Thermus thermophilus* phosphofructokinase (in preparation) Role of R55 in tight binding of phosphoenolpyruvate to *Thermus thermophilus* phosphofructokinase (in preparation) Enhancing allosteric response in *Thermus thermophilus* phosphofructokinase (in preparation)